Dissertation

submitted to the

Combined Faculty of Natural Sciences and Mathematics

of the Ruperto Carola University Heidelberg, Germany

for the degree of

Doctor of Natural Sciences

Presented by

M.Sc. Sonja Engels

born in: Linz am Rhein

Oral examination: 10th of July 2019

The role of human Hsp70
for survival and development of the human
malaria parasite
Plasmodium falciparum

Referees: Prof. Dr. Michael Lanzer

PD Dr. Jude Marek Przyborski

Acknowledgements

I would like to express my sincere gratitude to my thesis advisor, second referee and occasional blood donor PD Dr. Jude Przyborski. During the last 4 years Jude taught me to set up experiments with lots of controls to ensure that my results are reliable, to work independently and to take responsibility for students. I am thankful for being a member of the Przyborski lab with all the nice BBQs at our lab “outdoor waterbath” and really enjoyed my time in the lab.

Many thanks to Prof. Dr. Lanzer, who gave apart from accepting to be my first referee much valuable advice during my TAC meetings and Friday seminars.

I gratefully acknowledge the help of the Heat-shock protein 70 expert Prof. Dr. Mayer from the ZMBH, Heidelberg. He and his group were of great support concerning protein purification and luciferase refolding assays.

In addition, I would like to thank Dr. Faith Osier for accepting to be my fourth referee and for providing the pool of hyperimmune sera I used in some experiments.

I am indebted grateful to all the people who joined the lab during our time in Marburg. A special thanks to Dr. Qi Zhang, our queen of proteins, she really helped during the first years of my PhD and shared lots of her knowledge. Furthermore, Dr. Gabi Köllisch, Dr. Stefan Baumeister, Sigrid Stöhr and lots of students such as Bambi (Lisa-Maria Bieker) provided the lab with a friendly and welcoming atmosphere.

Moving from Marburg to Heidelberg was not easy and in the beginning really tough. Here, a special thanks to Miriam Griesheimer and Sandra Niebel. In addition, a big thanks to Marina Müller, Dr. Britta Nyboer, Dr. Tanja Marzluf, Dr. Klara Vochyanova, Kamil Wolanin and Monika Jankowska-Döllken. They were always up for a cup of tea or some burgers with cocktails. In particular I would like to thank Monika for becoming a close friend and a valuable cheating partner at “Bauch-Beine-Po”. Above all, I am grateful to Tanja for taking the time reading and correcting the thesis. She shared lots of useful tips and trips, thereby contributing to the success of this thesis.

Further, support was given by Jessica Kehrer and Marta Machado. Both were valuable assets in performing the mice infection and mosquito dissection.

Acknowledgements

The thesis could not be written without the support of Fauzia Musasia, Dennis Obonjo and Irene Nkumama who helped in particular with the sera experiments and answered all my FlowJo questions.
This work greatly benefited from a professional working atmosphere in the whole Przyborski lab. A special thanks to Laura Grob, Celine Rausch and Lena Rolling. Laura I would like to gratefully thank for taking the time to poof-read the thesis and for sunny afternoons we spent at the swimming pool.
I gratefully acknowledge the help of Mathias Diehl, “Toxic Ginger”, my partner in crime for the last 4 years. Thanks for introducing me to great artist such as, “the beards”, “Richard Cheese”, “The 24 hour insanity: Pink fluffy unicorns dancing on rainbows” or the weird Mongolian gangster rap.
During the long and winding road of my PhD Jessica Günnewig was of big support. I really enjoyed our time in Marburg and Heidelberg.
I would like to express my heartfelt gratitude to my former colleagues from the ZAI in Aachen, Alex Goltzmann, Dr. Christine Wirth, Dr. Meike Kiesow and Dr. Sandra Bennink. Thanks for keeping in contact and becoming close friends. Big thanks to Christine for the funny road trips to Aachen and for correcting the thesis.
Further, I would like to thank Ela Hoß, Lena Simon and Vanessa Boden for all the support during the last 4 years.
Finally, I want to thank all people for their support, without whose help this work would never have been possible.
Zum Schluss möchte ich mich sehr herzlich bei meiner ganzen Familie für die jahrelange Unterstützung bedanken. Ganz besonders möchte ich mich bei meinem Onkel Michael und meiner Tante Evi für das unerschütterliche Vertrauen in mich und meine Fähigkeiten bedanken.
Mein größter Dank gilt meinen Eltern. Vielen lieben Dank für die mentale sowie finanzielle Unterstützung während meines sehr langen Weges. Ihr habt immer an mich geglaubt und nie an meinen Erfolg gezweifelt.

Table of content

List of Figures

List of Tables

Abbreviations

APAD	3-Acetylpyridine adenine dinucleotide
APS	Ammonium persulfate
ATP	Adenosine triphosphate
BSA	Bovine serum albumin
CS promoter	Circumsporozoite promoter
CV	Column volumes
DAPI	4′,6-Diamidin-2-phenylindol
ddH_2O	Double distilled water
DMEM	Dulbecco´s modified eagle medium
DTT	Dithiothreitol
E. coli	*Escherichia coli*
EDTA	Ethylenediaminetetraacetic acid
EMP1	Erythrocyte membrane protein 1
ER	Endoplasmic reticulum
FCS	Fetal calf serum
FSC	Forward scatter
GAPDH	Glyceraldehyde 3-phosphate dehydrogenase
GFP	Green fluorescence protein
h	Hour/s
His-tag	6x Histidine tag
HsHsc70	*Homo sapiens* heat-shock cognate protein (HSPA8)
HsHsp40	*Homo sapiens* heat-shock protein 40
$HsHsp70^{K71M}$	*Homo sapiens* heat-shock protein 70 K71M (HSPA1)
$HsHsp70^{wt}$	*Homo sapiens* heat-shock protein 70 wildtype (HSPA1)
Hsp70x	*P. falciparum* heat-shock protein 70-x
HSPA1	*Homo sapiens* heat-shock protein A1 (HsHsp70)
IFA	Indirect immunofluorescence assay
iRBC	Infected red blood cell
irRBC	Infected resealed red blood cell
K	Lysine
L	Litre/s
LB agar	Luria-Bertani agar
LDH	Lactate dehydrogenase
M	Methionine
MACS	Magnetic activated cell sorting
MAHRP	Membrane-associated histidine-rich protein
mL	Millilitre/s
NBT	Nitro blue tetrazolium
NEF	Nucleotide exchange factor
Oval	Ovalbumin
P. berghei	*Plasmodium berghei*
P. falciparum	*Plasmodium falciparum*
PBS	Phosphate buffered saline
PC	Positive control
Pen/Strep	Penicillin/Streptomycin
PEXEL	*Plasmodium* export element
PHIS	Pool of hyperimmune sera from Kelifi, Kenya
PMSF	Phenylmethylsulfonyl fluoride
PNEP	PEXEL-negative exported protein
pos	Positive
PPM	Parasite plasma membrane
PV	Parasitophorous vacuole
PVM	Parasitophorous vacuole membrane
RBC	Red blood cells
RFP	Red fluorescence protein
Rhod	Rhodamine
RIPA buffer	Radioimmunoprecipitation assay buffer
RNA	Ribonucleic acid

RPMI 1640	Roswell Park Memorial Institute 1640 Medium
rRBC	Resealed red blood cells
s	Second/s
SB medium	Super broth medium
SBP	Skeleton-binding protein
scraRNA	Scrambled RNA
siRNA	Small-interfering RNA
SSC	Side scatter
SUMO	Small ubiquitin related modifier
vs	Versus
WB	Western blot
ZMBH	Zentrum für Molekulare Biologie der Universität Heidelberg

Summary

Plasmodium falciparum is one of the most deadly malaria parasites and causes the tropical disease “malaria tropica”. Most of the pathology can be explained by the drastic host cell modifications which are initiated by the parasite shortly after invasion. Moreover, upon the invasion of the mature human erythrocyte, the parasite encases itself with a parasitophorous vacuole (PV). It is known that the parasite exports 300-400 proteins to the host cell, to change the biophysical properties of the infected erythrocytes. However, up to date little is known about how the parasite sets up its own protein export machinery in a host cell devoid of any infrastructure. Scientific knowledge was significantly boosted with the discovery that ATP, a factor in the host cell cytoplasm and protein unfolding was pivotal to protein export across the PV membrane (PVM). Further, the discovery of the parasite-encoded protein translocon called PTEX (*Plasmodium* Translocon of EXported proteins) in the PVM shed more light on the underlying mechanism. In 2016, data was obtained that the human heat-shock protein 70 (HsHsp70) is essential for the transport across the PVM. Based on this observation, this study focussed on the question whether HsHsp70 is vital to the parasite’s intra-erythrocytic development. For this purpose, a resealing approach commonly used in pharmacology was established. Since the mature human erythrocyte cannot be easily genetically modified, the resealing approach was used to achieve a classic dominant negative effect by pre-loading the mature human erythrocytes with an excess amount of mutated recombinant HsHsp70. Afterwards the resealed erythrocytes were infected with *P. falciparum* parasites. Interestingly, the growth was not altered by the presence of the excess amount of the mutated HsHsp70. In addition, the protein export in the presence of the mutant protein was analysed using parasites encoding green fluorescently labelled, known exported, proteins. Surprisingly, the protein transport was not inhibited by the presence of the mutant, as well. Last, parasites depleted of a parasite-exported Hsp70 called Hsp70x, were used to infect the resealed cells pre-loaded with the mutated protein. The growth and protein export were not altered for the ΔHsp70x parasite. In conclusion, under the given experimental setup, no essential function of HsHsp70 for the growth and protein export of *P. falciparum* was revealed.

Zusammenfassung

Plasmodium falciparum ist einer der tödlichsten Malariaerreger und führt zur Tropenkrankheit „Malaria Tropica“. Der Großteil der Pathologie geht mit den drastischen Wirtszellmodifikationen, welche direkt nach der Invasion vom Parasiten induziert werden, einher. Zudem schließt sich der Parasit während der Invasion der Wirtszelle, dem reifen humanen Erythrozyten, in eine parasitophore Vakuole (PV) ein. Der Parasit exportiert 300-400 Proteine in die Wirtszelle und verändert dabei die biophysikalischen Merkmale der Wirtszelle. Dennoch ist bis heute nicht bekannt wie der Parasit eine Protein-Export-Maschinerie in eine Wirtszelle ohne jegliche Infrastruktur integriert. Unser Wissen konnte durch die Entdeckung, dass ATP, ein zytoplasmatischer Wirtszellfaktor und Proteinentfaltung entscheidend für den Transport über die PVM sind, erweitert werden. Die Entdeckung des PTEX-Translokons (*Plasmodium* Translocon of EXported proteins) in der PVM konnte mehr Licht auf die Mechanismen werfen. Im Jahr 2016 konnten Experimente eine essentielle Rolle des humanen Hitzeschock Proteins 70 (HsHsp70) im Protein-transport über die PVM nachweisen. Basierend darauf, wurde hier untersucht, ob HsHsp70 überlebenswichtig für die intra-erythrozitäre Entwicklung des Parasiten ist. Dazu wurde eine in der Pharmazie verwendete „Resealing“ Methode etabliert. Da der reife Erythrozyt sich nicht leicht genetisch manipulieren lässt, wurde durch das „Resealing“ ein klassisch dominant negatives Vorgehen ausgewählt, bei dem der Erythrozyt mit einem Überschuss eines mutierten Hsp70s beladen wird. Dann wurden die „resealten“ Erythrozyten mit *P. falciparum* infiziert. Interessanterweise wurde das Wachstum durch den Überschuss des mutierten HsHsp70s nicht beeinflusst. Auch der Proteinexport in Anwesenheit des mutierten HsHsp70s mit Parasiten, die grün-fluoreszierende exportierte Proteine exprimieren, zeigte keine Einschränkungen durch die Präsenz des mutierten HsHsp70s. Zuletzt wurden mutierte Parasiten ohne parasitäres exportiertes Hsp70, Hsp70x, für die Infektion von „resealten“ Erythrozyten verwendet. Das Wachstum und der Proteinexport der ΔHsp70x Parasiten wurden durch die Anwesenheit der Mutante nicht verändert. Unter diesen experimentellen Voraussetzungen konnte keine essentielle Funktion des HspHsp70 für das Wachstum und den Transport von *P. falciparum* enthüllt werden. .

1 Introduction

1.1 Introduction into Malaria

The subtropical and tropical disease malaria is caused by the obligate intracellular parasite genus *Plasmodium.* The disease was already described in 1880 by the French military surgeon Alphonse Laveran (Nye, 2002). Today, more than 100 *Plasmodium* species are known, including 5 that are pathogenic to humans: *Plasmodium vivax*, *Plasmodium ovale*, *Plasmodium malariae*, the recently identified simian agent *Plasmodium knowlesi*, and *Plasmodium falciparum*, causing the most severe and deadly form called malaria tropica (Cowman et al., 2016; Phillips et al., 2017). Despite the greatest efforts by the world health organisation (WHO), 219 million malaria cases were reported in 2017, of these 435,000 people did not survive the disease (WHO, 2018). The most deadly *Plasmodium* parasite represents *Plasmodium falciparum*, which accounted for 99.7% of the reported deaths in 2017 (WHO, 2018). Particularly, children under the age of 5 and pregnant women in malaria endemic regions such as Africa, South-East Asia and Latin America are at high risk for fatal malaria (Figure 1). The WHO recommends an Artemisinin-based combination therapy (WHO, 2018), but growing drug resistances make it hard to treat the disease and emphasise the need for the identification of new drug targets (Wells et al., 2015).

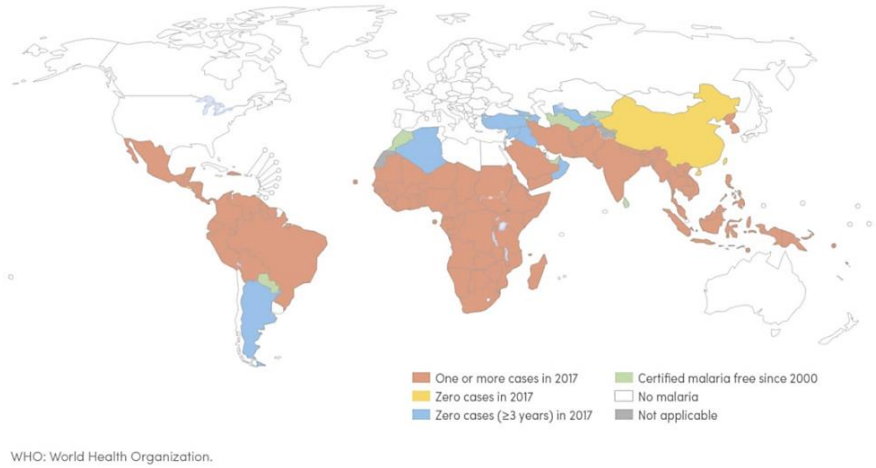

Figure 1 Comparison of the malaria cases in endemic areas in 2000 and their status in 2017.
Most of the malaria cases were still reported in Latin America, Africa and South-East-Asia (modified from the Malaria Report, WHO 2018).

1.1.1 Life cycle of Plasmodium falciparum

The complex life cycle of *Plasmodium falciparum* can be divided into an asexual multiplication, occurring in the mammalian host, and a sexual multiplication taking place in the invertebrate host (Cowman et al., 2016). The asexual multiplication can be further divided into an exo-erythrocytic phase referred to as liver stages and an intra-erythrocytic known as blood stages (Figure 2).

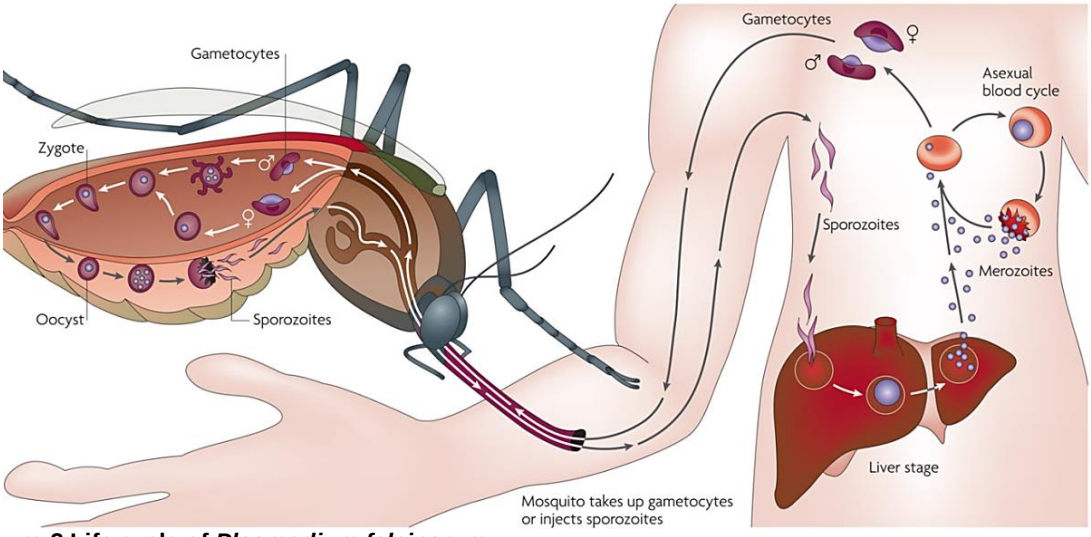

Figure 2 Life cycle of *Plasmodium falciparum*
The infection is initiated by an infected female *Anopheles* mosquito taking a blood meal from a human. Sporozoites are released and actively invade the hepatocytes, starting the exo-erythrocytic phase. After 1-2 weeks, merozoites are released and start the asexual blood cycle. Some merozoites become sexually committed and develop into mature female and male gametocytes which are able to infect a mosquito. In the mosquito, gametogenesis and fertilizations take place. Finally, a zygote is formed that develops into a motile ookinete, which breaks through the midgut epithelium and matures to an oocyst. The oocyst releases sporozoites that accumulate in the salivary glands of the mosquito (modified from Su et al. 2007).

A malaria infection starts with an infected *Anopheles* mosquito taking a blood meal from a human. During the blood meal sporozoites are released into the host dermis. The sporozoite actively migrates through the skin until it hits a blood vessel, which transports the parasite passively to the liver. In the liver, the sporozoite passes through endothelial cells, Kupffer cells (macrophage-like cells), and several hepatocytes before finally invading a liver cell (Tavares et al. 2013, Mota et al. 2001). Up to 2 weeks later, the sporozoite matures into a liver schizont (Amino et al., 2007). Then, merosomes are released into the blood stream and burst to discharge up to 40,000 merozoites (Sturm et al., 2006), marking the beginning of the intra-erythrocytic cycle. The merozoite actively invades the human erythrocyte by making use of its apical complex (complex of rhoptries, micronemes, apical polar ring and coniod) (Blackman and Bannister

2001). Upon the invasion of the host cell, the parasite encloses itself with a parasitophorous vacuole membrane (PVM), thereby separating itself from the host cytosol (Lingelbach and Joiner, 1998). Shortly after, parasitic development continues with the ring stage. Already in the ring stage the parasite starts to remodel its host cell by exporting parasite-encoded proteins to the erythrocyte cytosol (Das et al., 2015; Spielmann et al., 2006). 20-24 h post-invasion, the parasite progresses to the trophozoite stage in which more drastic host cell modifications are introduced (Cowman et al., 2016). One of the most striking modifications are small protrusions on the surface of the host cell known as knobs. On top of the knobs, the major virulence factor EMP1 (Erythrocyte Membrane Protein 1) is presented, which drastically changes the biophysical behaviour of the erythrocyte (Cowman et al., 2016; Phillips et al., 2017). The exact mechanisms of protein export and the thereby induced host cell modifications will be discussed in more detail in 1.2. The trophozoite develops into a schizont containing 16-32 merozoites (Cowman et al., 2016). During the intra-erythrocytic development, the parasite uses the host haemoglobin as a nutritional source and converts the accumulating toxic heme into hemozoin crystals (Slater and Cerami, 1992; Slater et al., 1991). Finally, the schizont and infected erythrocyte rupture, resulting in the release of mature merozoites into the blood stream. This step includes the release of hemozoin and pyrogens associated with the typical fever observed in malaria patients. After some rounds of asexual multiplication, some merozoites become sexually committed with a female bias (Silvestrini et al., 2000). In a process called gametocytogenesis, encompassing five stages (I-V), the parasite undergoes radical morphological changes resulting in a mature stage V male microgametocyte and female macrogametocyte. The mature stage V gametocytes are the only stage able to transmit the disease to a mosquito (Greenwood et al., 2008). Stage V gametocytes are taken up by the mosquito with a blood meal. The drop in temperature, the increased pH and the presence of xanthurenic acid in the midgut induce a process called gametogenesis (Billker et al., 1998; Garcia et al., 1998; Sinden et al., 1996; Sinden et al., 1983). The macrogametocyte starts to round up, becoming a macrogamete, while the microgametocyte differentiates into 8 mobile microgametes (Pradel, 2007). The fertilisation of a macrogamete with a microgamete resulting in a zygote completes the sexual development.

After 24 h, the zygote develops into an ookinete, which traverses the midgut epithelium. Finally, the ookinete matures to an oocyst that resides between the midgut epithelium and the basal laminal. After 10-12 days, the oocyst releases thousands of sporozoites, which accumulate in the salivary glands of the mosquito (Dimopoulos et al., 1998). Once the mosquito takes a blood meal from a human host, the life cycle starts anew.

1.2 Host cell modifications

Shortly after invading, the parasite starts to make it comfortable in its new home, the mature human erythrocyte. Already 8-12 h post-invasion, the parasite increases the erythrocyte's membrane permeability (Ginsburg et al., 1985; Kirk et al., 1994; Staines et al., 2000) by inducing Novel Permeation Pathways (NPP) (Baumeister et al., 2003, 2006; Kirk et al., 1999), thereby importing nutrients like sugars or amino acids, which the parasite cannot produce itself. The foundation for more drastic renovating events in the trophozoite stage is already laid in the ring stage. The parasite starts to export SBP1 (Skeleton-Binding Protein 1) (Blisnick et al., 2000) and MAHRP (Membrane-Associated Histidine-Rich Protein) (Spycher et al., 2003), 2 important components of the Maurer's clefts. The Maurer's clefts are an exomembrane structure directly underneath the erythrocyte membrane (Grüring et al., 2012; Lanzer et al., 2006).

In the trophozoite stage, an extremely active phase of protein export and severe host cell alteration is started. In the beginning, the parasite is restructured to the needs of this phase by increasing the size of the Endoplasmic Reticulum (ER) (Bannister et al., 2000), the centre of protein biosynthesis. One of the most striking modifications induced during this phase are small electron dense protrusions on the erythrocyte membrane, the so-called knobs (Gruenberg et al., 1983). On top of the knobs one of the most studied malaria proteins, EMP1 is presented (Figure 2) (Cowman et al., 2016; Przyborski et al., 2016). The already established Maurer's clefts are vital to EMP1 transport and presentation on the erythrocyte. EMP1 is encoded by members of the multigene family referred to as *var* genes (Su et al., 1995). With the help of the *var* genes, the parasite is able to undergo antigenic variation, thereby successfully evading the host immune

system (Baruch et al., 1995; Su et al., 1995). Moreover, EMP1 presentation on the erythrocyte surface allows the parasite to bind to host cell ligands like ICAM-1 (InterCellular Adhesion Molecule 1) and CD36 (Cluster of Differentiation 36) mediating cytoadherence (Smith et al., 1995). In the placenta, the EMP1 variant VAR2CSA enables the parasite to adhere to CSA (Chondroitin Sulfate A), thus harming the mother as well as the unborn child (Clausen et al., 2012; Salanti et al., 2004, 2003). Additionally, the infected red blood cell (iRBC) can bind to non-infected erythrocytes in a process known as rosetting, shielding the infected cell further from the immune system. Both processes, rosetting and cytoadherence, contribute to the disease's severity. As a result, small blood vessels are blocked, causing hypoxia and death by organ failures (Miller et al., 2002) (Figure 3).

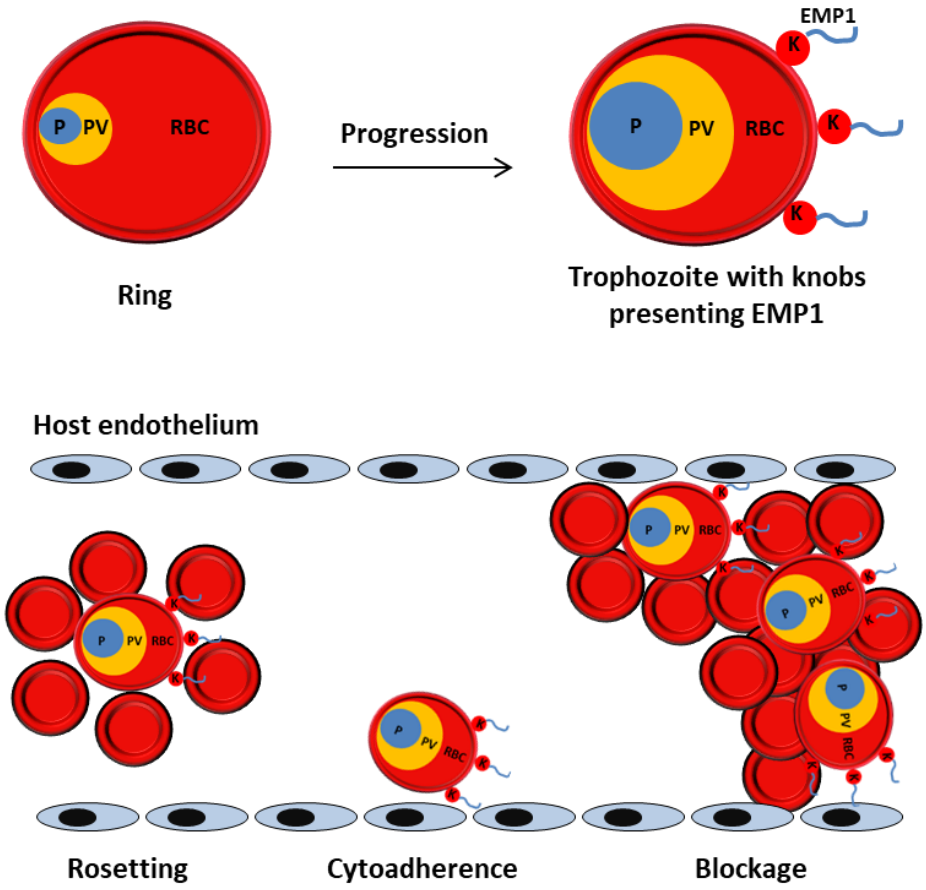

Figure 3 Rosetting and cytoadherence of *P. falciparum* infected erythrocyte
Top: In trophozoite stage, the drastic host cell modifications become obvious. These changes include small protrusions, the so-called knobs, as well as EMP1 presentation on the surface of the infected RBC.
Bottom: After host cell remodelling, the parasite is able to shield itself from the immune system by binding to non-infected RBC, a phenomenon known as rosetting. Further, the parasite avoids splenic clearance by binding to the host endothelium using the interaction between EMP1 and host ligands, resulting in cytoadherence. Both processes lead to a blockage of the vascular endothelium. P: Parasite, PV: Parasitophorous Vacuole, RBC: Red Blood Cell, K: Knob, EMP1: Erythrocyte Membrane Protein 1, (adapted from Yam et al. 2017).

An important prerequisite of all these modifications is the establishment of a protein export machinery introduced to the host cell by the parasite. To understand this complex process in more detail, a deeper knowledge of the host cell is required reviewed in the following.

1.2.1 The host cell

The human erythrocyte is commonly known as the major oxygen and carbon dioxide carrier. The gases are bound by the most abundant protein in the erythrocyte called haemoglobin, which is responsible for the typical red colour (Longeville and Stingaciu, 2017). Apart from this, erythrocytes are also associated with the transport of GPI-linked proteins (Kooyman et al., 1995) and iC3b/CBP (complement immune complexes) (Schifferli and Taylor, 1989). A proteomic study conducted by Pasini and colleagues found 340 membrane and cytoskeleton proteins in the erythrocyte (Pasini et al., 2006). Amongst these, most might be associated with the typical discoid shape of the cell. Additional 252 soluble proteins were revealed. Most of these proteins were involved in cellular metabolism, transport and the formation of protein complexes (Pasini et al., 2006). Interestingly, the human erythrocyte also contains chaperones such as, the heat shock protein 70 (Hsp70), Hsp90, Hsp60 and the heat shock cognate 70 (Hsc70) (D'Alessandro et al., 2010; Kakhniashvili et al., 2004; Pasini et al., 2006). In general, the erythrocyte is a fully differentiated and highly specialised cell. The mature human erythrocyte circulating in the peripheral blood went through some severe changes during its maturation. The cell lost most of the classical eukaryotic organelles e.g. the nucleus, mitochondria, ribosomes with ER, and the Golgi apparatus (Gronowicz et al., 1984). In consequence, the erythrocyte is devoid of any protein transport infrastructure. In summary, the human mature erythrocyte is a rather uncommon choice as host cell. With the aforementioned extreme host cell modifications in mind, it is fascinating how the parasite, without exploiting any host infrastructure, exports so many proteins to the host cell. The parasite even complicated transport by enclosing itself within a PV. In this way, the parasite needs to redress the PVM not only for protein export, but also for import of amino acids or sugars, it cannot produce.

1.3 Protein export to the human erythrocyte

The survival and propagation of the parasite largely depends on the export of 300-400 proteins to the human host cell (Hiller et al., 2004; Maier et al., 2009; Marti et al., 2004; Sargeant et al., 2006). Up to date, it is not completely resolved how the parasite assembles its own protein export machinery in a host cell devoid of any protein transport system. Nonetheless, it represents an outstanding drug target. Due to its parasite origin, drugs would specifically target the parasite and not harm the human host (Gilson et al., 2014). Yet, even better would be to target a human protein essential for this process, as the parasite can then not develop resistance.

1.3.1 Signal peptide sequences in *Plasmodium*

Usually proteins destined for export are marked by an N-terminal hydrophobic signal sequence and are transported to the ER (Wickham et al., 2001). Indeed, parasite proteins intended to be exported also encompass a distinct N-terminal RxLx/EDQ signal peptide sequence referred to as *Plasmodium* EXport ELement (PEXEL) or Host Targeting sequence (HT) (Hiller et al., 2004; Marti et al., 2004; Przyborski et al., 2005). The PEXEL motif undergoes several important modifications before it is ready for export. First, the ER-resident aspartyl protease, called plasmepsin V (Boddey and Cowman, 2013) cleaves off the arginine and lysine, leaving the xE/D/Q known as the mature PEXEL. Afterwards, the PEXEL motif is acetylated (Boddey et al., 2010; Chang et al., 2008). The processed proteins enter the secretory pathway and finally get secreted into the PV. Interestingly, not all exported proteins contain a PEXEL motif. The most extensively studied EMP1 does not have a PEXEL, representing an important member of the so called PEXEL-Negative Exported Proteins (PNEP) (Spielmann and Gilberger, 2010). The PNEP are characterised by the presence of an internal hydrophobic region, which is sufficient for entering the secretory pathway (Haase et al., 2009; Spielmann and Gillberger 2010).

1.3.2 How to reach the host cytoplasm?

It was long debated how proteins end up in the host cell cytoplasm. Experimental data was pointing towards the existence of a translocon in the PVM. Major evidence was obtained by Ansorge and colleagues revealing that a protein source and ATP in the host cell are needed for transport across the PVM (Ansorge et al., 1996). Additionally, Gehde and associates showed that protein unfolding is required to pass the PVM (Gehde et al., 2009). Both studies were strongly supporting the so far hypothesised and long debated existence of a translocon (Charpian and Przyborski, 2008). Finally, in 2009 the debate came to an end due to the identification of the *Plasmodium* Translocon of EXported proteins, in short PTEX (de Koning-Ward et al., 2009).

1.3.2.1 The *Plasmodium* Translocon of EXported proteins (PTEX)

The PTEX translocon is a 1,200 kDa complex containing 5 core proteins. The pore in the PVM is produced by EXP2 (EXported Protein 2) (de Koning-Ward et al., 2009), which was recently found to be involved in the transport of nutrients (Garten et al., 2018), as well. Additional components are Hsp101 (Heat-shock protein 101), a known ClpB-type-AAA-ATPase most likely associated with the unfolding of the cargo protein, and thioredoxin 2 (Trx2) (de Koning-Ward et al., 2009). Trx2 is probably involved in reducing disulfide bonds (de Koning-Ward et al., 2009). Finally, PTEX88 and PTEX150 complete the PTEX translocon and most likely perform structural tasks (de Koning-Ward et al., 2009). Recently, it was shown that both PNEP as well as PEXEL proteins use the translocon to redress the PVM (Elsworth et al., 2014; Grüring et al., 2012). Moreover, studies revealed that PTEX components such as PTEX150 and Hsp101 are produced during schizogony, emphasising the importance of PTEX (Bullen et al., 2012; Riglar et al., 2013).

As previously mentioned proteins destined for export enter the secretory pathway and are released into the PV (1.3.1). The transport mediated by a translocon typically includes protein unfolding (Eilers and Schatz, 1986; Paunola et al., 1998; Walker et al., 1996). In consequence, after translocation the protein also needs to be refolded in order to fulfil its task in the host cell (Figure 4).

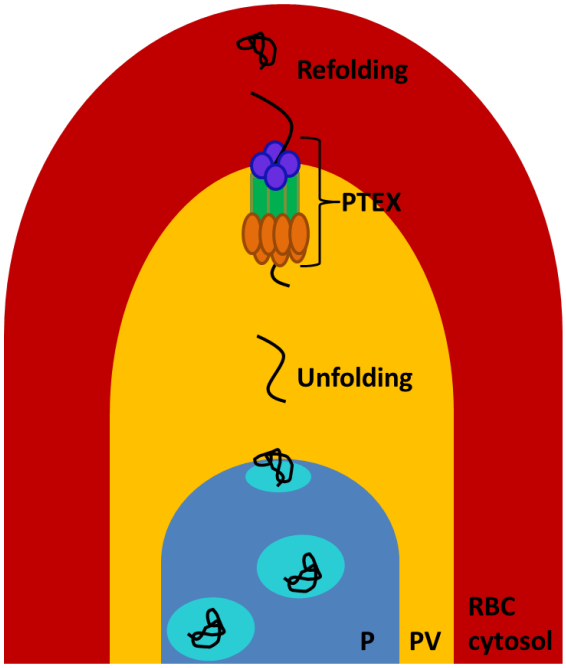

Figure 4 Overview of protein transport in the infected erythrocyte
Proteins destined for transport enter secretory pathway and get secreted into the PV. In the PV, proteins require unfolding in order to redress PVM by assistance of the PTEX translocon. Once in the RBC cytosol, proteins need to be refolded. P: Parasite (blue), PV: Parasitophorous Vacuole (yellow), RBC cytosol: Red Blood Cell cytosol (red), PTEX translocon: orange: Hsp101, green: PTEX150, dark blue: EXP2 (adapted from Boddey and Cowman, 2013).

The unfolding and refolding of proteins is usually performed by a highly conserved protein class known as chaperones (Eilers and Schatz, 1986; Paunola et al., 1998; Walker et al., 1996), reviewed in more detail in the following.

1.4 Chaperones

The nascent protein emerging from the ribosome requires folding, a task performed by so-called molecular chaperones (Gidalevitz et al., 2013). The highly conserved class of chaperones executes many jobs. Amongst these, chaperones are involved in protein translocation, resolve protein aggregates and assemble oligomers (Dekker et al., 2015; Goloubinoff, 2017). Molecular chaperones are crucial to the health of a cell and can be found in nearly all living cells (Lindquist, 1986). The Heat-Shock-Proteins (Hsp) are a well characterised chaperone group (Saibil, 2013). The Hsps are synthesised in particular during stress such as febrile episodes (Javid et al., 2007) and are named according to their molecular masses. Extensively characterised Hsp representatives are Hsp70 with its co-

chaperone Hsp40, Hsp90, Hsp60 also known as TRiC (TCP1 Ring Complex). In particular, Hsp70 and their co-chaperones Hsp40 are known to provide the motor power for protein translocation (Craig, 2018).

1.4.1 The molecular chaperone class Hsp70

One of the most ancient molecular chaperone classes is Hsp70 (Dekker et al., 2015). The 70 kDa protein contains an N-terminal 45 kDa Nucleotide Binding Domain (NBD) and a 25 kDa C-terminal Substrate Binding Domain (SBD) (Mayer and Bukau, 2005; Mayer and Kityk, 2015). Through its NBD the chaperone binds and hydrolyses ATP leading to drastic conformational changes (Mayer and Bukau, 2005; Mayer and Kityk, 2015). The chaperone requires its co-chaperone, known as Hsp40, and a nucleotide exchange factor to complete the cycle and for returning to the ATP-bound-state (Mayer and Kityk, 2015) (reviewed in more detail in 1.4.2). With the help of the SBP, the chaperone recognises hydrophobic motifs in their client proteins, which only get exposed during protein synthesis, protein translocation or protein denaturation in case of stress (Craig, 2018; Mayer and Kityk, 2015). Every 30-40 amino acids proteins contain such hydrophobic Hsp70 recognition motifs (Rüdiger et al., 1997). Further, at the C-terminus an EEVD motif can be found, enabling the formation of multi-chaperone complexes (Blatch and Lässle, 1999; Freeman et al., 1995) and targeting proteins to their destinations (Craig, 2018). Due to their function in protein translocation, Hsp70 proteins are interesting candidates to assist in protein translocation across PTEX (Koning-ward et al., 2009). In particular, their role in translocation processes to import proteins into the ER, chloroplast and mitochondria are well characterised and studied. In the ER, the chaperone BiP (Binding immunoglobulin Protein) helps proteins to pass the Sec61 translocon, to enter the ER after translation has been completed (Alder et al., 2005; Matlack et al., 1999). In the chloroplast, Hsp70 provides the driving force for importing proteins through translocons in the inner and outer chloroplast membrane (Shi and Theg, 2010). Finally, in the mitochondria, proteins are imported through TOM (Translocon Outer Membrane) and TIM (Translocon Inner Membrane) by using Hsp70 as “pulling” or motor force (Gambill et al., 1993). After passage Hsp70 can also assist in the refolding of cargo proteins (Horst et al., 1997).

There are 2 proposed models how Hsp70 assists in the translocation (Neupert and Brunner, 2002; Tomkiewicz et al., 2007): The power-stroke model suggests that Hsp70 actively pulls and unfolds the protein through the translocon via repeated ATP hydrolysis (Neupert and Brunner, 2002; Tomkiewicz et al., 2007). The other model called Brownian-rachet model relies, as the name indicates, on Brownian oscillations, which move the polypeptide chain forwards and backwards inside the translocon. Hsp70 binds tightly through ATP hydrolysis and stops the chain from moving backwards (Neupert and Brunner, 2002; Tomkiewicz et al., 2007).

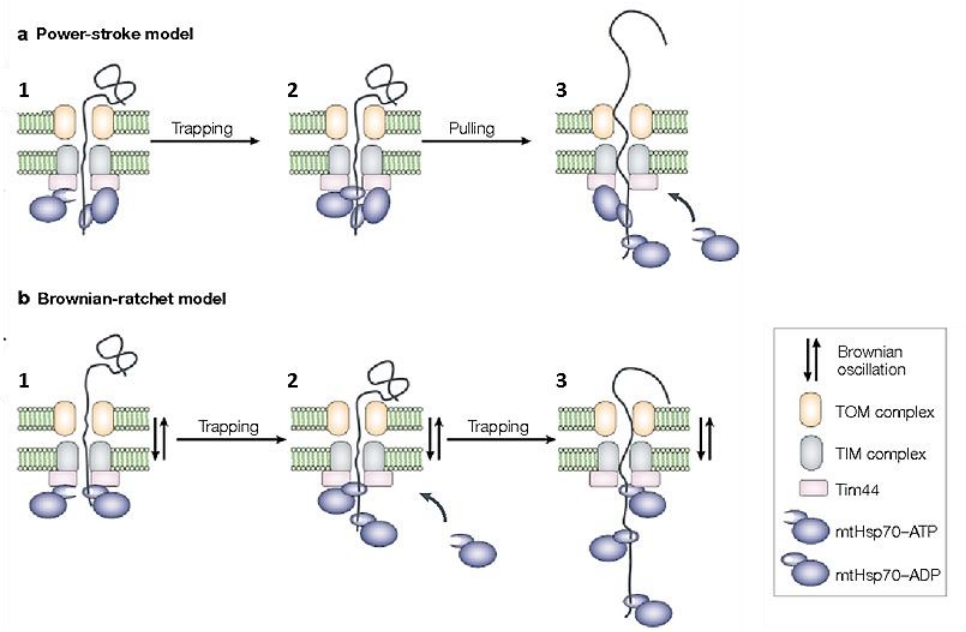

Figure 5 The power-stroke and Brownian-rachet model (explained by taking the example of mitochondria)

(a) Power-stroke model: The protein is actively pulled through the translocon by Hsp70. To this end, Hsp70 most probably uses the SBD as a lever arm. In its ATP-bound state, Hsp70 is recruited by Tim44 (component of the translocon) and binds the emerging polypeptide chain. Due to the conformational change the polypeptide chain is pulled through the translocon.

(b) Brownian-ratchet model: Based on the Brownian oscillation the polypeptide chain moves forwards and backwards inside the translocon. Hsp70, in its ADP-bound state, binds the polypeptide chain tightly and prevents it from sliding back. On the next forward move, the next Hsp70 binds and prevents the next piece from slipping back (modified from Neupert and Brunner, 2002).

1.4.2 The co-chaperone Hsp40

The Hsp70 protein family largely depend on their co-chaperones called Hsp40. The 40 kDa proteins are also referred to as J-proteins due the characteristic J-domain (Hennessy et al., 2005; Kampinga and Craig, 2010). These J-proteins are mainly involved in identifying client proteins and recruiting Hsp70s. In humans ~50 Hsp40 were identified (Kampinga and Craig, 2010). The Hsp40 display a big

variety in domains and can be divided into 3 classes according to their composition (Kampinga and Craig, 2010). This enormous Hsp40 diversity ensures Hsp70 specificity for many different proteins (Hennessy et al., 2005; Kampinga and Craig, 2010). Hsp40 and Hsp70 work in a complex cycle together with Nucleotide Exchange Factors (NEF) (Dekker et al., 2015). The co-chaperone Hsp40 first recognises and binds to client proteins by the J-domain. In the ATP-bound or also called “open conformation”, the Hsp70 SBD is able to bind the substrate. Afterwards, Hsp40 increase the low intrinsic ATPase domain (NBD) of the Hsp70, causing a fast ATP hydrolysis and drastic conformational changes. In the ADP-bound state, the “lid” is closed and the Hsp70 tightly binds its client. With assistance of NEF the ADP is replaced with an ATP, resulting in the opening of the “lid”. The client protein is released and the cycle can start over again (Dekker et al., 2015).

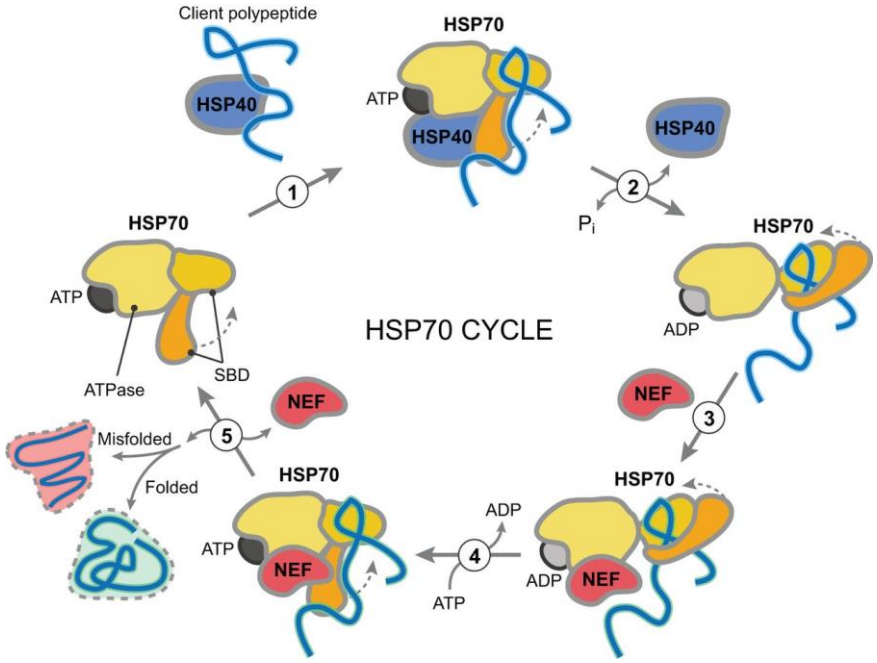

Figure 6 Overview of the Hsp70 cycle
Hsp40 recognises the client protein and recruits Hsp70. In the ATP-bound (“open conformation”) Hsp70 can bind the client. The low intrinsic ATPase activity of Hsp70 is stimulated by Hsp40 and results in fast hydrolysis, leading to the ADP-bound state (“closed conformation”). Finally, NEF is needed to open the lid by exchanging the ADP to an ATP, releasing the client protein (Brehme and Voisine, 2016).

Based on the aforementioned data, exported and parasite-encoded Hsp70 and Hsp40 would be the ideal candidates assisting in the protein translocation through the PTEX, and later refolding (Külzer et al., 2012, 2010).

1.4.3 Heat-shock proteins in *P. falciparum*

P. falciparum encodes 92 chaperones and co-chaperones, thus, dedicating 2% of its genome to their expression (Acharya et al., 2007). The most abundantly expressed chaperone classes are Hsp70 and Hsp90 (Acharya et al., 2007), while the co-chaperone Hsp40 protein family amounts to 49 known proteins, making it the biggest co-chaperone group in *P. falciparum* (Botha et al., 2007). There are 6 identified Hsp70s (PfHsp70-1, -2, -3, -z, -x and -y) in *P. falciparum* (Külzer et al., 2012; Przyborski et al., 2015; Shonhai, 2010). Based on *in silico* analysis it is predicted that the chaperones fulfil their classical jobs, e.g. in the parasite's mitochondria, PfHsp70-3 (Njunge et al., 2013) presumably forms a complex with Hsp90 and is involved in protein import (Przyborski et al., 2015; Young et al., 2003). The parasite also expresses a homologue to the ER-chaperone BiP (Binding immunoglobulin Protein) (Kumar et al., 1991, 1988; Kumar and Zheng, 1992). The plasmodial BiP is PfHsp70-2, which most likely assists in protein secretion as well as protein degradation (Przyborski et al., 2015). In 2012, Külzer and associates identified a parasite-encoded and exported Hsp70 chaperone called PfHsp70-x (in the following referred to as Hsp70x) (Külzer et al., 2012). Hsp70x is localised in the PV as well as in the host cytosol. In the cytosol, Hsp70x was revealed as a component of the so-called J-dots, which are mobile structures in the host erythrocyte containing also 2 PfHsp40 co-chaperones (PFA0660w and PFE0055c) (Külzer et al., 2012, 2010). First modelling and docking analysis pointed towards a functional PfHsp40-Hsp70x pairing (Hatherley et al., 2014) and later functional evidence for an interaction of PFA0660w and Hsp70x was obtained (Daniyan et al., 2016). Interestingly, the J-dots were associated with the major virulence factor EMP1 (Külzer et al., 2010). In consequence, it was hypothesised that Hsp70x might be involved in EMP1 trafficking (Külzer et al., 2012). Additionally, due to its presence in the PV, Hsp70x might assist Hsp101 in the unfolding of cargo proteins (Elsworth et al., 2016; Külzer et al., 2012; Seyffer et al., 2012; Zhang et al., 2017). This hypothesis was strongly supported by immunoprecipitation studies of the already introduced PTEX components PTEX150, EXP2 and Hsp101 (Elsworth et al., 2016; Rhiel et al., 2016). In general, all these data made Hsp70x a promising candidate to play an essential role in protein transport to the host cell. Recently generated Hsp70x-deficient parasites did surprisingly not display a growth defect

(Charnaud et al., 2017). However, parasites depleted of Hsp70x presented reduced EMP1 export resulting in a diminished cytoadhesion (Charnaud et al., 2017). In summary, Hsp70x is not essential, at least not *in vitro*, yet is closely linked to EMP1 transport (Charnaud et al., 2017).

Another likely candidate assisting in protein translocation and refolding in the host cytosol is the host's Hsp70 (Banumathy et al., 2002; Charpian and Przyborski, 2008; Külzer et al., 2010). As already mentioned, the mature human erythrocyte contains several HsHsp. At least 4 different HsHsp70 and HsHsc70 (HSPA2, HSPA1L, HSPA1and HSPA8) were identified by mass spectrometry (D'Alessandro et al., 2010). Further, Hsp60, Hsp90 (HSP90AA1 and HSP90AB1) as well as BiP (HSPA5) can be found in the mature human erythrocyte (D'Alessandro et al., 2010).

1.4.4 Is HsHsp70 exploited by *P. falciparum*?

It is well established that bacteria and viruses often use components of the host cell e.g. Hsp70 for their own purposes (Agostini et al., 2000; Awe et al., 2008). The chaperones DnaK and DnaJ, *E.coli* Hsp70 and Hsp40, were first identified as pivotal components of λ phage (bacteria virus) replication (Konieczny and Zylicz, 1999). There are also several indications that *Plasmodium* might exploit the host's Hsp70. A study conducted in 1991 by Gromov and Celis found Hsp70 to be membrane-bound in *P. knowlesi* infected erythrocytes (Gromov and Celis, 1991). Moreover, HsHsp70 and HsHsp90 were revealed to be recruited to the host membrane upon infection with *P. falciparum* (Banumathy et al., 2002). Interestingly, HsHsp70 was a member of a large complex with PfHRP1 (knob-associated protein) at the RBC membrane (Banumathy et al. 2002). In consequence, it was speculated that HsHsp70 was probably associated with knob formation or the transport of knob components (Banumathy et al., 2002). Indeed, a very recent study analysing the knob proteome, presented HsHsp70 as a so far unknown component of the knobs (Alampalli et al., 2018). In addition, a number of studies investigated whether parasite-encoded and exported Hsp40 might serve as co-chaperones of HsHsp70. Before it was known that the parasite itself exports Hsp70x, it was already speculated by Külzer et al. that the exported

PfHsp40 (PFE0055c or PFE55) interacts with HsHsp70 (Külzer et al., 2010). In 2017, a proteomic analysis by Zhang and colleagues investigated the J-dot proteome and showed HsHsp70 to be present in a complex amongst PFE55 and Hsp70x (Zhang et al., 2017). Additionally, experimental data obtained by a yeast-two hybrid screen identified exported Type II PfHsp40 as an interaction partner of HsHsp70 (Jha et al., 2017). Further evidence that a human chaperone acts as a motor force during the export of parasite proteins was obtained by pull-down assays of PTEX components (de Koning-Ward et al., 2009). These data can be supported by studies conducted by Dr. Stefan Charpian, which demonstrated that HsHsp70 is linked to the *trans*-side of the PVM (Charpian, 2008). In conclusion, it can be assumed that HsHsp70 is involved in assisting parasite-encoded proteins to pass the PTEX translocon and supporting experimental evidence was obtained. The translocation assay performed by Ansorge and colleagues already showed that a component in the host cell cytoplasm is needed for transport across the PVM (Ansorge et al., 1996). Remarkably, the addition of an excess amount of mutated Hsp70 to the host cell cytoplasm prevented the transport of the parasite-encoded protein GBP130 (Glycophorin-Binding Protein 130) (Günnewig, 2016). Taken together, all these data point towards a crucial role of HsHsp70 in the trafficking of parasite-encoded proteins.

1.5 Aim of the study

Based on the aforementioned data, the objective in this study was to investigate whether HsHsp70 has an essential role for the intra-erythrocytic development of the parasite. The mature human erythrocyte cannot be easily genetically modified, thus a new approach was needed to study the effect of HsHsp70 for parasite survival. In pharmacology, pre-loading also known as resealing, is used to allow the entrapment of small molecules into the mature erythrocyte (Bourgeaux et al., 2016; Magnani et al., 1998, 2002; Rossi et al., 2005). This method uses the pre-loaded erythrocytes as “carriers” for drugs, thereby avoiding degradation of the drug and ensuring biocompatibility if used erythrocytes originate from the identical patient in need of treatment (Bourgeaux et al., 2016; Magnani et al., 1998, 2002; Rossi et al., 2005). In this study, a resealing

approach was implemented and erythrocytes were pre-loaded with an excess amount of a mutated HsHsp70 to achieve a classical dominant negative effect. To this end, the inactive HsHsp70^{K71M} mutant was chosen. The K71M mutation, within the NBD of the chaperone, disrupts the chaperone's ability to hydrolyse bound ATP and renders it inactive (O'Brien et al., 1996). After establishing the resealing method, the resealed red blood cells (rRBC) pre-loaded with HsHsp70^{K71M} were infected with *P. falciparum* parasites. Further controls, e.g. rRBC pre-loaded with no protein and rRBC pre-loaded with a functional HsHsp70^{wt}, were used to compare growth rates in the presence of the HsHsp70^{K71M} mutant. The growth was analysed by lactate dehydrogenase assays and flow cytometry. Additionally, the localisation of HsHsp70 in the non-infected as well as in the infected erythrocytes was studied. Therefore, resealing assays with a fluorescently labelled HsHps70^{wt} were carried out. First, the localisation was determined in non-infected erythrocytes before these fluorescently labelled HsHsp70^{wt} rRBC were infected with *P. falciparum*.

2 Material and methods

2.1 Materials

2.1.1 Disposable consumables

If not stated differently all used disposable plastic ware, e.g. pipette tips, serological pipettes and falcons, was purchased from: Sarstedt (Hamburg), Greiner Bio-one (Frickenhausen), VWR (Darmstadt), Miltenyi Biotec (Bergisch Gladbach), Roth (Karlsruhe) or Eppendorf (Hamburg).

2.1.2 Chemicals

If not stated differently all used chemicals were purchased from: Sigma Aldrich (Taufkirchen), Peqlab (Erlangen), Roth (Karlsruhe), Applichem (Darmstadt), ThermoFisher (Dreieich) or Merck (Darmstadt).

2.1.3 Dyes

Table 1 List of used dyes with corresponding manufacturer

Name	Purpose and used concentration/dilution	Company
Cy2 succinimidyl ester	Labelling of HsHsp70: 0.3 mg dye/2.8 mg protein	ThermoFisher (Dreieich)
DAPI	IFA, flow cytometry: 1 µg/mL	Sigma (Taufkirchen)
Oregon green carboxylic-acid, succinimidyl ester	Labelling of HsHsp70: 0.3 mg dye/2.8 mg protein	ThermoFisher (Dreieich)
Rhodamine B-isothiocyanate-Dextran	Resealing: 40 mg/mL	Sigma (Taufkirchen)
SYBR green	Flow cytometry: 1:2000	Sigma (Taufkirchen)

2.1.4 Equipment

Table 2 List of used equipment with corresponding manufacturer

Equipment	Company
Centrifuge 5415R	Eppendorf (Hamburg)
Centrifuge 5417C	Eppendorf (Hamburg)
Centrifuge 5417D	Eppendorf (Hamburg)
Centrifuge Labofuge 400e	Heraeus (Hanau)
Centrifuge Mikro 220R	Hettich (Tuttlingen)
Centrifuge Universal 320	Hettich (Tuttlingen)

Citation 3 Imaging Reader	BioTek, (Bad Friedrichshall)
CO_2 Inkubator C200	Labotec (Göttingen)
FACS Canto	BD (Franklin Lakes, USA)
Heatblock DB1010	Alpha Labs (Hampshire)
HERAsafe HS 12	Heraeus (Hanau)
Light microscope Aixostar plus	Carl Zeiss (Göttingen)
Light microscope Primo Star	Carl Zeiss (Göttingen)
Lumat LB9507 luminometer	Berthold Technologies (Bad Wildbad)
Magnetic stirrer	IKA (Staufen)
pH-Meter GPRT 1400N	Greisinger Electronic GmbH (Regenslauf)
Power supply EPS 301	Amersham pharmacia biotech (Amersham, GB)
Precision balance portable	Sartorius (Göttingen)
Rolling Mixer TRM50	MAGV (Rabenau)
Semi-Dry Blotter	IDL (Nidderau)
Thermomixer 5436	Eppendorf (Hamburg)
Typhoon FLA 7000	Amersham GE Healthcare (Chalfont St Giles, GB)
VarioMACS	Milteny Biotec (Bergisch-Gladbach)
Waterbath Köttermann	Köttermann (Uetze)
Waterbath U3	Julabo (Seelbach)

2.1.5 Cell culture media

Table 3 Composition of used cell culture media

Media type	Composition
Adherent cells	
DMEM complete	DMEM 500 mL (Gibco, Karlsruhe) 10% FCS (CC Pro, Oberdorla) 0.5 mg Streptomycin (CC Pro, Oberdorla) 100 U Penicillin (CC Pro, Oberdorla)
DMEM incomplete	DMEM 500 mL (Gibco, Karlsruhe) 0.5 mg Streptomycin (CC Pro, Oberdorla) 100 U Penicillin (CC Pro, Oberdorla)
Plasmodium falciparum	
RPMI	RPMI 1640 500 mL (Gibco, Karlsruhe) 10% Human Plasma 0^+ 50 mg Neomycin (Sigma, Taufkirchen) 0.2 mM Hypoxanthine (CC Pro, Oberdorla)
RPMI-Albumax	RPMI 1640 500 mL (Gibco, Karlsruhe) 5% Human Plasma 0^+ 5% AlbuMAX II (Gibco, Karlsruhe) in

	RPMI 1640 50 mg Neomycin (Sigma, Taufkirchen) 0.2 mM Hypoxanthine (CC Pro, Oberdorla)

2.1.6 Bacteria media

Table 4 Composition of used bacteria media

Media	Ingredients
Luria-Bertani (LB) Agar	35 g/L LB agar
SOB medium	20 g/L Peptone 5 g/L Yeast extract 10 mM NaCl 2.5 mM KCl 20 mM $MgCl_2$
SOC medium	SOB medium 20 mM $C_6H_{12}O_6$
Super broth medium	35 g/L Tryptone 20 g/L Yeast extract 5 g/L NaCl

2.1.7 Cell culture reagents

Table 5 List of used cell culture reagents with corresponding manufacturer

Reagent	Company
Human plasma and erythrocytes, blood group 0, Rhesus factor +	Blood donation centre, Mannheim
Lipofectamine RNAiMAX	ThermoFisher (Dreieich)
Opti-MEM	ThermoFisher (Dreieich)
siRNA	
HSPA1A pre-designed siRNA (s6965)	Ambion ThermoFisher (Dreieich)
Silencer Select, Negative siRNA (AS029YZ6)	Ambion ThermoFisher (Dreieich)
WR99210	Jacobus Pharamaceuticals, (Princeton, USA)

2.1.8 Cell lineages

Table 6 List of used cell lineages

Strain	Description	Origin
Human		
HuH7	Immortalized hepatocellular carcinoma cell line (Nakabayashi et al., 1982)	Kind gift from AG Müller, Parasitology, Heidelberg

Parasite		
P. falciparum		
3D7 wildtype	Wildtype, Clone of NF54 (Walliker et al., 1987)	AG Przyborski, Parasitology
3D7-ΔPfHsp70x	Parasites deficient of PfHsp70x	Kind gift from Brendan Crabb, Burnet Institute, Australia
3D7-HsHsp70-mCherry	Parasites express a STEVOR 1-80-mCherry-HsHsp70 fusion protein	Produced during the thesis (construct: AG Przyborski, Parasitology)
P. berghei		
ANKA-red-green line	Parasites express mCherry under the CS promoter, while GFP is expressed under the ef1α promoter	Kind gift from AG Frischknecht, Parasitology
Bacteria		
E. coli BL21-Rosetta (DE3)	Expression strain	Kind gift from AG Mayer, ZMBH, Heidelberg

2.1.9 Protein size marker

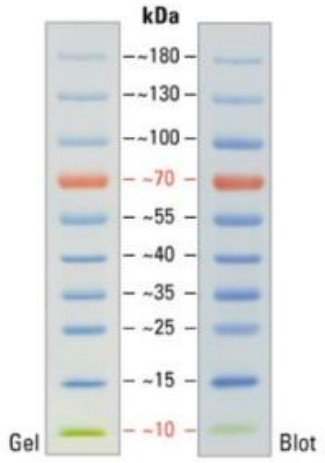

Figure 7 PageRuler Prestained protein ladder (ThermoFisher)

2.1.10 Vector maps

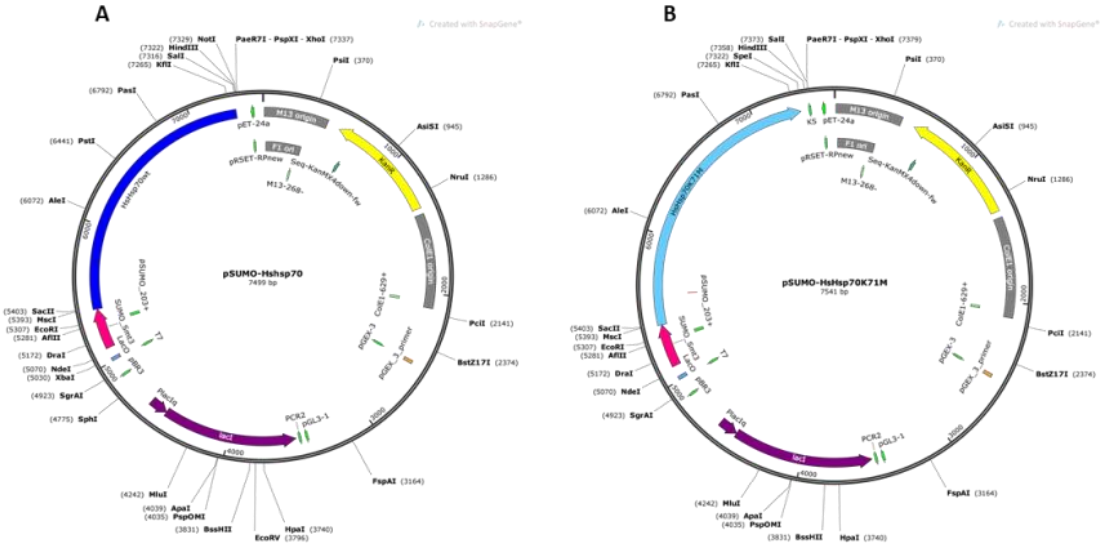

Figure 8 Expression vectors for HsHsp70^{wt} and HsHsp70^{K71M}
(A) pSUMO-HsHsp70^{wt}
(B) pSUMO-HsHsp70^{K71M}
Both vectors were a kind gift from AG Mayer, ZMBH, Heidelberg and express a 6xHis-tag fused to SUMO-tag and HsHsp70^{wt} or HsHsp70^{K71M}.

2.1.11 Antibodies

Table 7 List of primary antibodies

Name	Origin	Dilution	Manufaturer
α-Aldolase	Rabbit	WB: 1:5000	AG Przyborski
α-DnaK	Mouse	WB: 1:2000	Abcam (Cambridge, UK)
α-GAPDH	Mouse	WB: 1:500	Sigma (Taufkirchen)
α-Glycophorin A&B	Mouse	WB: 1:1000	AG Przyborski
α-HsHsc70	Mouse	WB: 1:1000	StressMarq (Victoria, British Columbia)
α-HsHsp70	Mouse	WB: 1:500	Santa Cruz (Heidelberg)
α-Ovalbumin	Rabbit	WB:1:500	AG Przyborski
α-PfHsp70x	Rabbit	WB: 1:500 IFA: 1:500	AG Przyborski
α-PfSBP1	Rabbit	WB: 1:1000 IFA: 1:500	AG Przyborski
α-RFP	Mouse	IFA: 1:500	Rockland (Limerick, USA)

Table 8 List of secondary antibodies

Name	Western blot IFA	Origin	Dilution	Company
α-mouse-Cy2	IFA	Goat	1:2000	Jackson (West

				Grove, USA)
α-mouse-Cy3	IFA	Goat	1:2000	Jackson (West Grove, USA)
α-mouse-HRP	WB	Goat	1:2000	Dako (Glostrup, Denmark)
α-rabbit-Cy2	IFA	Goat	1:2000	Jackson (West Grove, USA)
α-rabbit-Cy3	IFA	Goat	1:2000	Jackson (West Grove, USA)
α-rabbit-HRP	WB	Goat	1:2000	Dako (Glostrup, Denmark)

2.1.12 Buffers

Table 9 Compostion of buffers

Buffer	Ingredients
Ammonium peroxidsulfate (APS)	10% APS in ddH_2O
ATP	100 mM ATP pH 7 (NaOH) in ddH_2O
Blocking solution IFA	3% Bovine serum albumin in PBS (1x)
Blocking solution WB	5% milk powder in PBS (1x)
Blotting buffer (1x)	48 mM Tris HCl pH 9.5 39 mM Glycine 0.04% SDS 20% MeOH (add fresh) in ddH_2O
Coomassie Blue staining solution	25% MeOH 10% Acetic acid 0.1% Coomassie Brilliant Blue in ddH_2O
Coomassie destain	25% MeOH 10% Acetic acid in ddH_2O
Cytomix stock solutions	<u>Stock solution I</u> 10 M KOH in ddH_2O <u>Stock solution II</u> 250 mM HEPES 20 mM EGTA pH 7.6 with stock solution I <u>Stock solution III</u> 1 M Phosphate Buffer pH 7.6 in ddH_2O <u>Cytomix (100 mL)</u> 120 mM KCl 150 µM $CaCl_2$ 1 mL Stock solution III 10 mL Stock solution II 5 mM 1 M $MgCl_2$

D-Sorbitol	5% D-Sorbitol autoclaved before use in S2
ECL	250 mM Luminol in DMSO 90 mM P. commaric acid in DMSO 1 M Tris HCl pH 8.5 in ddH_2O
Fixation solution	4% PFA 0.0075 % Glutaldehyde in PBS (1x)
Freezing solution	28% Glycerol 3% D-Sorbitol 0.65% NaCl in ddH_2O, autoclaved before use in S2
LDH buffer	100 mM Tris HCl pH 8 50 mM Sodium-Lactate 0.25%Triton-X-100 in ddH_2O
Luciferase Refolding Assay	<u>Refolding Buffer</u> 25 mM HEPES KOH pH 7.6 100 mM KOAc 10 mM $Mg(OAc)_2$ 2 mM ATP pH 7 5 mM DTT in ddH_2O <u>Assay Buffer</u> 100 mM Phosphate Buffer pH 7.6 25 mM Glycly-glycine pH 7.4 100 mM KOAc 15 mM Mg(OAc)2 5 mM ATP pH7 in ddH_2O
PBS (10x)	1.4 M NaCl 28 mM KCl 83 mM K_2HPO_4 19 mM KH_2PO_4 pH 7.4, in ddH_2O
Ponceau	0.2% Ponceau S 3% Trichloroacetic acid in ddH_2O
Protein purification buffers	<u>Lysis buffer</u> 20 mM Tris HCl pH 7.9 100 mM KCl 1 mM PMSF (added before lysis) 1 mM Pepstatin (added before lysis) 1 mM Leupetin (added before lysis) 1 mM Aprotitin (added before lysis) in ddH_2O <u>Buffer A1</u>

	20 mM Tris HCl pH 7.9 100 mM KCl in ddH_2O <u>Buffer A2</u> 20 mM Tris HCl pH 7.9 1 M KCl in ddH_2O <u>Buffer B</u> 20 mM Tris HCl pH 7.9 100 mM KCl 250 mM Imidazol in ddH_2O <u>ATP Buffer</u> 40 mM Tris HCl pH 7.9 100 mM KCl 5 mM MgCl 5 mM ATP in ddH_2O <u>Buffer C</u> 40 mM HEPES KOH pH 7.6 10 mM KCl 5 mM $MgCl_2$ in ddH_2O <u>Buffer D</u> 40 mM HEPES KOH pH 7.6 10 mM KCl 5 mM $MgCl_2$ 10 mM beta-mercaptoehtanol 5% Glycerol in ddH_2O <u>Buffer E</u> 40 mM HEPES KOH pH 7.6 1 M KCl 5 mM MgCl 5% Glycerol in ddH_2O <u>Buffer F</u> 40 mM HEPES KOH pH 7.6 50 mM KCl 5 mM $MgCl_2$ 10 mM beta-mercaptoethanol 10% Glycerol in ddH_2O

Quencing solution	125 mM Glycine 1% Triton X in PBS (1x)
RIPA buffer	50 mM Tris HCl pH 7.5 1% Triton-X 0.1% SDS 5 mM EDTA 150 mM NaCl 50 mM NaF 0.5% NaDOC in ddH_2O
SDS running buffer (5x)	124 mM Tris 960 mM Glycin 0.05% SDS in ddH_2O
SDS-loading dye (2x)	100 mM Tris HCl pH 6.8 5 mM EDTA 20% Glycerol 4% SDS 0.2% Bromophenol blue 100 mM DTT in ddH_2O
Separating buffer (Tris-HCl pH 8.8)	1.5 M Tris HCl pH 8.8 0.4% SDS in ddH_2O
Stacking buffer (Tris-HCl pH 6.8)	500 mM Tris HCl pH 6.8 0.4% SDS in ddH_2O
Thawing solutions	<u>Solution I</u> 12% NaCl in ddH_2O <u>Solution II</u> 1.6% NaCl in ddH_2O <u>Solution III</u> 0.9% NaCl 0.2% $C_6H_{12}O_6$ in ddH_2O
WR 99210	20 mM WR99210 in DMSO Final concentration:2.5 nM

2.2 Methods

2.2.1 Cell culture techniques for human adherent cells: HuH7

2.2.1.1 *In vitro* culturing of human adherent cells

Cell culturing of human adherent cells (HuH7, liver carcinoma cells) was performed under sterile conditions and cells were maintained at 60-80% confluency. The standard culture medium DMEM was supplemented with 10% FCS, 100 U penicillin and 0.5 mg streptomycin. Cultures were kept at 37°C and 5% CO_2.

2.2.1.2 Splitting and counting of adherent cells

Every 2-3 days cells were splitted for continuous culturing or the desired number of cells was inoculated for experiments such as transfection. A confluent culture was first washed using DMEM media without any supplements. Afterwards, 6 mL trypsin/EDTA (1x) per T75-flask was added to detach cells from the culture flask. The trypsin/EDTA was incubated for 3 min at 37°C. Next, cell detachment was confirmed using an inverted microscope. To inactivate the trypsin/EDTA an equal amount of standard culture media (including FCS) was added. Subsequently, cells were centrifuged at 800xg for 2 min. The pellet was resuspended in the desired volume of standard cell media for splitting and transferred to a fresh flask with 12 mL standard medium per T75-flask. For counting, the pellet was resuspended in 10 mL culture medium (for T75-flask). The completely resuspended cells were mixed in a 1:1 ratio with trypan blue (0.04% in PBS) and 10 µL were applied to a Neubauer counting chamber. Cells present in 4 big squares were counted and the total cell number was calculated using the formula shown below.

$$\textbf{Cell number/mL} = \frac{counted\ number\ of\ 4\ squares}{4} * Dilution\ factor * 10^4$$

Table 10 contains numbers of seeded cells for the different culture flasks.

Table 10 Cell numbers seeded for different culture flasks

	24 well plate	96 well plate
Cm^2	1	0.2
Cell number	30,000 cells	10,000 cells

2.2.1.3 Thawing of human adherent cells

After 15 passages the cells usually started to grow slower and transfection efficiencies were reduced. To avoid such behaviour cultures were replaced with a freshly thawed aliquot after 15 passages. To this end, cells were allowed to thaw at 37°C and were subsequently transferred to a falcon containing 10 mL pre-warmed DMEM standard medium. Then, cells were centrifuged at 800xg for 2 min and washed once in standard media. Finally, a fresh culture flask was inoculated with the cells and grown at 37°C with 5% CO_2.

2.2.1.4 Freezing of human adherent cells

To preserve cells, a confluent flask was trypsinised as explained in 2.2.1.2. Afterwards, the pellet was resuspended in 200 µL 20% DMSO in DMEM, 200 µL 50% FCS in DMEM and cells were stored at -80°C.

2.2.1.5 siRNA transfection

A siRNA downregulation of HsHsp70 in HuH7, a liver carcinoma cell line, was used to investigate the role of HsHsp70 in parasite survival. The Lipofectamine RNAiMAX tranfection kit from ThermoFisher Scientific was used for this purpose. Transfection was conducted as described in the instruction manual with some slight variations explained in the following. Two pre-designed siRNAs, one directed against HsHsp70 (HSPA1A) and one scrambled RNA (scraRNA), were ordered from ThermoFisher Scientific. A reverse transfection, which means first DNA was added and afterwards the cells were added on top, was performed to introduce the siRNA into the cells. The following Table 11 shows a typical transfection in 96 and 24 well plates (volume/well).

Table 11 Transfection of HuH7 cells in 96 and 24 well plates

		96 well plate	24 well plate
Tube A	OptiMem media	10 µL	50 µL
	Lipofectamine RNAiMAX	0.6 µL	3 µL
Tube B	OptiMem media	10 µL	50 µL
	siRNA (10 µM)	0.2 µL	1 µL

After preparation of mastermixes, tube A and B were mixed and incubated at RT for 20 min. In the meantime, the cells were trypsinised and counted. Then, the lipofectamine siRNA mix was pipetted into each well (10 µL/96 well plate and 50 µL/24 well). Subsequently, the HuH7 cells, diluted in media without Pen/Strep, were evenly distributed on the plate. For a 24 well plate 30,000 and for a 96 well plate 10,000 cells/well were used. After 12-18 h the medium was replaced with DMEM complete containing Pen/Strep. Two days post-transfection *Plasmodium berghei* sporozoites (numbers and dissection explained in 2.2.1.6) were added and the western blot samples were taken to check the downregulation.

2.2.1.6 Dissection of *Anopheles* mosquitoes

In order to study the role of HsHsp70 on liver stage development of *P. berghei*, red-green sporozoites were used to infect the HsHsp70 downregulated HuH7 cells. The parasites express mCherry under the CS promoter, while GFP is expressed under control of the e1fα promoter (kind gift from AG Frischknecht). First, mice were infected with the help of frozen parasite stabilates. Due to the lack of a FELASA certificate for the author, infection experiments were performed by Jessica Kehrer (AG Frischknecht, Parasitologie). Once mice were infected and showed exflagellating gametocytes, mosquitoes were allowed to take a blood meal from the infected mice. The infection of the mosquitoes and all dissections were executed under S3 conditions. 17 days post-infection, the salivary glands were dissected to obtain sporozoites. With the help of a bottle of warm H_2O female mosquitoes were attracted to one side of the cage and were sucked in a tube using a small pump. Afterwards, mosquitoes were carefully transferred to a falcon and placed on ice for several minutes for immobilisation. The narcotised mosquitoes were placed on a slide with one drop of PBS and examined under a binocular microscope. Using 2 cannulas of different sizes the 6 legs of the

mosquito were removed. Afterwards, the bigger cannula was used to carefully secure the thorax of the mosquito, applying not too much pressure to avoid injuries of the thorax, which would contaminate the salivary glands dissection. The smaller cannula was used to apply pressure on the head, which was pulled slowly to the side. Salivary glands appeared shiny under the microscope and the head was in the final step removed from the glands. Depending on the infection rate, up to 100 mosquitoes were dissected to gain 500,000 sporozoites. After dissection, salivary glands were transferred to an Eppendorf tube and smashed with the help of a small plastic pestle to release sporozoites from the glands. The mixture was then applied to a cell strainer (0.2 µm) to separate the glands from the sporozoites and was centrifuged at 2,100xg for 2 min. Next, the supernatant was smashed and centrifuged again. The number of sporozoites per mL was determined using a Neubauer chamber. The dissection was performed with the help of Marta Marchado (AG Ganter, Parasitology). Finally, sporozoites were diluted to the desired number in DMEM complete medium and were allowed to infect HuH7 cells for 2 h. For a 24 well plate with 30,000 Huh7 cells, 40,000 sporozoites were added and for a 96 well plate with 10,000 HuH7 cells, 10,000 sporozoites were added. In the end, the media was changed every day and liver stages were analysed 48 h post-infection by flow cytometry.

2.2.2 Cell culture techniques for *Plasmodium falciparum*

2.2.2.1 *In vitro* culturing of *Plasmodium falciparum*

Cell culturing was performed under a lamina flow and cultures were cultivated in 4% haematocrit with RPMI 1640 medium supplemented with 10% human 0^+ plasma, 50 mg neomycin and 0.2 mM hypoxanthine (Trager and Jensen, 1976). All parasite cultures were maintained at 5% CO_2, 5% O_2 at 37°C in an incubator.

2.2.2.2 Giemsa staining of blood smears

Blood smears were prepared and stained using giemsa staining solution to monitor the parasitemia of the cultures. Therefore, a 5 µL sample of a culture was taken and a thin smear was prepared on a slide. Afterwards, the smear was fixed

for several seconds in 100% methanol. Thereafter, the slide was air dried and placed in giemsa staining solution (1:5 dilution in H_2O) for 10 min. The slide was rinsed with water and air-dried. Finally, the slide was analysed under the light microscope at 63x objective magnification with oil immersion.

2.2.2.3 Freezing of *P. falciparum*

In order to conserve parasite lines, a culture with high parasitemia around 10%, containing mainly ring stages, was centrifuged for 3 min at 2,100xg. The pellet was resuspended in the equal pellet volume of freezing solution and aliquoted (~500 µL/cryotube) to cryotubes. Subsequently, parasites were frozen in liquid nitrogen and stored at -80°C.

2.2.2.4 Thawing of *P. falciparum*

Stocks of parasite lines were thawed at 37°C, before slowly and gently mixing the freshly thawed parasites with 250 µL of pre-warmed 12 % sterile NaCl. After a 2 min rest, parasites were transferred to a 15 mL falcon and 5 mL pre-warmed 1.6% sterile NaCl was added dropwise. Followed by another 2 min rest, 5 mL of 0.2% glucose/0.9% NaCl was added dropwise. Afterwards, the parasites were centrifuged at 2,100xg, the supernatant was removed and parasites were washed in 10 mL culture media. Finally, the parasite pellet was filled up with fresh 0^+ blood (up to 500 µL) and 12 mL culture medium was added. Depending on the parasite line the appropriate antibiotic was added and parasites were maintained at 5% CO_2 and 5% O_2 at 37°C.

2.2.2.5 Synchronisation of *P. falciparum in vitro* culture by sorbitol

A synchronous *P. falciparum* culture is obtained by applying a sorbitol treatment, since trophozoites and schizonts are ruptured by sorbitol (Lambros and Vanderberg, 1979). Therefore, a mixed culture was transferred to a 15 mL falcon and centrifuged for 2 min at 2,100xg. Afterwards, the pellet was resuspended in the 10 times pellet volume with 5% sterile sorbitol. After an incubation of 10 min at 37°C, the parasites were centrifuged at 2,100xg for 2 min and washed in 10

mL culture medium. Finally, the pellet was resuspended in 12 mL culture medium.

2.2.2.6 Enrichment of *P. falciparum* trophozoites

In vitro P. falciparum cultures cannot reach a parasitemia above 10%. Therefore, some experiments require an enrichment to reach higher parasitemia. There are 2 methods to enrich parasites, a gelafundin treatment or Magnetic Activated Cell Sorting (MACS). In the following both techniques are explained in detail.

2.2.2.7 Trophozoite enrichment by gelafundin

Non-infected erythrocytes can be separated from infected ones using gelafundin (Pasvol et al., 1978). The infected erythrocytes contain so-called knobs that were introduced to the host cell shortly after infection with *Plasmodium*. If a culture is mixed with gelafundin non-infected erythrocytes sink to the bottom of the tube, while the infected erythrocytes stay longer in the supernatant. In consequence, the gelafundin treatment achieves 2 goals. First, it enriches the parasites and secondly, it helps to ensure that the *in vitro* culture still contains “knobby” parasites, as parasites tend to loose these knob structures under culture conditions (Langreth et al., 1979). Usually, a culture high in trophozoites was pelleted at 2,100xg for 2 min. Afterwards, the pellet was resuspended in the 10 times pellet volume with a 2.5% gelafundin solution (diluted in RPMI without any supplements). The falcon was incubated for 12-15 min in vertical position at 37°C. Finally, the supernatant was transferred to a fresh falcon, washed 2 times in culture medium and the parasitemia was determined via giemsa smears. In the end, a fresh plate with media and blood was inoculated with the desired parasitemia.

2.2.2.8 Magnetic Activated Cell Sorting (MACS) of *P. falciparum*

Magnetic activated cell sorting (MACS) allows the efficient enrichment of parasites, often leading to a 99% parasitemia. It exploits the formation of magnetic hemozoin crystals by the parasite as a result of its usage of

haemoglobin as a nutritional source, and its heme detoxification pathway (Kim et al., 2010). Therefore, only infected cells are held back to the column, which is attached to a big magnet and finally parasites can be eluted by removing the column from the magnetic field. All parasite enrichments using MACS were performed with 10% trophozoite cultures. The MACS column was equilibrated with 4 column volumes of pre-warmed PBS, followed by 4 column volumes of pre-warmed 3% BSA in RPMI during which the drop rate was set to 1 drop/s. Then, the parasites were applied to the column and the flow through was collected. After the first passage, the collected flow through was added a second time. Next, the column was washed with 3% BSA in RPMI until the flow through was not reddish any longer. Finally, the parasites were eluted by removing the column from the magnetic field and adding culture media. The eluate was centrifuged at 2,100xg for 2 min. The parasitemia was checked by giemsa smears.

2.2.2.9 Transfection of *P. falciparum*

Transfections were performed by electroporation, a technique that applies an electrical field to the parasite to increase membrane permeability and thereby allows the introduction of foreign DNA into the cell (Waters et al., 1997). Plasmid DNA was isolated and precipitated according to the QIAGEN Maxi Prep Kit instructions. A highly synchronous *P. falciparum* culture with a parasitemia of 5% and mainly ring stages was used for transfection. First, 500 µL (~100 µg) plasmid DNA was precipitated with the double volume of ice cold 100% ethanol and 10% 5 M sodium acetate (pH 5.2). The sample was centrifuged for 15 min at 36,000xg at 4°C. The supernatant was removed carefully and the pellet was washed in 500 µL 75% ice cold ethanol in ddH_2O. The supernatant was removed under sterile conditions and the pellet was carefully air-dried. Next, 30 µL TE buffer (pre-warmed to 50°C) was added to the pellet and the pellet was allowed to dissolve for 10 min at 50°C with shaking. In the meantime, a falcon with 12 mL albumax medium and 400 µL freshly obtained 0^+ blood (haematocrit 100%) was prepared and pre-warmed at 37°C. Next, a 400 µL aliquot of cytomix was pre-warmed at 37°C. After the pellet had completely dissolved, 370 µL of cytomix was added and well mixed with the DNA. Then, 200 µL of infected erythrocytes were added

and mixed well. The mixture was transferred to a 0.2 cm electroporation cuvette and electroporation was conducted at a voltage of 0.310 kV and a capacity of 950 µF, resulting in a time constant between 10-13 ms. Subsequently, the transfected cells were carefully transferred to the prepared falcon with Albumax medium and 0^+ blood. The cuvette was washed several times with the Albumax/blood mixture. The transfected culture was placed in a small culture dish and allowed to rest for the next 4-6 h. Finally, the culture was supplied with the appropriate selective agent. The used medium was exchanged daily with fresh medium and 20 µL of fresh human 0^+ erythrocytes were added until all parasites were killed. Afterwards, twice a week the culture was monitored for growth by giemsa smears and fresh medium, 20 µL fresh human 0^+ erythrocytes, the respective selective agent was added. Once parasites were detected and parasitemia reached 2% the culture was spilt and transfected strains were cryopreserved.

2.2.3 Methods of protein biochemistry

2.2.3.1 Transformation of *E. coli*

Foreign DNA is introduced into *Escherichia coli* (*E. coli*) in a process called transformation. The electrocompetent cells were slowly thawed on ice and 1 µL of plasmid DNA was added to 50 µL of cells. Then, the mixture was pipetted into a 0.2 cm electroporation cuvette and electroporation was performed at 2.5 kV, 25 µF and 200Ω. Subsequently, the cells were mixed with 1 mL SOC-medium and grown for 1 h at 37°C. Finally, bacteria were plated on LB agar with the required antibiotics and incubated at 37°C overnight.

2.2.3.2 Protein expression

The plasmids for recombinant protein expression and purification of $HsHsp70^{wt}$ and $HsHsp70^{K71M}$ were a kind gift from Prof. Mayer, ZMBH Heidelberg, and protein purification was performed in collaboration with the Mayer lab at the ZMBH. First, plasmids were introduced into *E. coli* Rosetta (DE 3) competent cells (provided from the research group Mayer) and plated on LB plates containing kanamycin (50 µg/mL) and chloramphenicol (50 µg/mL). On the next

day, 100 mL fresh SB medium with kanamycin (50 µg/mL) and chloramphenicol (50 µg/mL) were inoculated with a colony and grown overnight at 37°C with 200 rpm agitation. Then, 8 L of fresh SB medium with kanamycin (50 µg/mL) and chloramphenicol (50 µg/mL) were inoculated to an OD_{600} of 0.05-0.1 with the overnight culture. The bacteria were grown at 37°C with 200 rpm agitation until an OD_{600} of 0.8 was obtained. Preceding induction, a small sample was taken as a non-induced control of protein expression. Protein expression was induced by addition of 1 mM IPTG and 0.3 M NaCl. Afterwards, cells were incubated overnight at 20°C with agitation at 200 rpm. The bacteria were harvested at 3,000xg for 20 min at 4°C. Finally, the bacterial pellet was frozen at -80°C. The success of protein expression was checked via SDS-PAGE and Coomassie staining.

2.2.3.3 Protein purification

The 2 proteins were expressed as N-terminal 6-His-SUMO-tagged proteins to obtain pure untagged $HsHsp70^{wt}$ and $HsHsp70^{K71M}$. To this end, both proteins were affinity-purified using Ni-NTA (nickel charged affinity resin) beads. The elution is performed by adding imidazole and the His-SUMO-tag is cleaved off by usage of the Ulp1-protease. Afterwards, Ni-NTA beads will retain the His-SUMO-tag in the column, while the tagless protein can be eluted. Finally, depending on the protein purity, the protein can be further purified by ion-exchange chromatography (Figure 9).

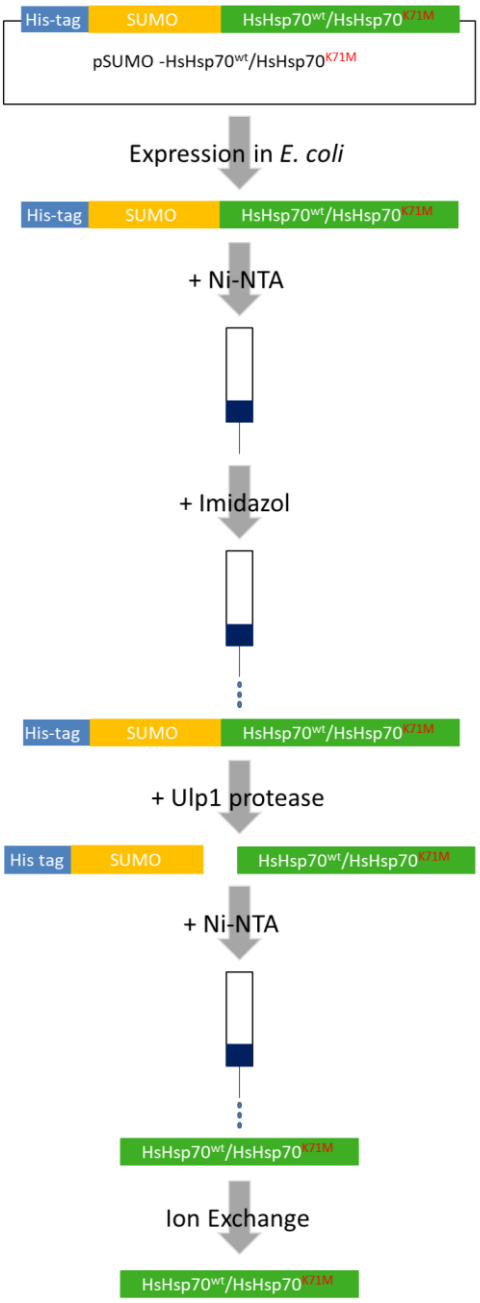

Figure 9 Schema of His-SUMO-tagged protein purification of HsHsp70^{wt} and HsHsp70^{K71M}
HsHsp70^{wt} and HsHsp70^{K71M} can be affinity-purified using Ni-NTA beads due to the N-terminal His-SUMO-tag. The elution is performed with imidazole. Afterwards, the N-terminal His-SUMO-tag is removed by cleavage with the Ulp1-protease and incubation with Ni-NTA beads. The purified protein can be found in the eluate. If needed protein purity can be increased by ion exchange chromatography.

All purification steps were performed on ice at 4°C to avoid protein degradation. The pellets were thawed on ice and 100 mL pre-cooled lysis buffer (with 1 mM pepstatin, 1 mM leupeptin and 1 mM aprototin) were added per 2 L of starting culture. Afterwards, the cells were lysed using a microfluidizer and centrifuged for 20 min at 20,000xg at 4°C. Then, the supernatant was centrifuged again for 2 h

at 100,000xg at 4°C. Afterwards, the supernatant was mixed with 5 mL Ni-NTA beads that were equilibrated against buffer A1 and incubated for 15 min at 4°C at end-over-end rotation. The mixture was transferred into a column. The column was first washed with 20 Column Volumes (CV) of buffer A1, afterwards with 20 CV of A2, then, with 2 CV of A1 again. Subsequently, 10 CV of ATP-buffer were added and after 2 CV had passed, a stop cock was applied to stop the flow. The ATP-buffer was incubated for 30 min at 4°C. After the wash with the ATP-buffer, the protein was eluted with double CV of buffer B. The purification was checked by SDS-PAGE and Coomassie staining. To cleave the His-tag off the protein, the eluates were pooled and the SUMO-protease Ulp1 was added during overnight dialysis against buffer C. On the next day, 1 mL Ni-NTA beads in buffer C was added and incubated for 15 min at 4°C at end-over-end rotation. Then, the mixture was applied to the column, the flow-through contained the pure-untagged $HsHsp70^{wt}$ or $HsHsp^{K71M}$. If required, the purity of the protein was further increased by ion exchange chromatography, using a Resource Q column (GE Healthcare). The column was equilibrated with buffer D and elution was achieved with a KCl gradient from 0-100% of buffer E. The flow rate was set to 1 mL/min and a fraction size of 0.5 mL was collected. Finally, fractions were screened for protein purity via SDS-PAGE followed by Coomassie staining. Protein fractions with high purity were pooled and dialysed against buffer F overnight. Protein concentration was determined and protein function was tested with the luciferase refolding assay. Afterwards, aliquots were frozen in liquid nitrogen and stored at -80°C.

2.2.3.4 Luciferase refolding assay

The firefly luciferase catalyses the conversion of luciferin to oxyluciferin, a reaction that is accompanied by the emission of light. If the luciferase is denatured, a functional Hsp70, Hsp40 and nucleotide exchange factor (NEF) are needed to refold the enzyme. The refolding process can then be visualised by the light emission that increases over time. A schematic overview of the luciferase refolding assay can be seen in Figure 10.

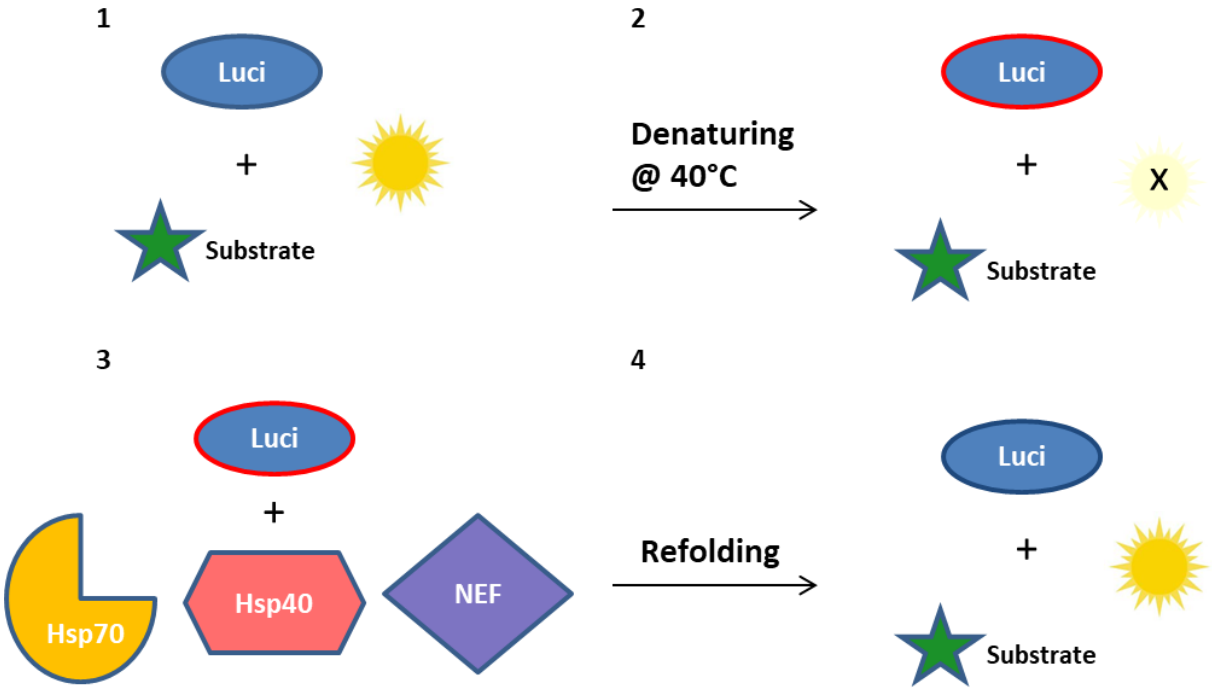

Figure 10 Schematic overview of the luciferase refolding assay
The firefly luciferase (luci) converts its substrate luciferin to oxyluciferin by which light is emitted **(1)**. If the firefly luciferase gets denatured by a short incubation at 40°C, the enzyme will be non-functional and no light will be emitted **(2)**. The luciferase's function can be restored by mixing the protein with a functional Hsp70, Hsp40 and nucleotide exchange factor (NEF) **(3)**, which leads to the refolding and light will be emitted again **(4)**.

In this thesis, the assay was used to test whether the 2 purified untagged proteins HsHsp70^{wt} and HsHsp70^{K71M} were functional and non-functional, respectively. First, it was tested whether the firefly luciferase was functional. For this purpose, 1 µL firefly luciferase was diluted in 124 µL refolding buffer (final concentration 80 nM firefly luciferase). Afterwards, luciferase activity was assessed by a luminometer by adding 1 µL of the luciferase sample to 124 µL of assay buffer. In advance to each measurement, the luminometer injected 125 µL 80 µM luciferin. $2*10^6$-10^6 RLU (relative light units) were measured and set as 100% for normalisation. Afterwards, the luciferase was incubated at 40°C for 10 min and the denaturing process was controlled by measuring the RLU. After denaturing ~10^4 RLU were set as the starting point (t_0). The 80 nM of the denatured firefly luciferase were either mixed with 2 µM purified-untagged HsHsp70^{wt} or the HsHsp70^{K71M} and additionally 1 µM Hdj1, 0.2 µM Apg2 (both kind gifts from the AG Mayer, ZMBH) were added to 125 µL refolding buffer. The control did not contain any of the 2 purified HsHsp70s. The samples were incubated at 30°C and measurements were done in triplicates after 5, 10, 20, 30, 45, 60 and, 90 min. For each measurement 1 µL sample was diluted in 124 µL assay buffer.

2.2.3.5 Dialysis

Before the purified proteins were used for a growth assay, the storage buffer containing harmful chemicals for the parasite, e.g. beta-mercaptoethanol, was dialysed against PBS. Only a small volume of the protein was needed and in consequence, a special dialysing method was established for this. A normal Eppendorf tube was opened and with the help of a heated glass pasteur pipette a small whole was inserted in the lid of the tube. Afterwards, the dialysis membrane (Spectra/Por Dialysis Membrane, MWCO: 6-8 kDa) was soaked for several minutes in ddH_2O. In the meantime, the protein was thawed on ice. Afterwards, the protein was transferred to the prepared Eppendorf tube and the dialysis membrane was pinched between the now “open” lid. Then, the Eppendorf tube was placed in a float and positioned in a beaker with PBS (1x) (100,000x more than protein volume). Before turning the float upside down, a little PBS was pipetted on the open lid to avoid air bubble formation. Finally, the protein was dialysed overnight in the cold room with a magnetic stirrer at a slow stirring speed.

2.2.3.6 Fluorescent labelling of HsHsp70

In order to study localisation of HsHsp70 in the non-infected as well as in infected erythrocytes, purified HsHsp70^{wt} was fluorescently labelled by coupling the protein to a dye. For the labelling either Cy2 or Oregon-green were used. Pure untagged HsHsp70 was dialysed overnight. 2.8 mg protein was mixed with 0.3 mg dye solved in 100% DMSO and incubated for 1 h in the dark. Afterwards, the PD Midi-Trap G-25 (GE, Healthcare) column was used to remove unbound dye according to the manufacturer’s instructions. Finally, the labelled proteins were separated on SDS-PAGE and protein labelling was controlled via a laser scanner at 488 nm.

2.2.3.7 Resealing

To assess the effect of HsHsp70 for parasite survival and development, erythrocytes were pre-loaded with an excess amount of a mutated HsHsp70-protein. This pre-loading method is called resealing and is widely used in the

pharmacology to pre-load erythrocytes with drugs. In this approach, the erythrocytes are used as “carriers” to deliver drugs to the target site and thereby minimising the risk of side effects of the drug (Bourgeaux et al., 2016; Magnani et al., 1998, 2002; Rossi et al., 2005). This method was exploited to gain erythrocytes that were fluorescently labelled and contained an excess amount of HsHsp70^{K71M}. The protocol was adapted from Frankland et al. 2006 and Bakar et al. 2010. In brief, erythrocytes were lysed via hypotonic lysis. Afterwards, the erythrocytes were mixed with a dye called rhodamine to label all cells that were successfully resealed. Furthermore, either the purified HsHsp70^{wt} or the HsHsp70^{K71M} was added or no protein, resulting in resealed RBC (rRBC) with HsHsp70$^{wt/K71M}$ or rRBC that were only pre-loaded with rhodamine (Figure 11).

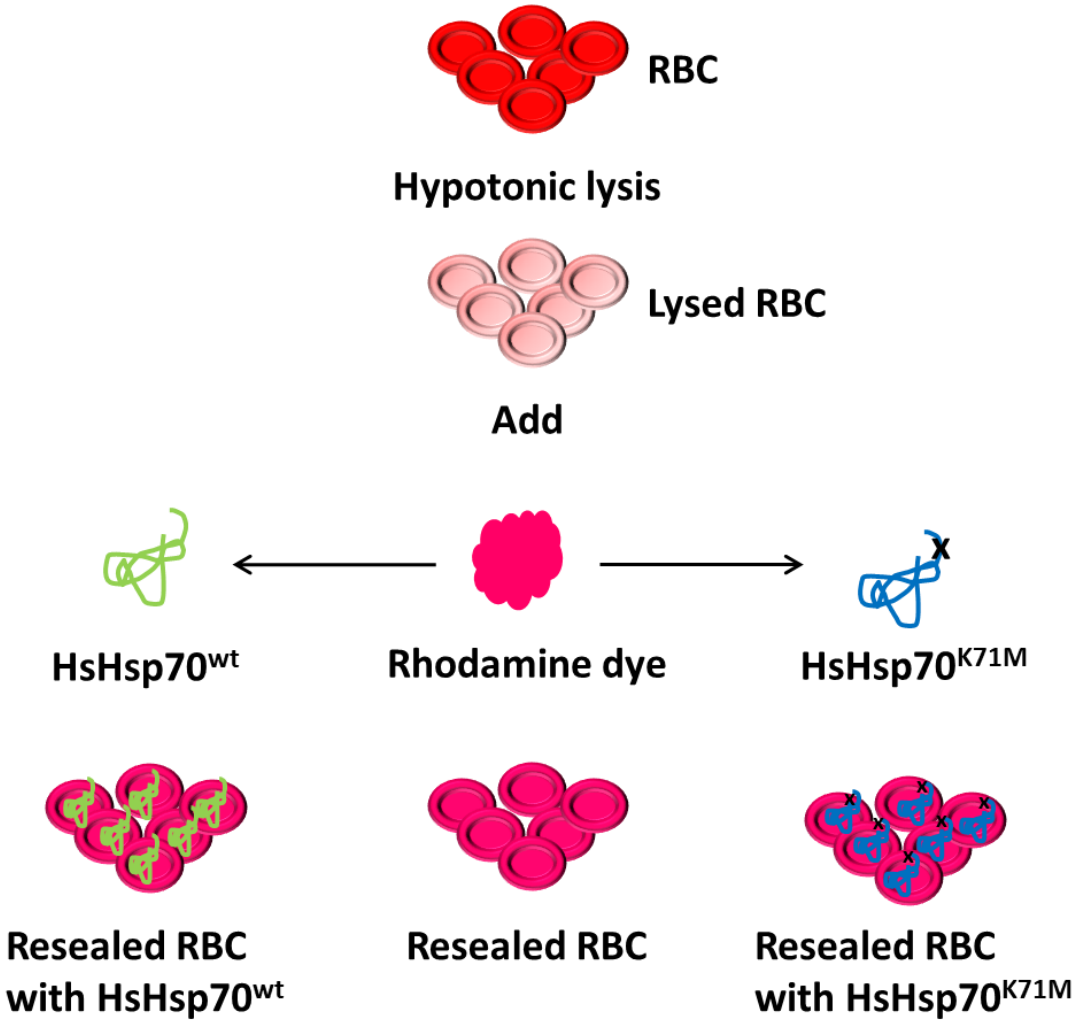

Figure 11 Overview of the resealing process
Fresh RBC were lysed by hypotonic lysis. Afterwards, the lysed cells were mixed with rhodamine to label cells that were resealed. Further, HsHsp70^{wt} or HsHsp70^{K71M} pure untagged protein was added. In the end, either resealed RBC containing rhodamine (middle) or resealed RBC pre-loaded with rhodamine and HsHsp70^{wt} (left) or HsHsp70^{K71M} were produced.

During the test phase it was noted that the resealing process worked the best with freshly obtained blood not older than 24 h. In consequence, all resealing experiments were performed with freshly obtained blood. First, an ice cold master mix was prepared containing 5 mM sodium phosphate buffer (pH 7.4) with 20 mM glucose, 0.3 mM DTT, 1 mM Mg-ATP and 40 mg Rhodamine B isothiocyanate. $5x10^9$ freshly obtained erythrocytes were mixed with 4 times the volume of the master mix. Afterwards, the dialysed proteins were added. Usually, 120 µg of protein ($HsHsp70^{wt}$ or $Hsp70^{K71M}$) was added per $5x10^9$ packed erythrocytes. This resulted in a 1.5- to 1.8-fold HsHsp70 uptake compared to non-resealed (wildtype) erythrocytes (see Figure 18). Afterwards, the cells were lysed for 20 min on ice while shaking. In order to avoid insufficient haemoglobin amounts after the resealing, an erythrocyte lysate was added. The lysate was prepared by repeated freezing and thawing of wildtype erythrocytes in liquid nitrogen. Afterwards, the lysate was centrifuged at 36,000xg for 10 min at 4°C. After cells lysis was completed, 1 mL of erythrocyte lysate was added and cells were resealed by the addition of 800 µL 37°C pre-warmed 1 M NaCl. Finally, cells were allowed to reseal for 1 h at 37°C. At the end, the resealed red blood cells (rRBC) were centrifuged at 2,100xg for 2 min with decreased brake (level 4 out of 9) and washed 3 times with complete RPMI. After the resealing the haemoglobin amount, the protein uptake and the resealing efficiency was checked.

2.2.3.8 Measurement of haemoglobin

After each resealing experiment the haemoglobin amount was checked. Therefore, rRBC were diluted 1:40 and 1:80 in RPMI. A sample of non-resealed (wildtype) erythrocytes was used as a control. 100 µL of the dilutions were pipetted into a 96-well-flat-bottom plate and the absorbance at 570 nm was measured. The absorbance of the non-resealed cells was set as 100% and the rRBC haemoglobin amount was calculated accordingly.

2.2.3.9 Preparation of HuH7 western blot samples

The downregulation of HsHsp70 in HuH7 cells using siRNA was checked by western blot. The cells were harvested 48 h post-transfection and washed twice

in ice cold PBS. Afterwards, 80 µL/well RIPA buffer with 1:200 PIC and 1 mM PMSF was added to the cells. The cells were incubated on ice for 15 min. Next, a pipette tip was used to scratch the cells from the plate and the samples were transferred to a tube. The collected cells were centrifuged at 36,000xg for 15 min and the supernatant was kept. Afterwards, total protein amount was determined using a plate reader. Then, the samples were complemented with 2x SDS loading dye, boiled at 100°C for 10 min and equal protein amounts around 10 µg were loaded on a 12% SDS gel.

2.2.3.10 Preparation of RBC western blot samples

For non-infected red blood cells, 10^7 cells were directly added to 2x SDS loading dye, boiled at 100°C for 10 min and centrifuged at 36,000xg for 10 min. Afterwards, 10^7 cells were loaded per lane on a 12% SDS gel.

2.2.3.11 Sodium dodecylsulphate polyacrylamide gel electrophoresis (SDS-PAGE)

A sodium dodecylsulphate polyacrylamide gel electrophoresis (SDS-PAGE) separates proteins according to their molecular weight. Every SDS gel consists of a stacking gel, which is used to concentrate the samples and a separating gel, which allows separation of proteins. The SDS gels used in this thesis were prepared according to the recipe in Table 12.

Table 12 Composition of stacking and separation gel

Component	Stacking gel (5%)	Separating gel (12%)
ddH_20	5.6 mL	7.6 mL
Tris-HCl	2.5 mL	5 mL
Acrylamide	1680 µL	7.4 mL
APS	100 µL	160 µL

The samples were prepared using 2x SDS loading dye and boiling for 10 min at 100°C. The samples were separated at 90 V for 15-20 min until the samples entered the separating gel before increasing the voltage to 145 V for 1.5 h.

2.2.3.12 Coomassie blue gels

After electrophoresis, proteins on SDS gels were visualised by Coomassie blue staining for 1 hour, followed by destaining using destain-solution. The destain-solution was changed occasionally and ultimately replaced by ddH_2O for further destaining overnight.

2.2.3.13 Western blot

In a western blot the protein of interest can be detected and quantified based on the interaction between antigen and antibody. First, proteins were separated by SDS-PAGE and transferred onto a nitrocellulose membrane (Towbin et al., 1979). In the semi-dry blotting system a “sandwich” containing 3 blotting papers, the SDS gel, nitrocellulose membrane and 3 other blotting papers was assembled on a semi-dry blotter. Before setting up the blotting, all components of “the sandwich” were soaked in transfer buffer. The positive electrode was applied to the top of the semi-dry blotter and protein transfer was performed at 2 $mA/1cm^2$ for 1.5 h. After blotting, the membrane was blocked in 5% blocking milk for 1 h. The membrane was incubated overnight with the appropriate primary antibody diluted in 5% blocking-milk at 4°C. At the next day, the primary antibody was removed and the membrane was washed 3 times in PBS, 10 min each. Afterwards, the appropriate HRP conjugated secondary antibody (1:2,000 dilution) in 5% blocking milk was added to the membrane for 2 h at RT. Next, the membrane was washed 3 times in PBS for 10 min. Afterwards, the membrane was placed in a developing cassette. Henceforth, all steps were performed in the dark. A mix of H_2O_2 and ECL (1:1,000 dilution) was added to the membrane. A photographic film was laid on the nitrocellulose membrane and closed for some seconds. Afterwards, the photographic film was placed in developer, water, fixation buffer, water and finally air-dried.

2.2.3.14 ImageJ quantification of immunoblots

To analyse the downregulation or protein uptake of HsHsp70, bands detected on the immunoblot where quantified using the freeware ImageJ. Therefore, the immunoblot photographic film was scanned at 600 dpi. Afterwards, the resulting

data file was opened with ImageJ and converted to the greyscale 8 bit format. The picture was calibrated by usage of the function “uncalibrated optical density”. Then, a square was used to enclose the band of interest and a measurement of the optical density (OD) was performed. The square was moved without changing the square’s size and the OD of the remaining bands was determined. In total 3 independent measurements were performed. Finally, the downregulation or protein uptake was calculated normalised based on a loading control.

2.2.3.15 Sera experiment

To test whether different resealed host cells (with HsHsp70^{wt} and HsHsp70^{K71M}) have a different surface expression of e.g. PfEMP1, 2 sera (German naïve or a Pool of HyperImmune Sera (PHIS) from Kenya (kind gifts from AG Osier, Parasitology)) were incubated with infected rRBC. Afterwards, binding of antibodies in the sera was detected using anti-human IgG conjugated to Alexa-488. For this experiment, resealed erythrocytes were infected with MACS purified trophozoites. 48 h post-invasion, 0.5 µL of 4-5% trophozoite culture, 1 µL sera and 11 µL 0.5% BSA in PBS were added to each well on a 96-well-U-bottom plate. The sera were incubated for 30 min at RT. Afterwards, cells were washed 3 times in 200 µL 0.5% BSA in PBS and centrifuged at 800xg for 3 min. The wash buffers were discarded by flipping the plate over the sink to avoid cell loss. Then, the second antibody staining was performed using a 1:50 dilution of mouse-anti-human-Alexa-488 for 30 min at RT in the dark. Cells were washed 3 times in 200 µL 0.5% BSA in PBS with 800xg for 3 min. Finally, the cells were fixed in 4% PFA in PBS at 4°C overnight and samples were prepared for flow cytometry. As a control, non-infected RBC were used to exclude unspecific binding of the antibodies due to any reaction of the host RBC with the naïve serum and PHIS sera. Furthermore, a background control of infected rRBC, which was only stained with the secondary antibody, was included.

2.2.3.16 Indirect immunofluorescence assay

The indirect immunofluorescence assay exploits the specific recognition of an antigen by an antibody. Thereby, localisation of a certain protein can be

determined and even co-localisation studies can be performed. First, a methanol fixation in ice-cold 10% methanol and 90% acetone was performed. Parasite smears were carried out on a slide and samples were fixed for 10 min in the acetone/methanol mixture at -20°C. The blocking was performed using 3% BSA in PBS for 1 h. Afterwards, the primary antibody was diluted in 3% BSA in PBS and incubated overnight at 4°C in a wet chamber. On the next day, slides were washed 3 times in PBS and the appropriate secondary antibody was diluted in 3% BSA and incubated for 2 h at RT. Following, the slides were washed 3 times in PBS and the nuclear staining was performed using DAPI. To this end, slides were incubated with 1 µg/mL DAPI in PBS for 10 min. At last, slides were washed once with ddH_2O to remove salt crystals from the PBS and analysed by fluorescence microscopy at a 63x objective magnification with immersion oil.

2.2.4 Analysis of Parasite Growth

2.2.4.1 Setting up the growth assay

All growth assays were performed in 96-well flat-bottom plates. One well contained 200 µL RPMI complete medium with a 2% haematocrit and 0.1% starting parasitemia. The growth was analysed by either a LDH assay (2.2.4.2) or by flow cytometry (2.2.4.3) after 48 h and 96 h. Several controls were included in the setup. The first control was a sample of non-infected RBC acting as a background control for the LDH assay or for the DAPI/SYBR green staining. Further, parasites were treated with 50 µg/mL BFA acting as positive control showing parasite death.

2.2.4.2 Lactate dehydrogenase assay

The LDH assay exploits the ability of plasmodial lactate dehydrogenase (pLDH) to convert lactate to pyruvate (Basco et al., 1995) with the help of the cofactor 3-acetylpyridine adenine dinucleotide ($APAD^+$), which is reduced to APADH. Upon the addition of the yellow dye nitroblue tetrazolium (NBT) and diaphorase (also called lipoamide dehydrogenase), the APADH is oxidised to $APAD^+$ while NBT is converted to the coloured product formazan (Markwalter et al., 2016). The

harvest was performed at the trophozoite stage after 48 h and 96 h. To harvest the cells for the LDH assay, 100 µL of the used medium was removed and parasites were resuspended in the remaining medium. Afterwards, parasites were frozen at -20°C for at least 24 h. For the LDH assay 50 mL LDH-buffer was used to dissolve 1 Nitro Blue Tetrazoilum (NBT) tablet (in the dark). Afterwards, the LDH-NBT buffer was complemented with diaphorase from *Clostridium kluyveri* (final concentration 1U/mL) and 3´-acetylpyridine adenine dinucleotide (APAD) (final concentration 50 µg/mL). The parasites were thawed for 30 min at RT and then, mixed 1:1 with the prepared LDH-buffer. The reaction was incubated at RT in the dark for 20 min. Afterwards, the reaction was measured at $A_{650\ nm}$ using a plate reader.

2.2.4.3 Flow cytometry analysis

All flow cytometry measurements were performed at the ZMBH FACS core facility under the supervision of Dr. Monika Langlotz. The BD Canto uses the BD Diva software for analysis. Depending on the experiments gates were set with the appropriate controls and lasers (e.g. 561-C, 408-B, 488-B). All experiments were measured in 96-well U-bottom plates with 200 µL using the HTS loader. HTS loader settings were as following: sample flow rate (0.5 µL/s), sample volume (160 µL), mixing volume (100 µL), mixing speed (180 µL/s), number of mixes (4) and, wash volume (400 µL). After measuring the data was saved as PDF as well as FCS file, which was then further analysed using the FlowJO software (version 10.4.2).

2.2.4.3.1 Preparation of HuH7 *Plasmodium berghei* infected flow cytometry samples

48 h post-infection with *P. berghei* liver stages, the cells were harvested for flow cytometry. The cells were washed twice with DMEM incomplete (no FCS) medium and 80 µL trypsin/EDTA was added for 3-5 min. For inactivation 160 µL DMEM complete was added and cells were transferred to a tube. The samples were centrifuged at 600xg for 2 min and washed once in 200 µL 1x PBS. Finally, cells were resuspended in 400 µL 1x PBS and transferred into FACS tubes.

2.2.4.3.2 Preparation of *Plasmodium falciparum* iRBC flow cytometry samples

The growth of *P. falciparum* in the different resealed host cells was analysed by flow cytometry. After 48 h and 96 h at the trophozoite stage parasites were fixed. To this end, the 200 µL spent culture medium was replaced with 100 µL 4% PFA with 0.0075% Glutardelyhde and fixed overnight at 4°C. At the next day, samples were either DAPI stained or stained with SYBR green to allow for differentiation of the ring/trophozoite or schizont stages.

DAPI staining:

Parasites were washed in PBS after fixation and then DAPI stained with 1 µg/mL DAPI in PBS for 10 min. Afterwards, the 96 well plate was centrifuged at 1,000xg for 2 min and 5 times washed in 150 µL PBS. Finally, cells were resuspended in 200 µL fresh PBS. Lastly, cells were diluted 1:6 in a fresh 96-well U-bottom plate with 200 µL PBS.

SYBR green staining:

For SBYR green staining cells were washed once in PBS and then resuspended in 100 µL (1:2,000) SYBR green. Afterwards, cells were washed 3 times in 150 µL PBS and finally diluted 1:6, as described for the DAPI staining.

3 Results

3.1 Establishing the resealing method

In this study, the role of HsHsp70 for the intra-erythrocytic development of *P. falciparum* was elucidated. Unfortunately, human erythrocytes cannot be easily genetically modified to study the effect of a certain host protein on parasite survival and development. In consequence, a different approach was needed. Here, a pre-loading or also called resealing method of human mature erythrocytes, which is widely used in the pharmacology, came in handy (Bourgeaux et al., 2016; Magnani et al., 1998; Rossi et al., 2005). Erythrocytes can be lysed and pre-loaded with e.g. an excess amount of a mutated protein of interest, leading to a classical dominant negative. In this thesis, a non-functional HsHsp70 called HspHsp70^{K71M} (unable to hydrolyse ATP) (O'Brien et al., 1996) is added during the resealing, thereby resealed red blood cells (rRBC) loaded with an excess amount of HspHsp70^{K71M} are produced that can be used as host cells for the infection with parasites. As a control, rRBC were pre-loaded with a functional HsHsp70 called HsHsp70^{wt} protein. In the beginning, various resealing protocols and methods were tested. Each method contained major drawbacks considering the resealing efficiency and the reproducibility (data not shown). After a long test phase, the combination of several resealing protocols led to satisfying results. During this test phase a dye called rhodamine was added, without adding any HsHsp70 protein, to check the pre-loading. In the end, rRBC were analysed by fluorescence microscopy. Indeed, using the newly established protocol, rRBC showed fluorescence labelling (Figure 12).

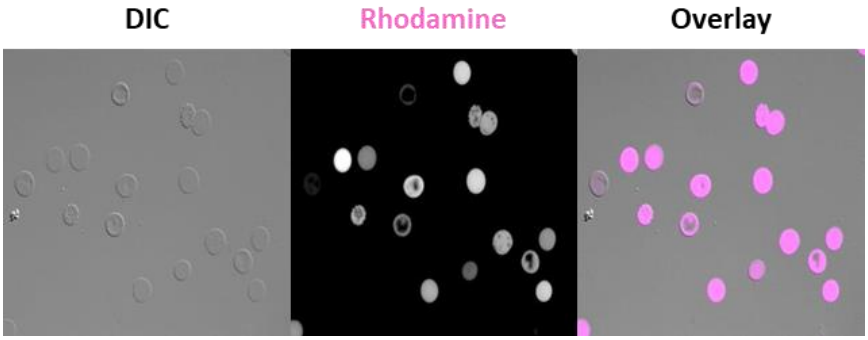

Figure 12 Fluorescence microscopy of resealed red blood cells (rRBC)
Microscopy of non-fixed and non-infected rRBC labelled with rhodamine. DIC: Differential Interference Contrast, 63x objective magnification.

After establishing the resealing method it was tested, whether the rRBC were still susceptible to *P. falciparum* infection. Therefore, parasites expressing a cytosolic Green Fluorescent Protein (GFP) were enriched by Magnetic Activated Cell Sorting (MACS) to a parasitemia of nearly 100%, thereby avoiding that non-infected erythrocytes from the culture were diluting the rRBC. 48 h post-invasion, rRBC were checked by live cell imaging. As seen in Figure 13, GFP-expressing parasites infected the rhodamine labelled rRBC and even double infections of rRBC were observed (Figure 13). Interestingly, the rhodamine signal co-localised with hemozoin, characteristic of the food vacuole, thereby indicating that the rhodamine was located in the food vacuole of the parasite.

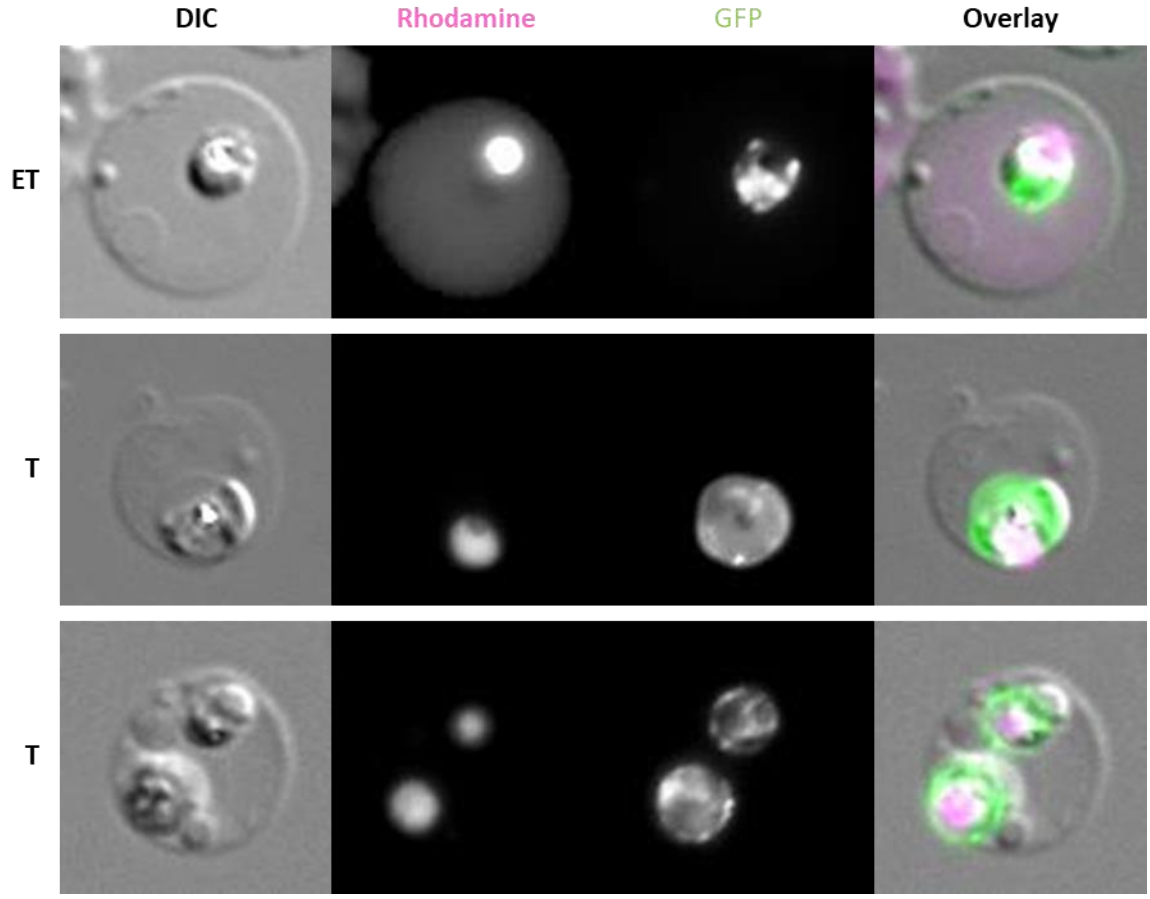

Figure 13 Resealed red blood cells infected with parasites expressing GFP
Live cell imaging of rRBC labelled with rhodamine and infected with *P. falciparum* parasites expressing GFP. DIC: Differential Interference Contrast, ET: Early Trophozoite, T: Trophozoite, GFP: Green Fluorescent Protein, 63x objective magnification.

Next, the protein purification of the 2 proteins needed for the dominant negative effect was performed. During the resealing process either the mutated HsHsp70^{K71M} or the wildtype HsHsp70^{wt} was used. The latter acted as a positive

control. The 2 His-SUMO-tagged proteins were expressed in *E. coli* and purified by affinity chromatography. Finally, the His-SUMO-tag was removed by the Ulp1-protease. The 2 untagged proteins were separated on a SDS-PAGE and stained with Coomassie. Both proteins presented pure protein bands around 70 kDa (Figure 14).

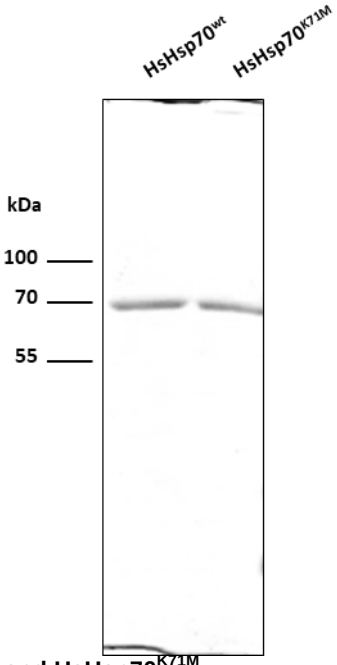

Figure 14 SDS-PAGE of HsHsp70^{wt} and HsHsp70^{K71M}
Pure and untagged HsHsp70^{wt} and HsHsp70^{K71M} separated on a 12% SDS-PAGE. Bands were visualised with Coomassie staining. Size marker indicated on the left side in kDa.

Following purification, both purified proteins were checked for contamination with *E. coli* Hsp70, called DnaK, which often is found as contaminant. The purified proteins as well as an *E. coli* protein lysate used as positive control for DnaK were separated by SDS-PAGE. Afterwards, an immunoblot analysis using antisera raised against DnaK was carried out. DnaK was only detected in the positive control (*E. coli* lysate) around 70 kDa, but was absent in the HsHsp70^{wt} and HsHsp70^{K71M}, indicating the purity of the 2 protein samples (Figure 15A). As a loading control, the same samples were analysed by immunoblot using antisera directed against HsHsp70. The positive control (RBC) as well as the purified proteins showed bands around the expected 70 kDa (Figure 15B).

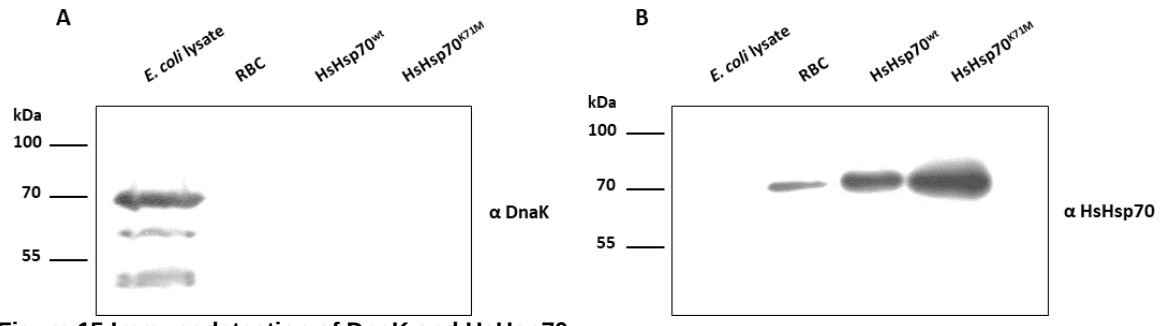

Figure 15 Immunodetection of DnaK and HsHsp70
(A) Immunoblotting against DnaK with *E. coli* lysate, 10^7 non-infected RBC, HsHsp70^{wt} and HsHsp70^{K71M}.
(B) Immunoblotting against HsHsp70 with *E. coli* lysate, 10^7 non-infected RBC, HsHsp70^{wt} and HsHsp70^{K71M}.
Size markers indicated on the left side in kDa.

To assess whether the purified proteins were functional and non-functional, a luciferase refolding assay was conducted. Briefly, the function of a denatured firefly luciferase can be restored by the refolding capacity of an active Hsp70 in concert with its co-chaperone Hsp40 and the help of a NEF. The denatured firefly luciferase was incubated with an Hsp40, a NEF (both kind gifts from Dr. Roman Kityk, research group Mayer, ZMBH) and either the functional HsHsp70^{wt} or the inactive HsHsp70^{K71M}. The control sample did not contain either of the 2 proteins. The refolding was visualised by light emission, which was monitored over 90 minutes. Only HsHsp70^{wt} was able to refold the luciferase, whereas both the control and the inactive mutant HsHsp70^{K71M} displayed only small to no refolding capacity (Figure 16). In the literature usually up to 80% of luciferase refolding is reported (Morán Luengo et al., 2018; Schröder et al., 1993). Here, only a smaller refolding was achieved, but a similar trend could be observed upon the addition of a functional HsHsp70^{wt}. In consequence, a pure, untagged and functional HsHsp70^{wt} as well as non-functional HsHsp70^{K71M} have been purified.

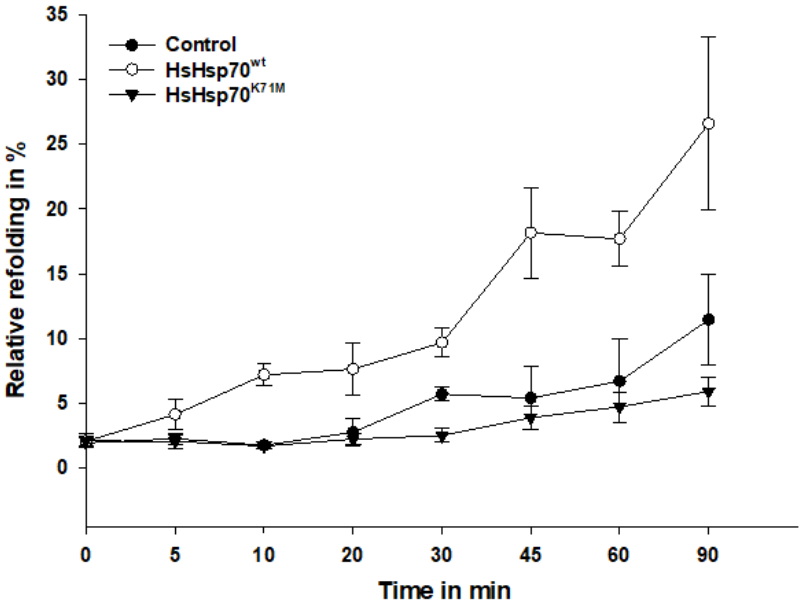

Figure 16 Luciferase refolding assay with HsHsp70^{wt} and HsHsp70^{K71M}
The blot shows relative refolding over time of denatured firefly luciferase with HsHsp70^{wt} or HsHsp70^{K71M}, Hsp40 and NEF. The control did not contain either one of the 2 purified proteins. The highest measured relative light unit was set as 100% to calculate the relative refolding in percent. Result of 1 experiment in triplicates.

Next, the average protein amount of HsHsp70 in mature human erythrocyte was determined. Therefore, 10^7 RBC were separated on a SDS-PAGE together with 20, 40 and 100 ng of purified HsHsp70. Immunoblotting against HsHsp70 was used to visualise the proteins and protein quantification was performed with the freeware ImageJ. The measurement indicated that 10^7 erythrocytes contained approximately 10 ng HsHsp70 (Figure 17A). Afterwards, it was verified whether Hsp70^{wt} and HsHsp70^{K71M} can be successfully entrapped into the rRBC. Based on the determined amount of endogenous HsHsp70, different concentrations of HsHsp70$^{wt/K71M}$ were added during the resealing to achieve a double to triple protein excess for the dominant negative effect. The protein uptake was confirmed by immunoblotting (data not shown). In the end, approximately 80 ng of purified protein were added per 10^7 erythrocytes, which presented intensive bands in the immunoblot. The exact amount of HsHsp70 entrapped in RBC was determined by immunoblotting. First, RBC, rRBC with no protein and rRBC with HsHsp70^{wt} (HsHsp70^{wt}) or with HsHsHsp^{K71M} (HsHsp70^{K71M}) were subject to SDS-PAGE, followed by an immunoblot against HsHsp70 and Glycophorin A&B.

The latter acted as loading control (Figure 17A). Afterwards, the quantification with ImageJ revealed that rRBC contained little less HsHsp70 compared to the wildtype RBC. However, protein uptake during the resealing of HsHsp70$^{wt/K71M}$ was confirmed and was determined to approximately 30 ng of HsHsp70 for both proteins (Figure 17B). Furthermore, the amount of the cognate form HsHsc70 was determined. Therefore, the same samples were separated by SDS-PAGE followed by immunoblotting against HsHsc70 (Figure 17C). ImageJ quantification indicated that the HsHsc70 amounts were similar in all 4 samples (Figure 17D). Additionally, both HsHsp70 and HsHsc70 antisera were tested for their specificity with purified HsHsp70 and HsHsc70 recombinant proteins (shown in the appendix, Figure 44).

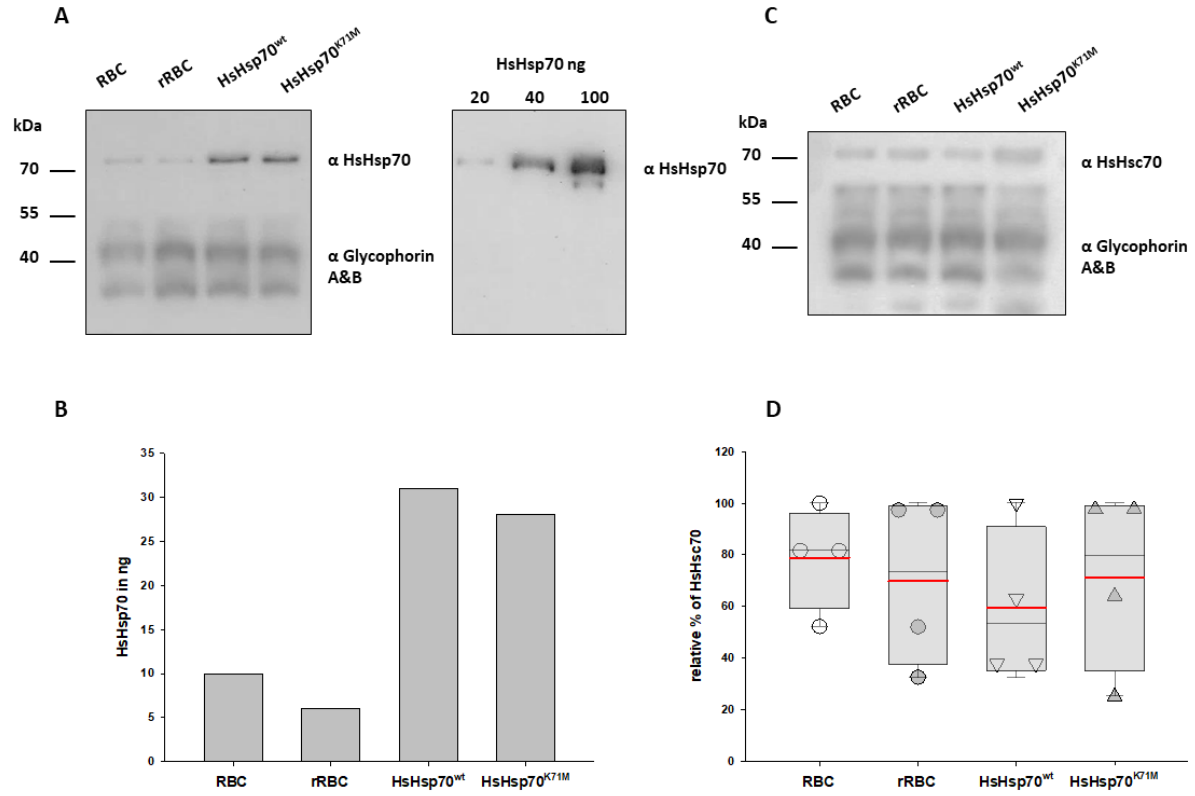

Figure 17 Immunodetection of HsHsp70 and HsHsc70 with ImageJ quantification

(A) Immunoblot against HsHsp70 with RBC, rRBC and rRBC with HsHsp70^{wt} or HsHsp70^{K71M} as well as 20, 40,100 ng purified HsHsp70. Glycophorin A&B was used as a loading control. Size markers are indicated on left side in kDa.

(B) ImageJ quantification of HsHsp70 in ng based on (A). The amount of HsHsp70 was determined according to the standard curve of 20-100 ng purified HsHsp70. Result of 1 quantification.

(C) Immunoblot against HsHsc70 with RBC, rRBC and rRBC with HsHsp70^{wt} or HsHsp70^{K71M} and Glycophorin A&B (loading control). Size markers are indicated on left side in kDa.

(D) Dot blot with boxes shows relative percent of HsHsc70 determined by ImageJ quantification of (C). Relative percent of HsHsc70 was normalised against Glycophorin A&B. Results of 4 independent resealing experiments.

It was shown in previous translocation experiments, using the same dominant negative approach, that HsHsp70 has an important impact on the transport of parasite proteins across the PVM (Günnewig, 2016). Thus, it was tested with immunoblotting whether a similar HsHsp70 fold increase was obtained due to the resealing as for the translocation assay. Therefore, wildtype erythrocytes, rRBC and rRBC with $HsHsp70^{wt}$ or $HsHsp70^{K71M}$ were separated on a SDS-PAGE followed by immunoblotting against HsHsp70 and Glycophorin A&B as a loading control (Figure 18A). Afterwards, the visualised bands were quantified by ImageJ. An approximately 2-fold increase in the HsHsp70 concentration compared to wildtype erythrocytes was measured for $HsHsp70^{wt}$ and $HsHsp70^{K71M}$ (Figure 18B). The direct comparison between the resealing and the translocation assay can be seen in Figure 18C. In the resealing assay, the amount of HsHsp70 was compared to the rRBC, whereas in the translocation assay the amount of HsHsp70 was compared to the positive control of the assay, where no HsHsp70 was added. Both assays achieved an approximate 6-fold increase of $HsHsp70^{wt/K71M}$ (Figure 18C). Therefore, the resealing experiments and the translocation assays used equal protein amounts for the dominant negative effect. At last, the haemoglobin amount in the 3 different resealed cell types was checked, as any variation might affect the expected growth. The haemoglobin amount was determined by measuring the absorbance at 570 nm, while setting a sample of wildtype erythrocytes (non-resealed) as 100% and calculating the respective percentages for the rRBC samples. In general, similar amounts of ~40% haemoglobin were achieved for all 3 samples (Figure 18D).

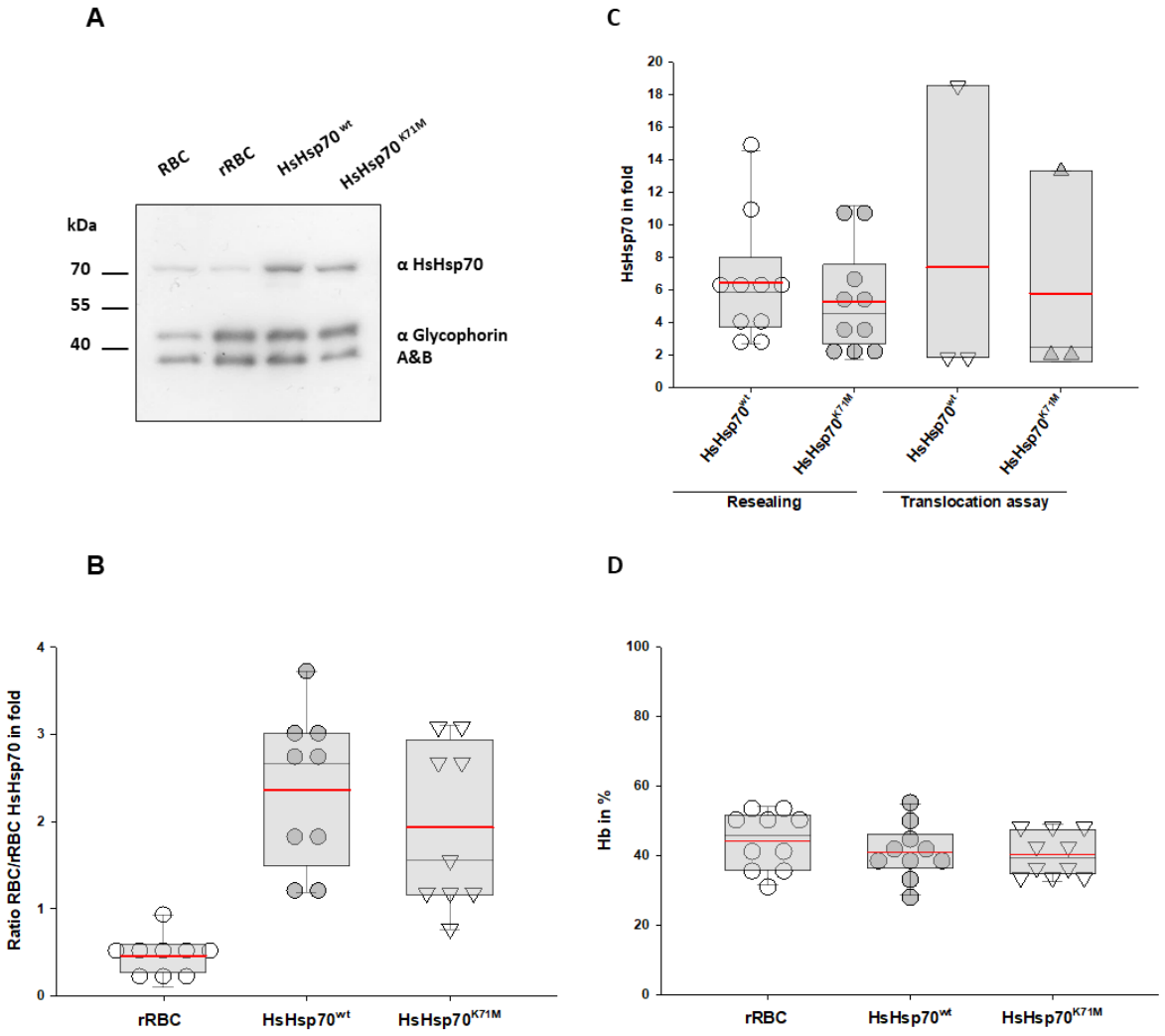

Figure 18 Protein uptake and haemoglobin concentration in rRBC

(A) Immunoblot against HsHsp70 with RBC, rRBC and rRBC with HsHsp70^{wt} or HsHsp70^{K71M} and Glycophorin A&B was used a loading control. Size markers are indicated on left side in kDa.

(B) Dot blot with box presents HsHsp70 amount in fold compared to wildtype erythrocytes normalised against Glycophorin A&B determined by ImageJ quantification of (A). Results of 9 independent resealing experiments.

(C) Dot blot with box visualising HsHsp70 amount in resealing and translocation assays (Günnewig, 2016). For the resealing HsHsp70 amounts were calculated in comparison of rRBC. The HsHsp70 amount in the translocation assay was calculated in comparison to the positive control of the assay.

(D) Haemoglobin amount in percent of rRBC and rRBC with HsHsp70^{wt} or HsHsp70^{K71M} compared to non-resealed wildtype erythrocytes.

To sum everything up, a successful resealing protocol was established enabling the pre-loading of mature human erythrocytes. With this method cells were resealed and were still capable of being infected by *P. falciparum*. During the resealing the pure, untagged functional HsHsp70^{wt} and inactive HsHsp^{70K71M} can be entrapped into the rRBC, resulting in a 6-fold excess compared to rRBC where no protein was added. All 3 rRBC contained ~40% haemoglobin compared to wildtype erythrocytes that were non-resealed.

3.2 Localisation of HsHsp70 in non-infected and infected erythrocytes

Apart from the investigation of HsHsp70 for parasite survival and development, analysing the localisation of HsHsp70 was also of interest. In previous studies, several fruitless attempts were made to localise HsHsp70 in non-infected as well as in the infected erythrocyte using classical immunofluorescence assays (Jude Przyborski, personal communication). Here, the resealing method was used to entrap fluorescently labelled HsHsp70 to the mature human erythrocytes, to localise the protein in the non-infected erythrocyte. To achieve this, the purified HsHsp70^{wt} was coupled to an Oregon green dye and as a control Bovine Serum Albumin (BSA) was coupled to Oregon green, as well. Afterwards, HsHsp70^{wt}-Oregon green, BSA-Oregon green and a sample of the dye itself were separated by SDS-PAGE and bands were visualised with the help of a laser scanner. Indeed, protein labelling was confirmed by an intensive band around the expected 70 kDa for HsHsp70^{wt}-Oregon green and for the control BSA-Oregon green.

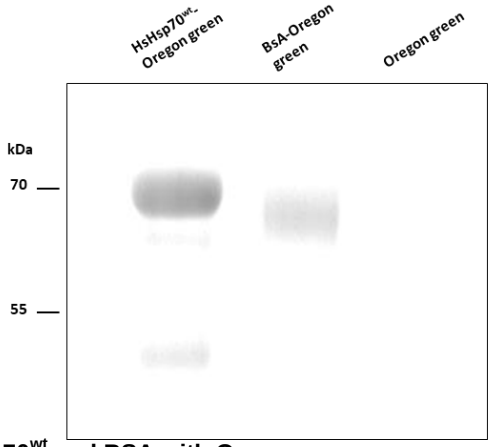

Figure 19 Labelling of HsHsp70^{wt} and BSA with Oregon green
HsHsp70^{wt}-Oregon green, BSA-Oregon green and Oregon green dye were separated on a 12% SDS gel and bands were visualised using a laser scanner at 488 nm. Size markers are indicated on left hand side in kDa.

After confirming the coupling of the proteins to the dye, 3 resealing reactions with mature human erythrocytes were performed using either HsHsp70^{wt}-Oregon green, BSA-Oregon green, or only the dye. Moreover, for all 3 reactions rhodamine was added to label cells that were resealed. Afterwards, rRBC were analysed by fluorescence microscopy for the localisation of the proteins. The HsHsp70^{wt}-Oregon sample displayed dot-like structures all over the non-infected

cell. At a closer look, the dot-like structures were mobile foci presenting no directed movement, but rather a randomised motion. However, BSA-Oregon as well as the dye itself displayed an equal fluorescence throughout the cytosol in accordance to the rhodamine signal (Figure 20).

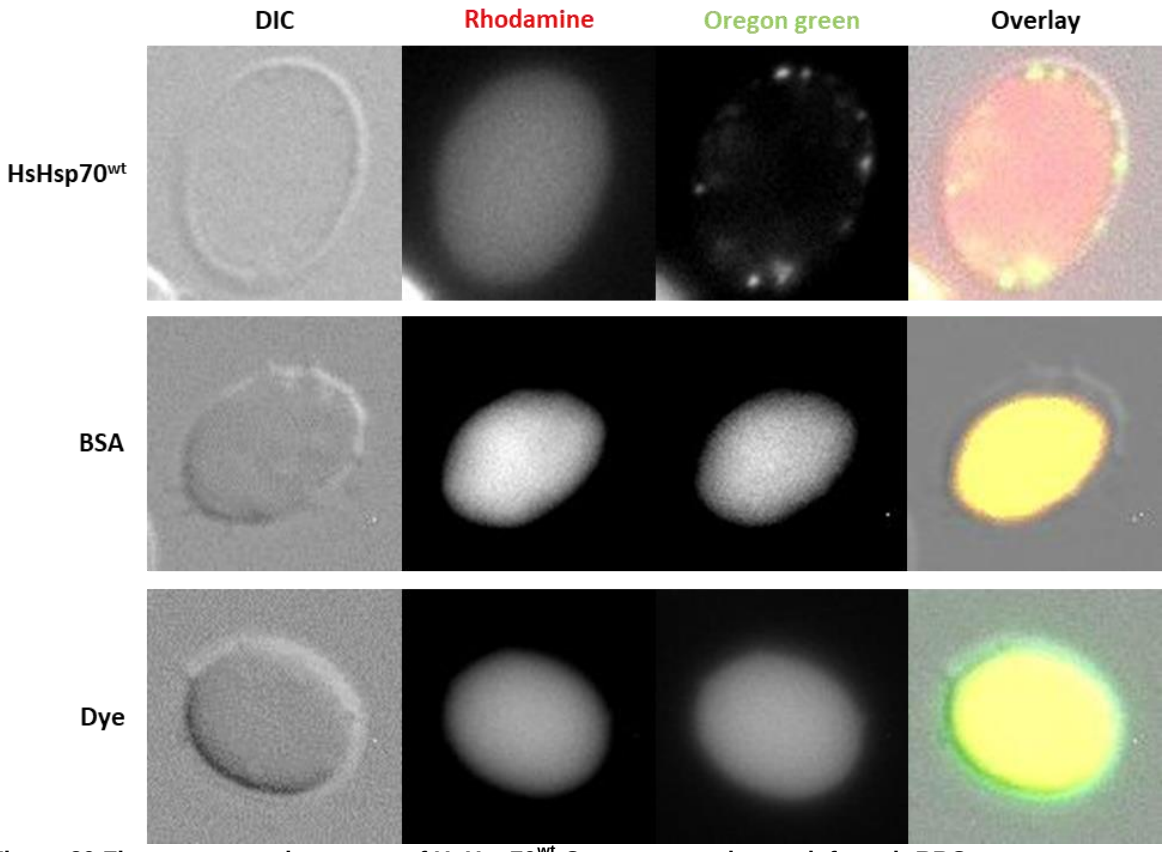

Figure 20 Fluorescence microscopy of HsHsp70^{wt}-Oregon green in non-infected rRBC
Live cell imaging of HsHsp70^{wt}-Oregon green (HsHsp70^{wt}), BSA-Oregon green (BSA), and dye (dye) in rRBC. 63x objective magnification, DIC: Differential Interference Contrast.

After localising HsHsp70 in the non-infected erythrocyte, its localisation in the infected erythrocytes was investigated. Unfortunately, the previously used Oregon green dye was emptied and due to time restriction HsHsp70 was labelled with another available Cy2 dye. First, HsHsp70 coupling to Cy2 was verified using the laser scanner. HsHsp70 labelling was confirmed by the presence of an intense band around the expected 70 kDa (Figure 21).

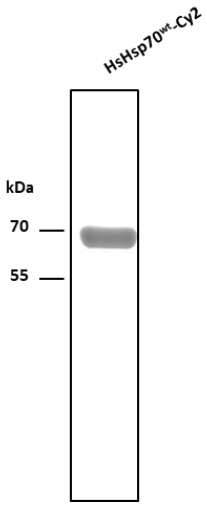

Figure 21 Labelling of HsHsp70^{wt} with Cy2
HsHsp70^{wt}-Cy2 separated on a 12% SDS-gel visualised by typhoon laser scanner at 488 nm. Size markers are indicated on left hand side in kDa.

Next, a resealing in presence of the HsHsp70^{wt}-Cy2 was performed and rRBC were infected with MACS purified *P. falciparum* wildtype parasites. After 48 h, rRBC with HsHsp70^{wt}-Cy2 were subjected to life cell imaging. Uninfected rRBC were used as a control and the incorporation of HsHsp70^{wt}-Cy2 was checked, revealing the same dot-like structures as observed for the HsHsp70^{wt}-Oregon green labelling. Contrary to the initial expectations, HsHsp70^{wt}-Cy2 was identified inside the parasite and not in the host cell.

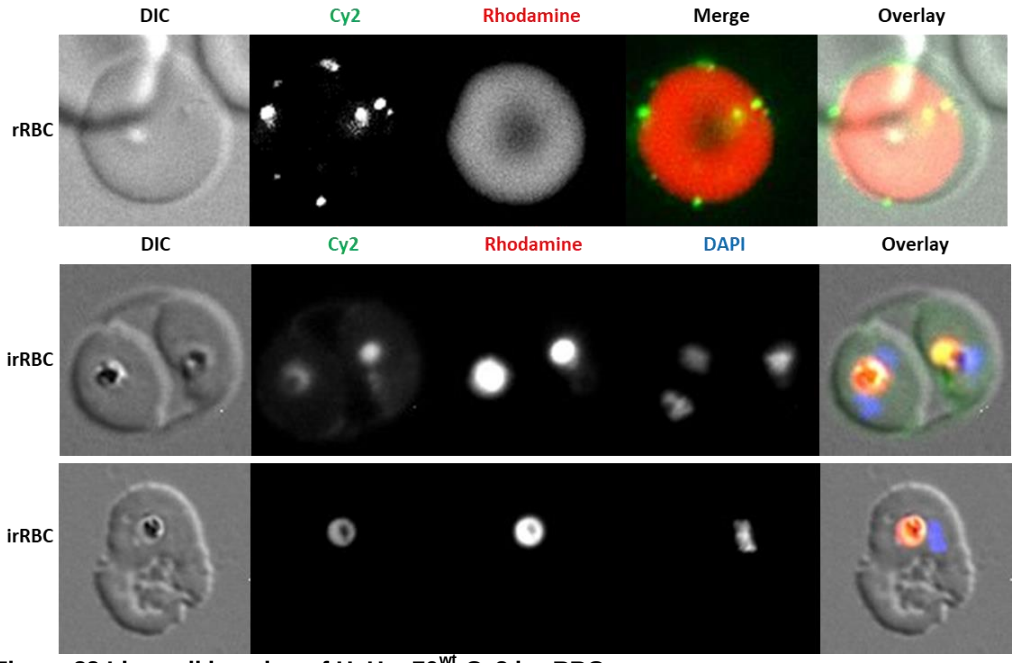

Figure 22 Live cell imaging of HsHsp70^{wt}-Cy2 in rRBC
Live cell imaging of HsHsp70^{wt}-Cy2 in the non-infected rRBC (rRBC) and the infected rRBC (irRBC). 63x objective magnification, DIC: Differential Interference Contrast.

Inevitably, no progress on the localisation of HsHsp70 in the infected erythrocyte was made with the resealing and in consequence, another approach was needed. The new idea was to genetically modify *P. falciparum* in a way, leading to the parasite itself exporting a tagged HsHsp70 to its own host cell, which would enable the localisation of the protein. Thus, a construct containing the first 80 amino acids of STEVOR (a known exported protein of the parasite, with the first 80 amino acids being sufficient to direct any protein to the host cell), an mCherry tag allowing the localisation of the fusion protein as well as the full sequence of HsHsp70 was introduced into the parasite (Figure 23A). Transfection of the parasites was successful and parasites showed a detectable mCherry signal upon live cell imaging. Similarly, to the localisation experiments using the resealing, the infected erythrocytes showed mobile dots (data not shown), as well. Unfortunately, the signal was not strong enough to acquire good pictures and consequently an ImmunoFluorescence Assay (IFA) was performed using antisera directed against mCherry. The fusion protein localised to the host cell cytosol displaying a dot-like structure. Some of the protein was localised inside of the parasites, leading to the presumption that protein export was not complete (Figure 23B).

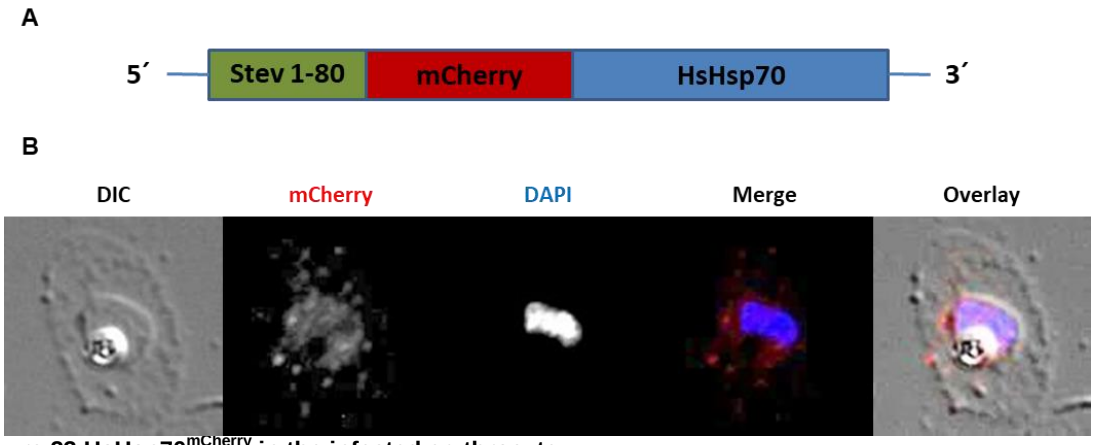

Figure 23 HsHsp70^{mCherry} in the infected erythrocyte
(A) Construct of STEVOR 1-80 with mCherry and HsHsp70.
(B) Immunofluorescence assay against mCherry showing the fusion protein HsHsp70^{mCherry}. Nucleus visualised with DAPI. As a negative control the fixed cells were stained with the secondary antibody, which did not show any fluorescence. 63x objective magnification, DIC: Differential Interference Contrast.

There are already 2 known dot-like structures described in the infected erythrocyte. The so called J-dots, which contain parasite encoded chaperones and co-chaperones, appear as mobile dot-like structures in the infected RBC.

Further, Maurer's clefts, which are single membrane structures close to the host cells, also show punctuate structures in the infected erythrocyte and even present motion in younger trophozoite stages. Hence, it was analysed whether the HsHsp70^{mcherry} fusion protein co-localised with any of the known structures. Therefore, co-localisation studies with antisera directed against mCherry and either Hsp70x ((70x), a parasite-encoded and exported chaperone, J-dot marker) (Külzer et al., 2012) or SBP1 (a known component of the Maurer's clefts) (Blisnick et al., 2000) was performed. The J-dot marker 70x showed the expected dot-like structures and surprisingly, a partial co-localisation could be detected. The Maurer's cleft marker SBP1 did not demonstrate co-localisation with HsHsp70^{mcherry} (Figure 24).

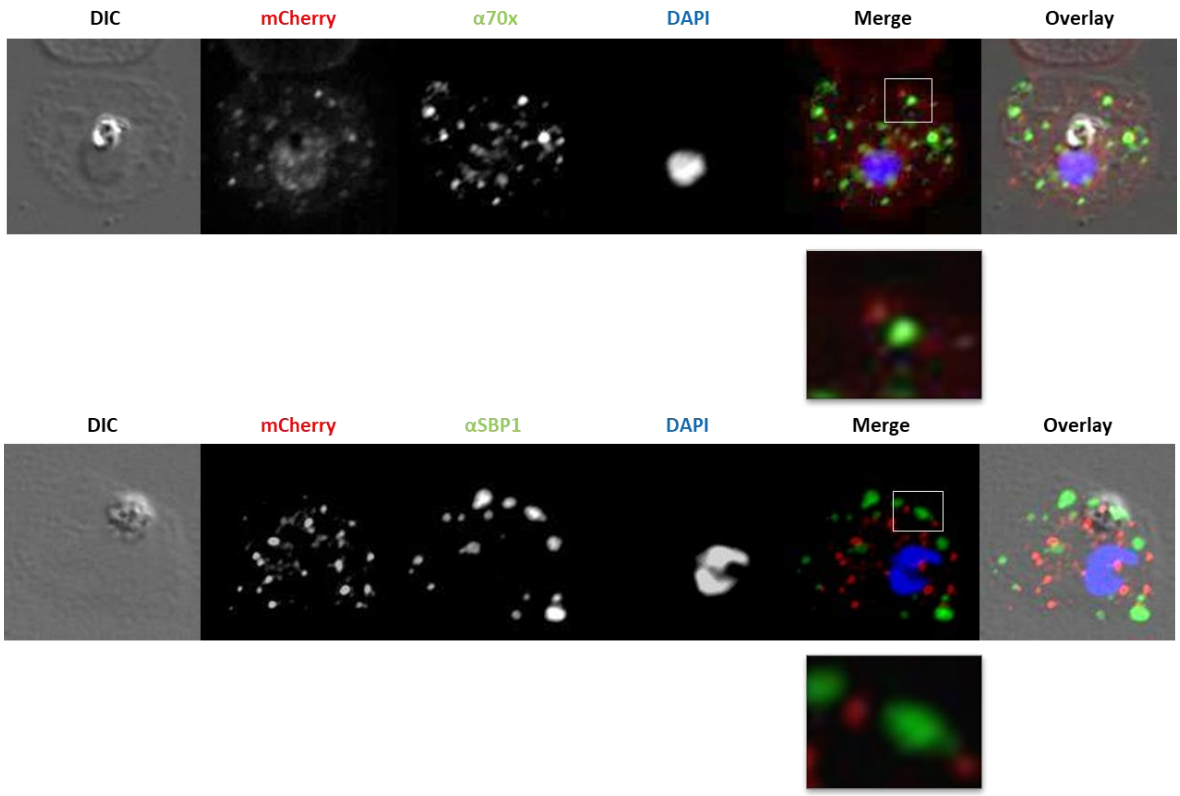

Figure 24 Co-localisation study of HsHsp70^{mCherry} with 70x and SBP1
Co-localisation study of HsHsp70^{mcherry} with the J-dot marker 70x and the Maurer's cleft marker SBP1. Pictures below merge show close up from the indicated boxes. Staining with the secondary antibodies did not present fluorescence. 63x objective magnification. 70x: PfHsp70x, SBP1: Skeleton-Binding Protein 1, DIC: Differential Interference Contrast.

To sum up, the results of the localisation study using the resealing approach presented HsHsp70 as mobile foci in the non-infected erythrocyte, but also revealed in addition to the immunoblots that protein uptake during the resealing was achieved. However, regarding the localisation of HsHsp70 in the infected

erythrocyte, no satisfying results were obtained. Still, HsHsp70^{mCherry} expression and the export of the protein to the host cell was possible. The fusion protein displayed a dot-like structure in the infected RBC, which partially co-localised with the J-dot marker Hsp70x, but not with the Maurer's clefts marker SBP1.

3.3 Growth analysis of HsHsp70 in 3D7 wildtype parasites

After showing that rRBC can be pre-loaded with an excess amount of HsHsp70 and can still be infected by *P. falciparum*, the role of the host cell protein in the intra-erythrocytic development of the parasite was analysed. First, a classical growth assay followed by a Lactate DeHydrogenase assay (LDH) was performed. In this study, several rRBC types were analysed for growth; (i) rRBC pre-loaded with no additional protein, (ii) rRBC pre-loaded with an excess amount of HsHsp70^{wt} and (iii) rRBC with an excess amount of the inactive HsHsp70^{K71M}. All 3 host cell types were infected with MACS purified 3D7 wildtype parasites. Further, non-infected rRBC samples were included, acting as background control for the LDH assay. At last, a control of BFA, a substance that causes the death of the parasite, was added to the experimental setup. Parasite growth was monitored for 48 and 96 h and analysed using the LDH assay. The LDH assay exploits the anaerobic metabolism of the parasite, which includes the conversion of lactate to pyruvate and can be visualised upon the addition of a yellow substrate that is converted into a product of blue-brownish colour (Markwalter et al., 2016). The colorimetric assay was measured using a laser at 650 nm, with the absorbance at this wavelength being proportional to the parasitemia. The results of 4 independent LDH assays after 48 h and 96 h can be seen in Figure 25. After 48 h, the BFA control worked well for all 3 samples and showed low relative absorbance, indicating the death of the parasites. However, some assays showed decreased growth for parasites grown in either the presence of HsHsp70^{wt} or HsHsp70^{K71M}. Overall, there were statistically significant differences for HsHsp70^{wt} and HsHsp70^{K71M} compared to the rRBC control. Incubation for 96 h displayed big variations for the growth of HsHsp70^{wt} and HsHsp70^{K71M} samples. Here, a significantly smaller growth rate in the rRBC containing HsHsp70^{K71M} was observed (Figure 25).

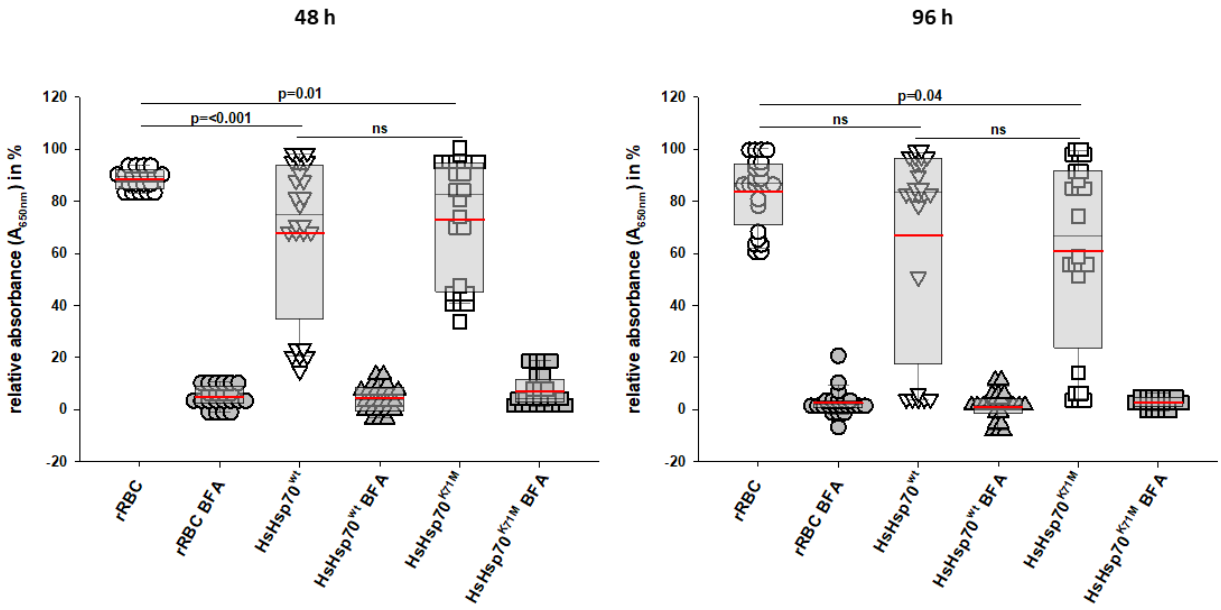

Figure 25 Lactate dehydrogenase assay of 3D7 grown in rRBC
LDH assay of 3D7 parasites grown in rRBC, rRBC pre-loaded with an excess amount of HsHsp70^{wt} or HsHsp70^{K71M}. Parasites were treated with BFA (50 µg/mL) as a positive control for parasite death (BFA). Absorbance at 650 nm in percent of 4 independent experiments is visualised. The relative absorbance was calculated based on the highest absorbance in the single assays. Background of non-infected rRBC, HsHsp70^{wt} and HsHsp70^{K71M} were subtracted, respectively. The mean values are indicated by a red dash and statistical significance was determined by the One-Way ANOVA-Holm Sidak test.

Using the LDH assay no consistent results were obtained due to limitations of the assay. With the LDH assay no distinction between non-resealed and resealed cells was made. Nevertheless, resealing efficiencies may differ between the 3 rRBC types and can thereby already influence the results. In consequence, the next step was to adjust the read-out method to flow cytometry. Here, the growth of only successfully resealed RBC was analysed by assistance of the rhodamine labelling and parasites can be easily visualised by a DAPI staining. The same experimental setup as previously explained for the LDH assay was used, but growth was now analysed by flow cytometry with some smaller adjustments. The parasites were fixed using 4% ParaFormAldehyde (PFA) in PBS and stained with DAPI. Additionally, the study was blind, therefore, each resealing protein name was coded during the process.

First, controls were used to set the gates for the analysis. With the help of non-infected and non-resealed wildtype erythrocytes (RBC) the gate for rhodamine positive cells was set. Next, a sample with rRBC that were non-infected, but stained with DAPI was used to confirm the rhodamine gate and to set the gate for the DAPI positive cells. At last, the gating process was checked by infected

rRBC, which were stained with DAPI (irRBC DAPI) (Figure 26). In the appendix an example for the gating strategy with the FlowJo software can be seen (appendix Figure 45).

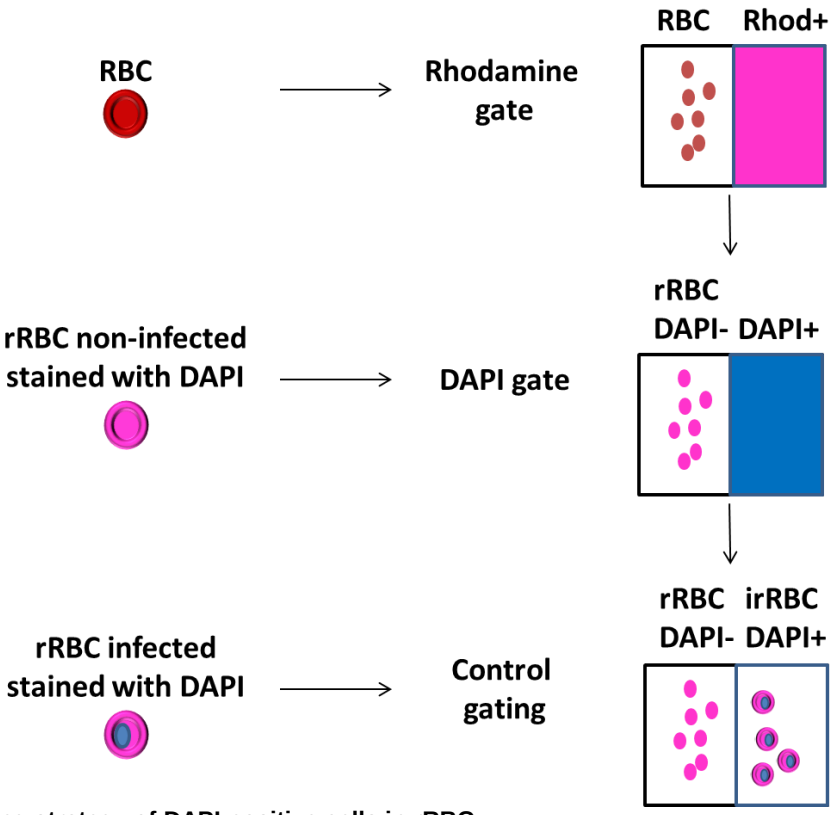

Figure 26 Gating strategy of DAPI positive cells in rRBC
Flow cytometry gating strategy of DAPI positive cells detected in rRBC. Non-infected and non-resealed RBC (RBC) were used to set the gate for rhodamine positive cells. rRBC non-infected but stained with DAPI were used as a control for the DAPI gating. Finally, infected rRBC stained with DAPI were used to confirm the gating strategy.

After 48 h parasites presented less growth in the presence of HsHsp70^{K71M} compared to rRBC, although not significant. Interestingly, the growth rate in the rRBC with HsHsp70^{wt} was significantly increased compared to the rRBC control after 96 h. The BFA controls after 48 h and 96 h showed low relative growth. For all samples, a DAPI background control with non-infected DAPI stained rRBC was included. Sometimes the measured background was higher compared to the actual parasitemia obtained for BFA treated samples, explaining the negative values seen for the BFA controls (Figure 27).

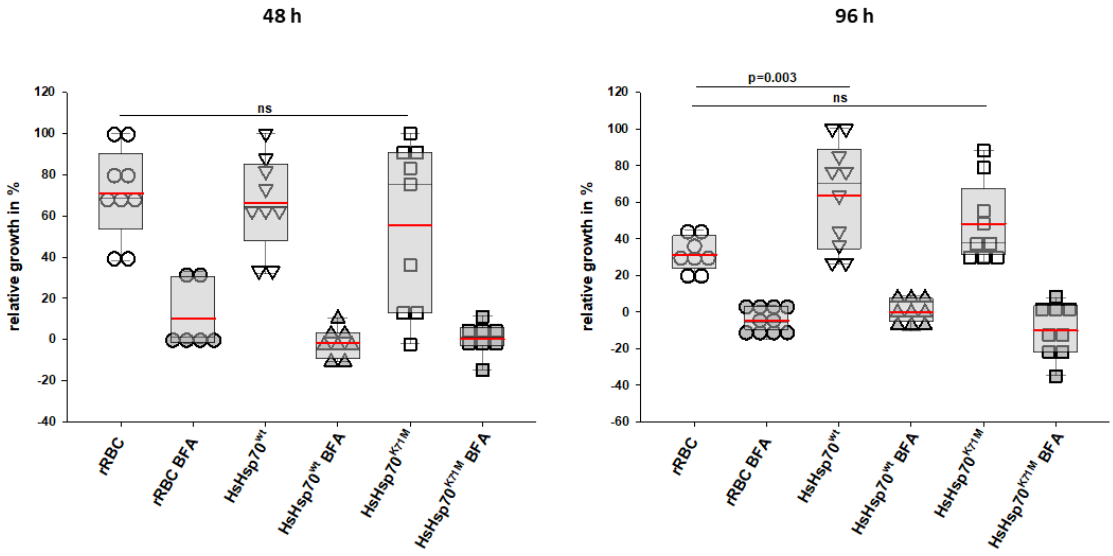

Figure 27 3D7 growth in rRBC with HsHsp70^{wt} and HsHsp70^{K71M}
Flow cytometry assay of 3D7 parasites grown in rRBC, rRBC containing an excess of HsHsp70^{wt} or HsHsp70^{K71M}. As a positive control for parasite death, parasites were treated with BFA (50 µg/mL) (BFA). The relative growth in percent was determined by setting highest parasitemia of the single assay as 100%. Background of non-infected rRBC, HsHsp70^{wt} and HsHsp70^{K71M} stained with DAPI were subtracted, respectively. The mean values are indicated by a red dash and statistical significance was determined by the One-Way ANOVA-Holm Sidak test.

As there was no statistically significant effect on the growth of the parasite in the presence of an excess amount of HsHsp70^{K71M}, the developmental stages of the parasites were analysed in more detail using a SYBR green staining. The staining of the fixed parasites enabled differentiation between the single-nucleated stages of the parasite, the ring and trophozoite stage, and the multi-nucleated schizont stage.

Again, proper gating was ensured as for the DAPI analysis and non-infected and non-resealed cells (RBC) were used to set the gate for rhodamine cells. This time, non-infected and SYBR green stained rRBC were used set the gate for SYBR green positive cells. Finally, a sample of rRBC infected with mixed stages (ring, trophozoite and schizont) acted as a control for the ring/trophozoite gate (RT) and the schizont (S) gate (Figure 28). In the appendix, Figure 45 shows an example for the gating process.

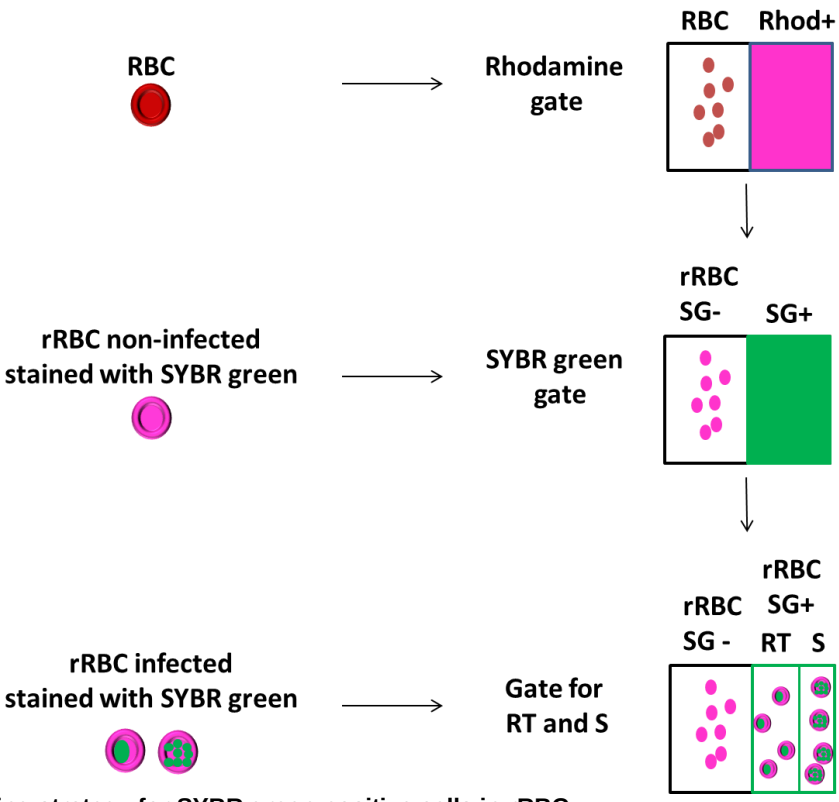

Figure 28 Gating strategy for SYBR green positive cells in rRBC
Flow cytometry gating strategy of SYBR green (SG) positive cells detected in rRBC to differentiate single-nucleated ring/trophozoites (RT) and multi-nucleated schizonts (S). Non-infected and non-resealed RBC (RBC) were used to set gate for rhodamine positive cells. Non-infected but SYBR green stained rRBC acted as a control for the SYBR green gating. Finally, infected rRBC stained with mixed stages were used to set the gates for the ring/trophozoites (RT) and for schizonts (S).

Again, rRBC and rRBC with HsHsp70$^{wt/K71M}$ were infected with MACS purified 3D7 wildtype parasites and fixed after 48 and 96 h. Afterwards, the cells were stained with SYBR green and analysed by flow cytometry. No difference for ring and trophozoite stages (RT) was observed between the samples. However, HsHsp70^{K71M} presented significantly less schizonts compared to the rRBC control. 96 h post-infection, no statistical difference was detected between parasites grown in the different host cell types. Tough, the power of the performed statistical test was below the desired one and a smaller power indicates that it is less likely to detect a difference when one actually exists. There are big variances in the obtained data, in particular for the determined RT numbers, and in general more repeats are needed to validate the results.

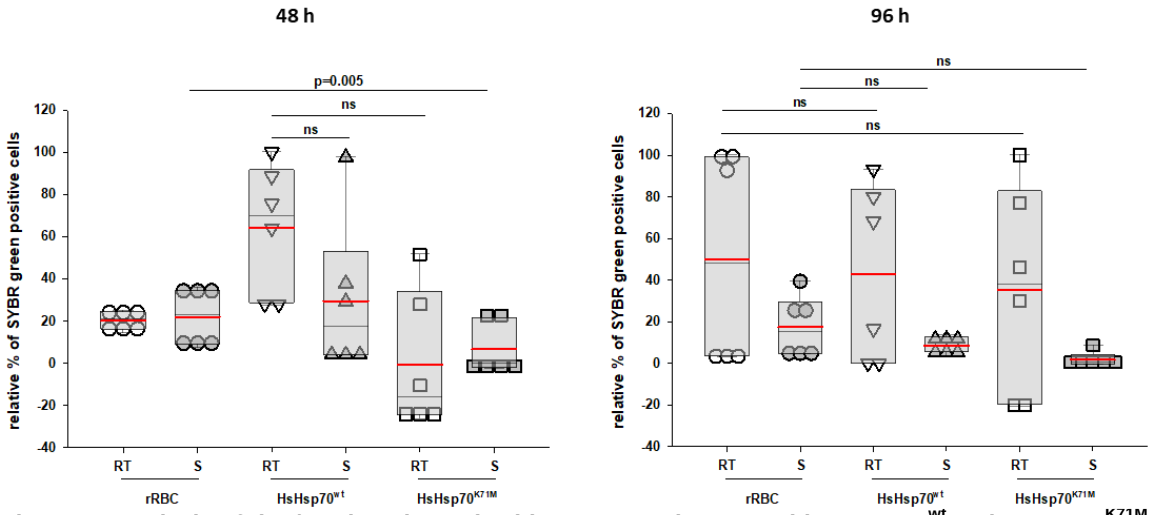

Figure 29 Analysis of ring/trophozoite and schizont stages in rRBC with HsHsp70^{wt} and HsHsp70^{K71M}
Flow cytometry assay of 3D7 parasites grown in rRBC, rRBC with HsHsp70^{wt} and rRBC with HsHsp70^{K71M}. Dot blot with box shows relative percent of SYBR green positive cells from 2 independent experiments. The relative percent of SYBR green positive cells was calculated based on the highest parasitemia in the single assays. Background of non-infected rRBC, HsHsp70^{wt} and HsHsp70^{K71M} stained with SYBR green were subtracted, respectively. The mean values are indicated by a red dash and statistical significance was determined by the One-Way ANOVA-Holm Sidak test.

Even if there are no detectable differences in the intra-erythrocytic development, protein export and thereby the surface expression of major cytoadherence proteins might still be altered. Usually, differences on the surface of the infected erythrocyte are analysed using a binding assay. Unfortunately, the rRBC limit the portfolio of classical methods used for normal infected erythrocytes. During the study it was noted that rRBC react more sensitive to e.g. PFA fixation. As a result, the rRBC protein surface expression was analysed using 2 different sera. A Pool of HyperImmune Sera (PHIS) from the endogenous malaria region Kelifi, Kenya (kind gift from Dr. Osier, Parasitology, Heidelberg) was used. It is already well-established to use such sera from endemic malaria regions to recognise surface antigens on the infected erythrocyte (Maier et al., 2008). Mostly EMP1 is recognised by such sera (Beeson et al., 2006). In this study, naïve serum from Germany obtained from donors who did not acquire any immunity against malaria acted as negative control. The 3 different rRBC types were infected with MACS purified wildtype 3D7 parasites. After 48 h, parasites were incubated either with the PHIS or the naïve serum. The antibodies bound to the surface of the irRBC were visualised by an anti-human-Alexa-488 staining. After intensive washing, the parasites were fixed in 4% PFA and subject to flow cytometry analysis.

First, gates were set by usage of the proper controls. Again, non-resealed erythrocytes were used set the gate for the rhodamine positive cells. Afterwards, a sample of non-infected but DAPI stained erythrocytes secured the gating for DAPI positive cells. The gate for Alexa-488 positive cells was set with the help of infected rRBC stained by DAPI and incubated with the secondary antibody. Finally, a sample of irRBC treated with PHIS and stained with Alexa-488 as well as DAPI validated the whole gating process. An example of the gating process with the FlowJo software can be seen in Figure 47 (appendix).

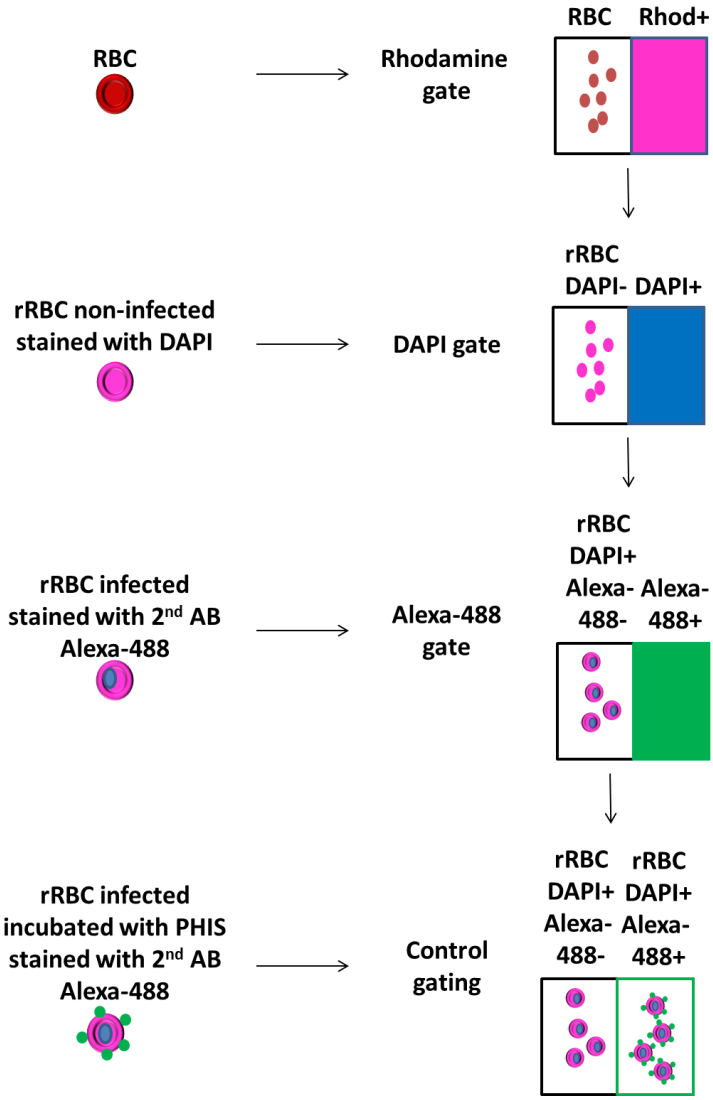

Figure 30 Gating strategy of irRBC stained with Alexa-488
Flow cytometry gating strategy of Alexa-488 positive cells detected in rRBC treated with PHIS from Kelifi, Kenya. Rhodamine gate (Rhod) was set with the help of non-infected and non-resealed RBC (RBC). rRBC non-infected but stained with DAPI were used for the DAPI gating. The infected rRBC stained with DAPI and the secondary antibody were used for the gating of Alexa-488 positive cells. Finally, infected rRBC treated with PHIS and stained with DAPI as well as the secondary antibody were used to ensure a proper gating

Every experiment contained an internal control with non-infected RBC to ensure that antibody binding of the sera was not due to differences in the host cell factors e.g. kell factor. The non-infected RBC control never showed any binding, indicating that the sera did not react to host cell factors (data not shown). Further, another internal control with non-resealed RBC (RBC), which were incubated with naïve serum or the PHIS, was included. There was a highly statistically significant difference between the relative percentages of Alexa-488 positive cells of RBC treated with naïve serum compared to the PHIS sera. The German naïve serum was not able to detect infected RBC specified by the relatively low binding of ~10%. It was expected that there would be differences in the binding of the sera for the different rRBC. Indeed, there was a lower binding affinity of the PHIS for parasites grown in the HsHsp70^{K71M} however this difference was not statistically significant. Taken together, all 3 rRBC samples showed low binding with the naïve serum and a significant increase was achieved by the use of the PHIS (Figure 31).

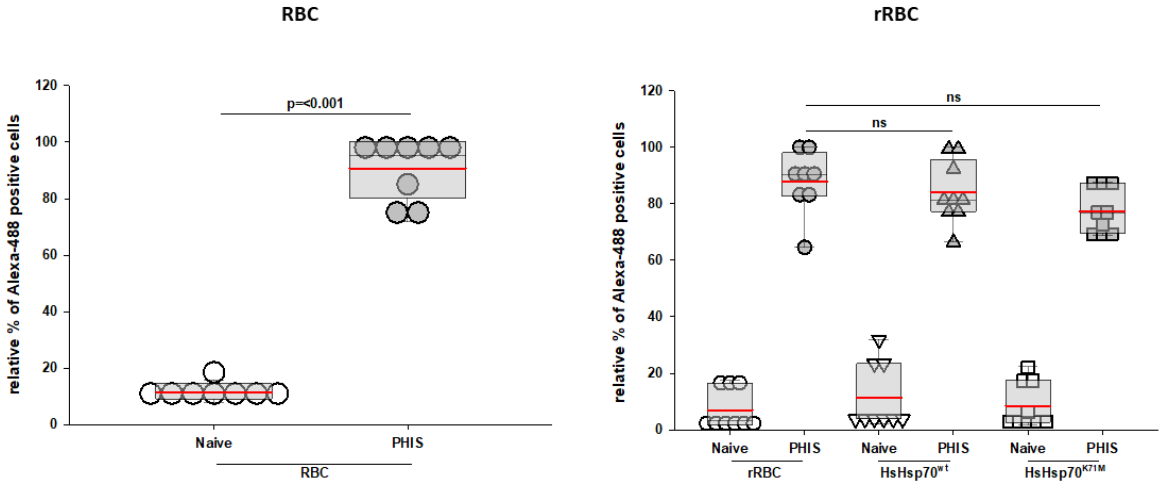

Figure 31 Alexa-488 positive cells with Naïve serum and PHIS in rRBC
Dot blot with boxes of RBC and rRBC, rRBC pre-loaded with HsHsp70^{wt} (HsHsp70^{wt}) or with HsHsp70^{K71M} (HsHsp70^{K71M}) incubated with either naïve serum or PHIS from Kelifi, Kenya. Infected RBC and rRBC only stained with the secondary antibody acted as background and was always subtracted. Data are shown as the relative percentage of Alexa-488 positive cells calculated based on the highest amount of Alexa-488 cells for each experiment. The mean values of the 3 independent experiments are indicated by red dashes and statistical significance was determined by the One-Way ANOVA-Holm Sidak test.

In the end, the change from the LDH assay to the flow cytometry cleared the confusion regarding the effect of HsHsp70 for parasite survival and made results much more reliable as well as reproducible. Using flow cytometry it was seen that there is no effect of HsHsp70 on the intra-erythrocytic development, but

interestingly after 96 h, addition of the HsHsp70^{wt} revealed a positive effect on parasite growth. The analysis of the parasite stages displayed a significantly lower amount of schizonts after 48 h for parasites grown in the presence of HsHsp70^{K71M} compared to the control. Finally, the expression of antigens on the surface of the irRBC was unaltered by the presence of the HsHsp70^{K71M} as shown by the sera experiments.

3.4 Growth analysis of HsHsp70 in PfHsp70x knockout parasites

It has been demonstrated that the parasite itself also exports an Hsp70-protein called PfHsp70x (from now on referred to as Hsp70x) to the host cell. Recent studies did not demonstrate an essential function of Hsp70x regarding the parasite development, leading to the assumption that the function of Hsp70x might be covered by the host chaperone (Charnaud et al., 2017). As the aforementioned analysis of HsHsp70 in the infected erythrocyte did not show any essential function of the host chaperone, it was speculated that the function might be compensated by the parasite chaperone. To address this hypothesis, it was analysed whether parasites depleted of Hsp70x (∆Hsp70x) are able to survive in the presence of HsHsp70^{K71M}. The same experimental setup as already explained for the wildtype 3D7 parasites was chosen but this time, ∆Hsp70x parasites were used. Before starting the growth experiments, it was ensured that the used ∆Hsp70x parasites were depleted of Hsp70x by immunoblotting. Indeed, ∆Hsp70x were lacking Hsp70x compared to a wildtype control (shown in the appendix, Figure 48). Afterwards, ∆Hsp70x parasites were MACS purified and mixed with rRBC, rRBC with an excess amount of HsHsp70^{wt} or HsHsp70^{K71M}. After 48 and 96 h, parasites were fixed with 4% PFA and stained with DAPI followed by flow cytometry analysis. The gating was performed as explained in Figure 26. As previously mentioned, parasites were treated with BFA acting as a positive control for dead parasite, which did not display any relative growth. Further, there were no significant differences in the growth of the 3 rRBC after 48 h. Yet, a significantly increased growth was observed after 96 h in the presence of the 2 proteins HsHsp70^{wt} and HsHsp^{K71M} compared to the control (Figure 32).

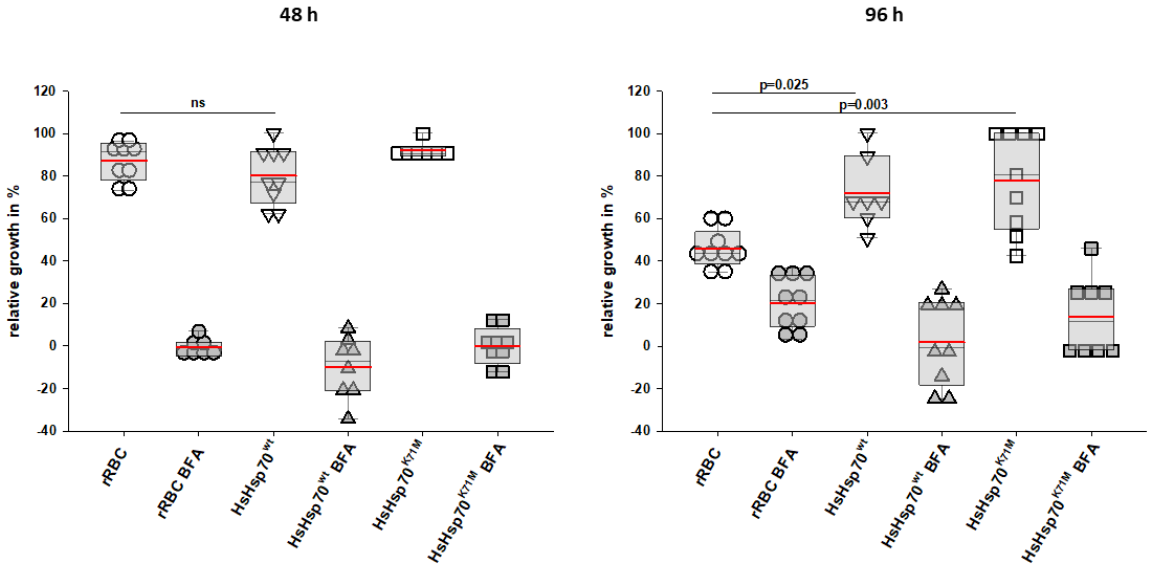

Figure 32 ΔPfHsp70x growth in rRBC with HsHsp70^{wt} and HsHsp70^{K71M}
Flow cytometry analysis of ΔHsp70x parasites grown in rRBC, rRBC with excess of HsHsp70^{wt} or HsHsp70^{K71M}. Parasites were treated with BFA (50 µg/mL) as a positive control for death. Dot blot with box indicates relative growth in percent of 3 independent experiments. The relative growth was calculated based on the highest parasitemia in the single assays. Background of non-infected rRBC, HsHsp70^{wt} and HsHsp70^{K71M} stained with DAPI were subtracted, respectively. The mean values are indicated by a red dash and statistical significance was determined by the One-Way ANOVA-Holm Sidak test.

In the next step, ΔHsp70 parasites were analysed via SYBR green staining for rings/trophozoites and schizonts. The experimental setup, staining as well as gating, was performed as previously explained in chapter 3.3. No difference in the ring/trophozoite and schizont stages between the 3 rRBC samples was observed after 48 h. Although, the power of the performed statistical test was below the desired power and in consequence it is less likely to detect a difference when one actually exists. After 96 h, statistical significance was determined with confidence resulting in no difference in growth for the ring/trophozoite stage of rRBC, HsHsp70^{wt} and HsHsp70^{K71M} (Figure 33). It was observed that the determined ring/trophozoite numbers displayed big variances and in consequences more repeats are needed to validate the data.

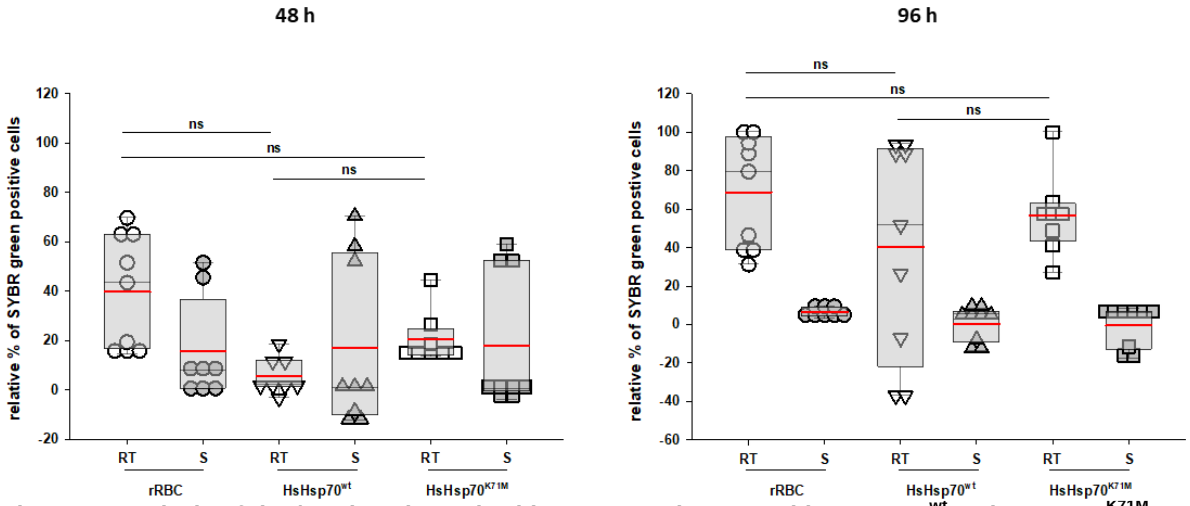

Figure 33 Analysis of ring/trophozoite and schizont stages in rRBC with HsHsp70^{wt} and HsHsp70^{K71M}
Flow cytometry analysis of ΔHsp70x parasites grown in rRBC, rRBC pre-loaded with an excess amount of HsHsp70^{wt} or HsHsp70^{K71M} for 48 h and 96 h stained with SYBR green. Box blot with box presents relative percent of SYBR green positive cells from 3 independent experiments. The relative percent of SYBR green positive cells was calculated based on the highest parasitemia in the single assays. Background of non-infected rRBC, HsHsp70^{wt} and HsHsp70^{K71M} stained with SYBR green were subtracted, respectively. The mean values are indicated by a red dash and statistical significance was determined by the One-Way ANOVA-Holm Sidak test.

Any potential difference in the surface expression of the ΔHsp70x infected rRBC was analysed using naïve German sera from donors who never acquired immunity against malaria and PHIS from the endemic malaria region in Kelifi, Kenya. The experiment was performed as explained in chapter 3.3. Additionally, an internal positive control of wildtype erythrocytes was incubated with naïve serum and the PHIS. The incubation with the PHIS led to a significant increase of Alexa-488 positive cells, thereby indicating a correct experimental setup. Surprisingly, incubation of infected rRBC, rRBC with HsHsp70^{wt} and HsHsp70^{K71M} with PHIS did not display statistically significant differences (Figure 34).

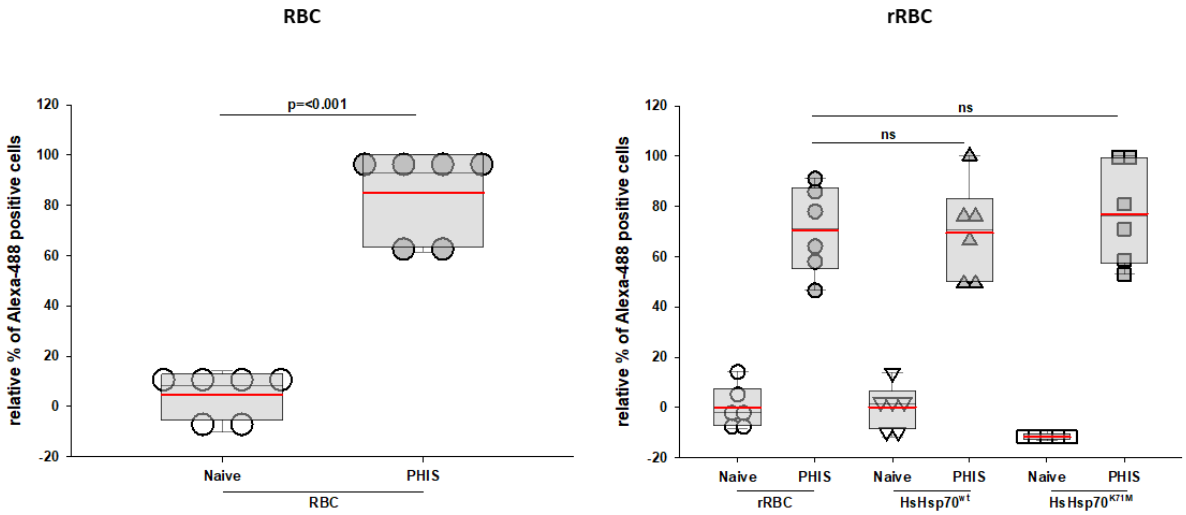

Figure 34 Alexa-488 positive cells with naïve serum and PHIS in rRBC
Dot blot with box of ΔHsp70x cultivated in RBC and rRBC, rRBC pre-loaded with HsHsp70^{wt} or HsHsp70^{K71M} incubated with either naïve serum or PHIS from Kelifi, Kenya. Infected RBC and rRBC only stained with the secondary antibody acted as background and were always subtracted. Data are shown as the relative percentage of Alexa-488 positive cells, calculated based on the highest amount of Alexa-488 cells for each experiment. The mean values of the 2 independent experiments are indicated by a red dash and statistical significance was determined by the One-Way ANOVA-Holm Sidak test.

In summary, the use of ΔHsp70x parasites disclosed no essential function of HsHsp70 for parasite survival. Yet again, a positive effect upon the addition of HsHsp70^{wt} as well as HsHsp70^{K71M} on the parasite growth after 96 h was revealed. Further, no differences in surface expression of the 3 ΔHsp70x infected rRBC were detected.

3.5 Microscopy analysis of known exported proteins in rRBC

In addition to the performed sera experiments (explained in the chapters 3.4 and 3.5), the protein export in rRBC was evaluated by microscopy analysis of 2 exported GFP-tagged proteins. In this regard, rRBC, rRBC pre-loaded with an excess of HsHsp70^{wt} or HsHsp70^{K71M} were infected with MACS purified SBP1-GFP tagged parasites (SBP^{GFP}). The SBP^{GFP} parasites localise to the Maurer's clefts in the infected erythrocyte (Saridaki et al., 2009). 48 h post-invasion, the parasites were examined by fluorescence microscopy. The rRBC sample revealed export of the fusion protein SBP^{GFP}. The pattern of the fusion protein was altered compared non-resealed cells (Saridaki et al., 2009), which might be caused by the morphology of the rRBC. Remarkably, the presence of

HsHsp70^{K71M} did not block the protein export of SBP^{GFP} to the host cell cytosol (Figure 35).

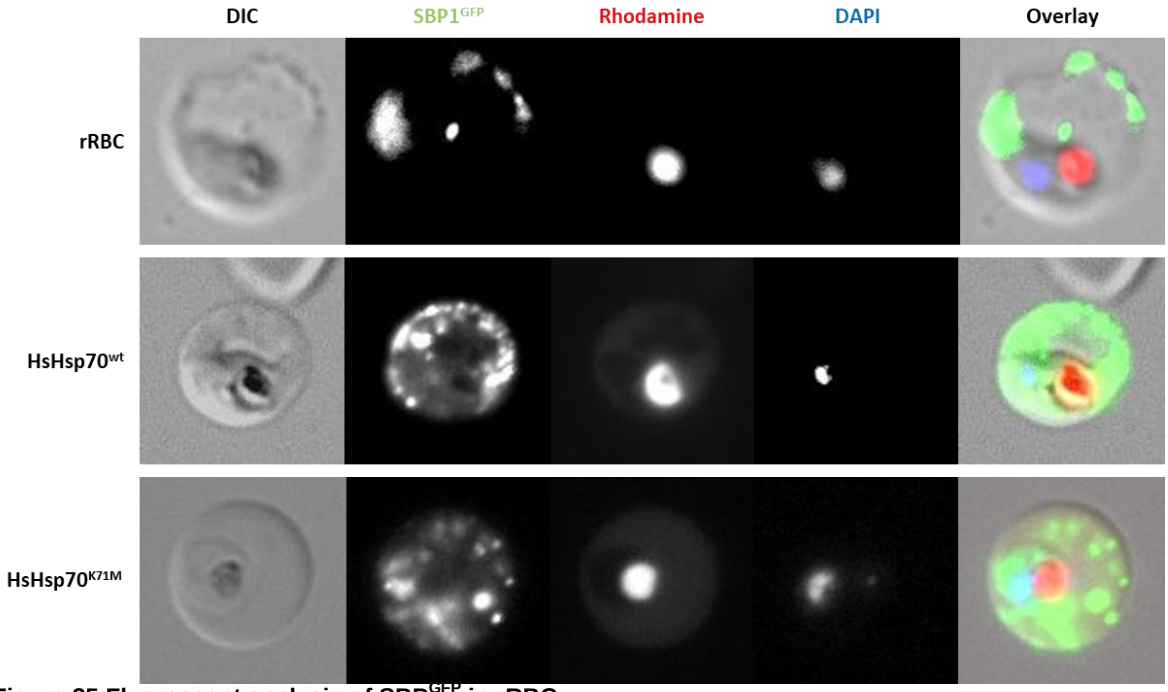

Figure 35 Fluorescent analysis of SBP^{GFP} in rRBC
Live cell imaging of SBP^{GFP} infecting rRBC (rRBC), rRBC pre-loaded with an excess amount of HsHsp70^{wt} (HsHsp70^{wt}) or HsHsp70^{K71M} (HsHsp70^{K71M}). The nucleus was visualised by DAPI. 63x objective magnification, DIC: Differential Interference Contrast.

Secondly, the export of a STEVOR-GFP fusion protein (STEVOR^{GFP}) to the host cell cytosol was analysed by the same experimental setup. STEVOR is a known exported protein and localises to the Maurer's cleft and is associated with antigenic variation (Przyborski et al., 2005). The control using rRBC confirmed export of the fusion protein, although the localisation appeared slightly different compared to wildtype infected erythrocytes (Przyborski et al., 2005), which might be due to the altered appearance of the rRBC. Surprisingly, the presence of HsHsp70^{K71M} did not inhibit the protein transport of STEVOR^{GFP} to the host cell.

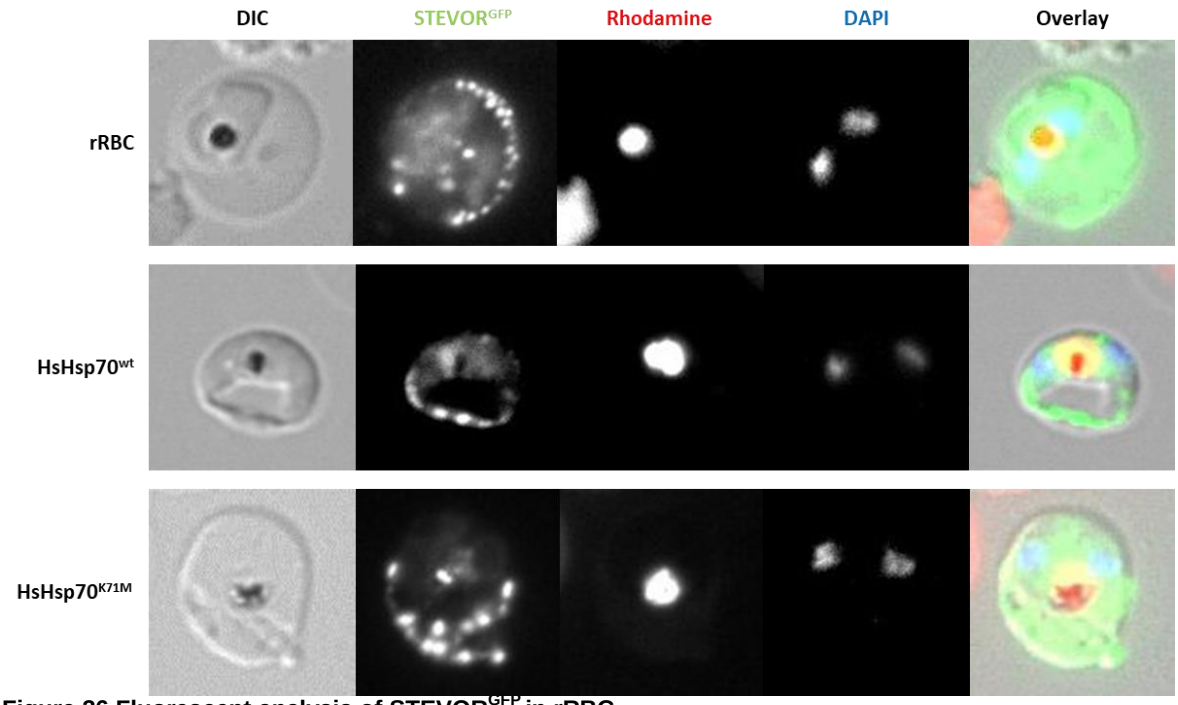

Figure 36 Fluorescent analysis of STEVOR^{GFP} in rRBC
Live cell imaging of STEVOR^{GFP} in rRBC (rRBC), rRBC pre-loaded with an excess amount of HsHsp70^{wt} (HsHsp70^{wt}) or HsHsp70^{K71M} (HsHsp70^{K71M}). Nucleus was visualised by DAPI. 63x objective magnification, DIC: Differential Interference Contrast.

In closing, in both SBP1 and STEVOR infected cells, the pattern looked different to non-resealed cells, but there appeared to be no recognisable difference between the 3 resealed cell populations. These data imply that the parasite does not hijack HsHsp70 for its own purposes and are supporting the obtained data from the previous sera experiments.

3.6 Evaluating the function of ovalbumin for the intra-erythrocytic development

It was noted that during the growth analysis of wildtype 3D7 and ΔHsp70x in rRBC, both displayed a significant increased growth profile after 96 h upon addition of protein compared to the control rRBC. The 3D7 showed an increased growth upon the addition of HsHsp70^{wt} (Figure 27), while the ΔHsp70x revealed an increased growth in the presence of both HsHsp70^{wt} and HsHsp70^{K71M} (Figure 32). These results raise the possibility that parasites used the added HsHsp70 as a nutritional source, leading to a growth advantage. To address this hypothesis, it was tested whether the addition of a random protein to the rRBC led to the same

positive effect. For this purpose, ovalbumin, a common protein in chicken egg white, was pre-loaded to the RBC. First, the pre-loading and entrapment of ovalbumin to the erythrocyte was analysed. The immunoblot analysis using an anti-ovalbumin antibody revealed that protein uptake during the resealing process was achieved (Figure 17A). Further, with a standard consisting of different ovalbumin concentrations the exact amount in ng was determined by ImageJ quantification, revealing an approximately 28 ng uptake of ovalbumin/10^7 erythrocytes. This is in good agreement with the determined 30 ng of HsHsp70$^{wt/K71M}$ observed in the previous experiments (Figure 17B). Additionally, the haemoglobin amount was determined for rRBC and the rRBC containing ovalbumin (Oval) by measuring the absorbance at 570nm. A sample consisting of wildtype erythrocytes (non-resealed) was set as 100% and the respective percentages for the rRBC samples were calculated accordingly. Both rRBC and rRBC pre-loaded with ovalbumin showed 40% haemoglobin compared to wildtype RBC (Figure 17C).

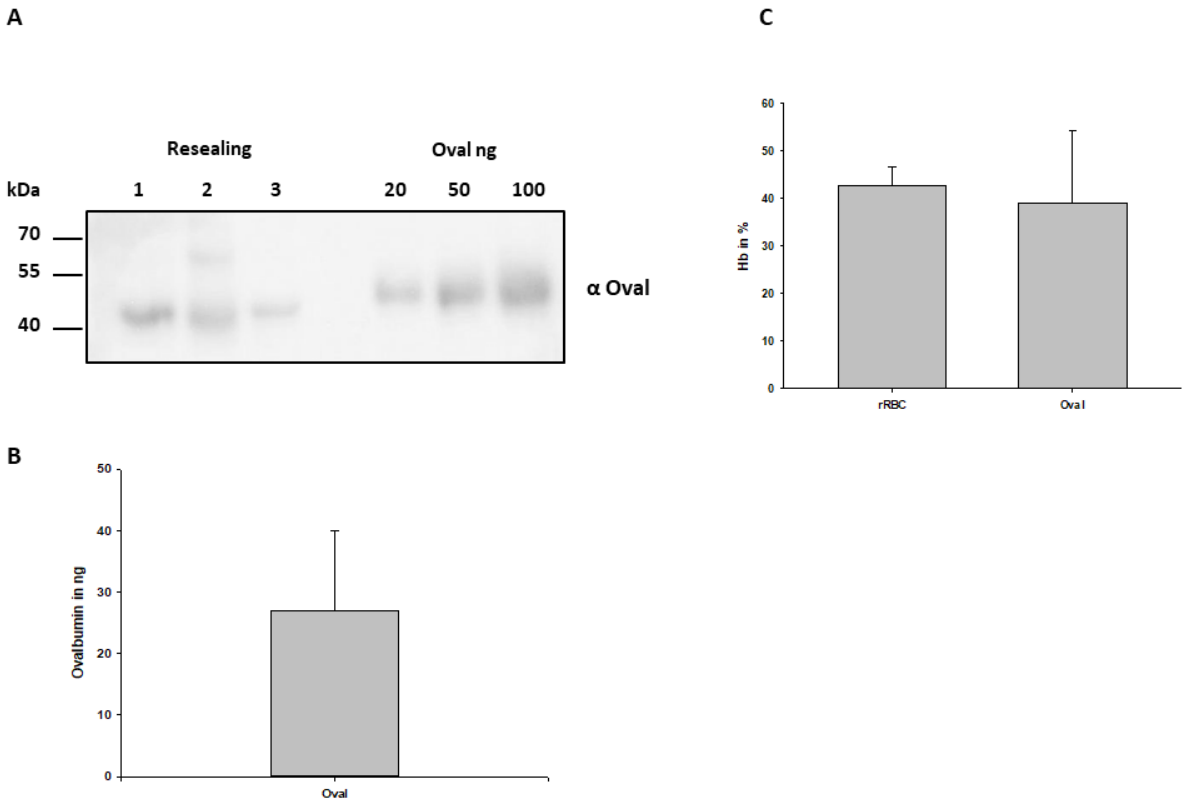

Figure 37 Immunodetection of ovalbumin in rRBC

(A) Immunoblot of rRBC (10^7) pre-loaded with ovalbumin (Resealing 1-3) separated on a 12% SDS gel. A standard of different ovalbumin concentrations ranging from 20-100 ng were loaded, as well. Bands were visualised with an anti-ovalbumin sera and the size marker in kDa is indicated on the left side. Oval: Ovalbumin.

(B) ImageJ quantification of ovalbumin (Oval) enclosed in rRBC during the resealing in ng/10^7 RBC. The concentration was determined with the help of the standard of 20-100 ng ovalbumin. Bar chart with standard deviation shows results of 3 independent resealing reactions.

(C) Haemoglobin amount in percent of rRBC (rRBC) and rRBC preloaded with ovalbumin (Oval) compared to non-resealed wildtype erythrocytes determined with the absorbance at 650 nm. Bar chart with standard deviation marks results of 3 independent resealing reactions.

After ensuring that the rRBC were pre-loaded with ovalbumin and equal haemoglobin amounts were achieved, the pre-loaded rRBC were used in another growth assay, which in contrast to previous experiments also included non-resealed wildtype erythrocytes. The RBC, rRBC and rRBC with ovalbumin were infected with MACS purified 3D7 wildtype parasites. Growth was monitored after 48 h and 96 h. The parasites were fixed with 4% PFA and stained with DAPI to visualise the parasites. Finally, growth was analysed using flow cytometry and gating was performed according to Figure 26. There was significant less growth observed for the rRBC and rRBC with ovalbumin compared to the RBC after 48 as well as 96 h. Interestingly, parasites grown in the presence of ovalbumin presented a slight increase in growth after 48 h compared to the rRBC, although not significantly. Surprisingly, irrelevant of the rRBC pre-loaded with or without

protein, parasites showed small relative growth after 96 h, comparable to the BFA control samples. However, the addition of ovalbumin caused a small, but insignificant difference in growth compared to the rRBC control (Figure 38).

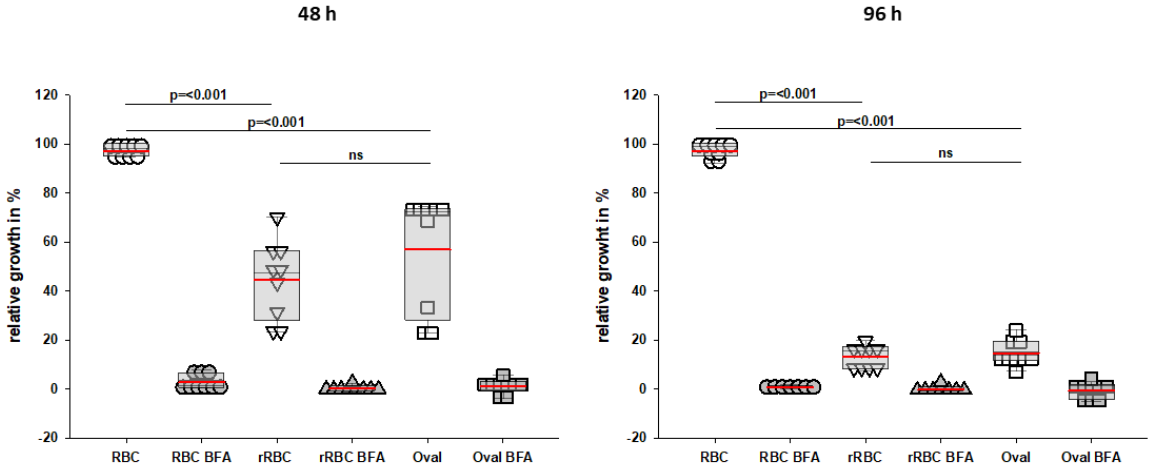

Figure 38 Growth analysis of 3D7 wildtype parasites in rRBC pre-loaded with Ovalbumin
Flow cytometry assay of 3D7 parasites grown in RBC, rRBC, rRBC pre-loaded with an excess amount of ovalbumin (Oval) for 48 h and 96 h. Parasites were treated with BFA (50 µg/mL) as a positive control for parasite death. Dot blot with box indicates relative growth in percent of 3 independent experiments. The parasitemia of RBC was set as 100%. Background of non-infected RBC, rRBC and rRBC with ovalbumin stained with DAPI were subtracted, respectively. The mean values are indicated by a red dash and statistical significance was determined by the One-Way ANOVA-Holm Sidak test.

This analysis revealed only a slightly increased growth for rRBC compared to the BFA control after 96 h and suggested that parasites cannot propagate efficiently in rRBC for 2 full cycles. For this reason, the parasitemia in percent was compared between RBC and rRBC. Indeed, parasites grown in the rRBC presented lower parasitemia after 48 h and were, compared to the RBC control, not able to increase their parasitemia after 96 h (Figure 39).

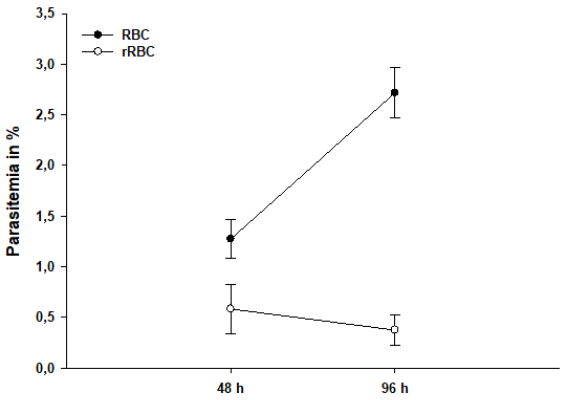

Figure 39 Parasitemia in rRBC and RBC determined after 48 and 96 h
3D7 wildtype parasites grown in RBC as well as rRBC for 48 and 96 h. Parasitemia was determined in percent by flow cytometry and results of 3 independent experiments with standard deviation is presented.

In sum, the ovalbumin experiments did not verify the hypothesis that the addition of protein alone had a favourable effect on parasite growth in rRBC. However, parasites barely propagate in the rRBC after 48 h.

3.7 Growth analysis of HsHsp70 *P. berghei* infected human liver cells

Results so far have not shown an essential function of HsHsp70 for the intra-erythrocytic development of *P. falciparum*. Yet, HsHsp70 may still be important for other stages of the complex parasite life cycle e.g. the liver stages. To clarify whether HsHsp70 is vital to the liver stages of *P. berghei*, the agent causing rodent malaria, a growth analysis was performed. To this end, an HsHsp70 downregulation using siRNA in the human carcinoma liver cells, HuH7, was performed. A siRNA directed against HsHsp70 as well as scrambled RNA (negative control) were purchased. First, different concentrations of the siRNA and scrambled RNA (scraRNA) were tested and introduced by a lipofectamine transfection into the cell. Additionally, a control which was only treated with lipofectamine (Mock) and a positive control (PC) were included. The downregulation was controlled using immunoblotting against HsHsp70 and GAPDH (loading control). In fact, all used siRNA concentrations showed downregulation of HsHsp70, while usage of the scraRNA did not lead to a downregulation (Figure 40A). The ImageJ quantification determined a good downregulation to ~35% of HsHsp70 already with the lowest concentration of 5 pmole siRNA. At the same concentration the scrambled siRNA revealed no downregulation (Figure 40B).

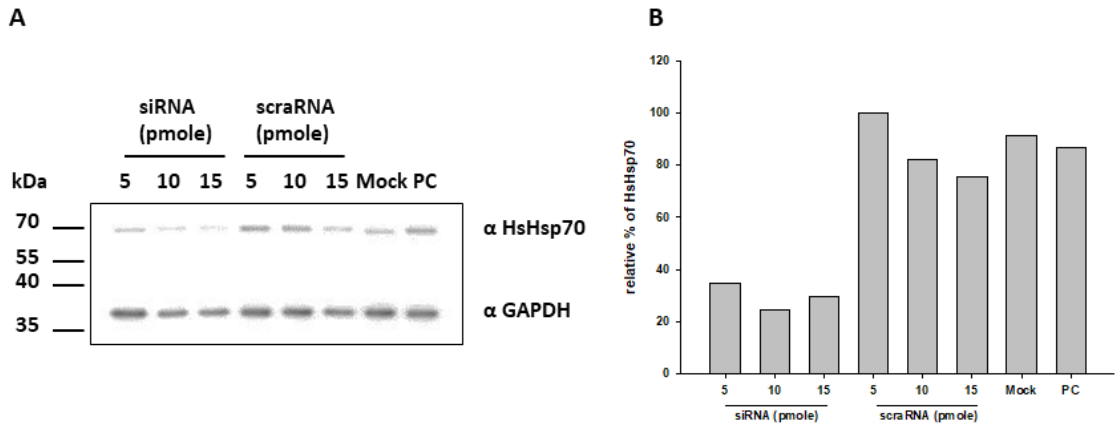

Figure 40 HsHsp70 siRNA downregulation in HuH7 cells

(A) Immunoblot analysis of HuH7 liver cells transfected with different concentrations of siRNA and a control scrambled RNA (scraRNA). Bands were visualised with sera directed against HsHsp70 and GAPDH acting as a loading control. The mock control was only treated with lipofectamine and the positive control (PC) was untreated. The size marker in kDa is indicated on the left side.

(B) ImageJ quantification of relative HsHsp70 amount in percent from (A). The HsHsp70 amount was normalised against GAPDH and the relative HsHsp70 amount was calculated according to the highest determined value by ImageJ. Result of 1 experiment is shown.

As 5 pmole siRNA resulted in a downregulation with the cells still appearing healthy, this concentration was chosen for all further experiments. The HuH7 cells were reverse transfected with 5 pmole of either siRNA, scraRNA or were only treated with lipofectamine (mock). 48h post-transfection, cells were harvested and analysed by immunoblotting for downregulation. Indeed, only a faint band for HsHsp70 was detected in cells treated with the siRNA. Both controls scraRNA and mock showed presence of HsHsp70 (Figure 41A). An ImageJ quantification revealed that only ~20% HsHsp70 remained after the siRNA downregulation. In comparison to both controls, the HsHsp70 amount was significantly decreased by the siRNA (Figure 41B). To assess the specificity of the used siRNA, which was only directed against HsHsp70 and not the cognate form HsHsc70, the same samples of HuH7 cells treated with either the siRNA, scraRNA or the mock control were examined by immunoblotting against HsHsc70. All 3 samples displayed a comparable amount of HsHsc70 and did not show a downregulation of HsHsc70 by the siRNA (Figure 41C). The ImageJ quantification did not present any downregulation of HsHsc70, as well (Figure 41D).

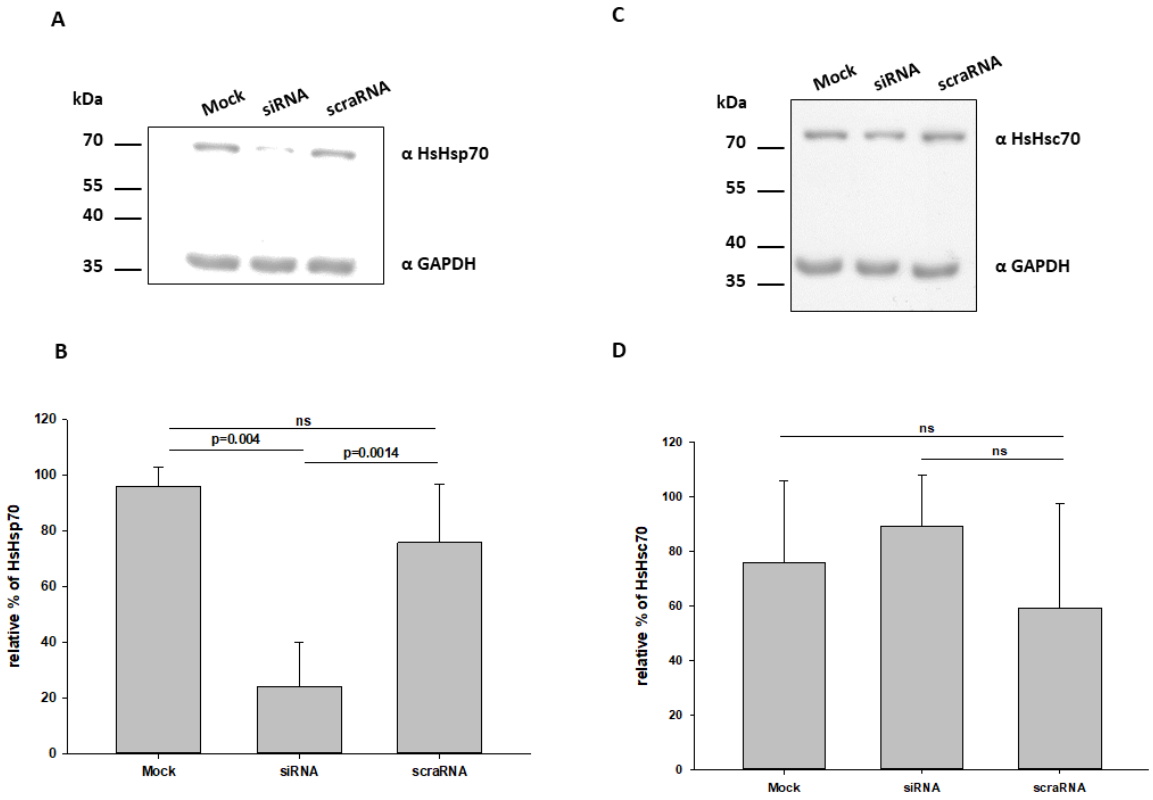

Figure 41 Amount of HsHsp70 and HsHsc70 in downregulated HuH7 cells

(A) Immunoblot analysis of HuH7 liver cells transfected with 5 pmole siRNA or a control scrambled RNA (scraRNA). Bands were visualised with sera directed against HsHsp70 and GAPDH acting as a loading control. The mock control was only treated with lipofectamine and the positive control (PC) was untreated. The size marker in kDa is indicated on the left side.

(B) ImageJ quantification of relative HsHsp70 amount in percent from (A). The HsHsp70 amount was normalised against GAPDH and the relative HsHsp70 amount was calculated according to the highest determined value by ImageJ. Bar chart with standard deviations shows results of 3 independent experiments. The statistical significance was determined by the One-Way ANOVA-Holm Sidak test.

(C) Immunoblot analysis of HuH7 liver cells transfected with 5 pmole siRNA and a control scrambled RNA (scraRNA). Bands were visualised with sera directed against HsHsc70 and GAPDH used as loading control. The mock control was only treated with lipofectamine and the positive control (PC) was untreated. The size marker in kDa is indicated on the left side.

(D) ImageJ quantification of relative HsHsc70 amount in percent from (C). The HsHsc70 amount was normalised against GAPDH and the relative HsHsc70 amount was calculated according to the highest determined value by ImageJ. Results of 3 independent experiments are shown in bar chart with standard deviation. The statistical significance was determined by the One-Way ANOVA-Holm Sidak test.

Additionally, 48 h post-transfection the downregulated HuH7 cells were infected with *P. berghei* sporozoites. After 2 h, sporozoites that did not infect the liver cells were washed away and non-fixed parasite liver stages were analysed 48 h post-infection by flow cytometry. The used sporozoites expressed GFP under control of the CircumSporozoite promoter (CS promoter), while RFP was expressed under the elongation factor 1 α (eF1α) promoter. The CS promoter is only active till 24 h post-invasion thus, only GFP-expressing liver stages were analysed. First, using non-infected HuH7 the gate for GFP positive cells was set. Finally,

the gating was controlled by a sample of infected HuH7 cells (Figure 42). An example of the whole gating strategy can be seen in Figure 49 (appendix).

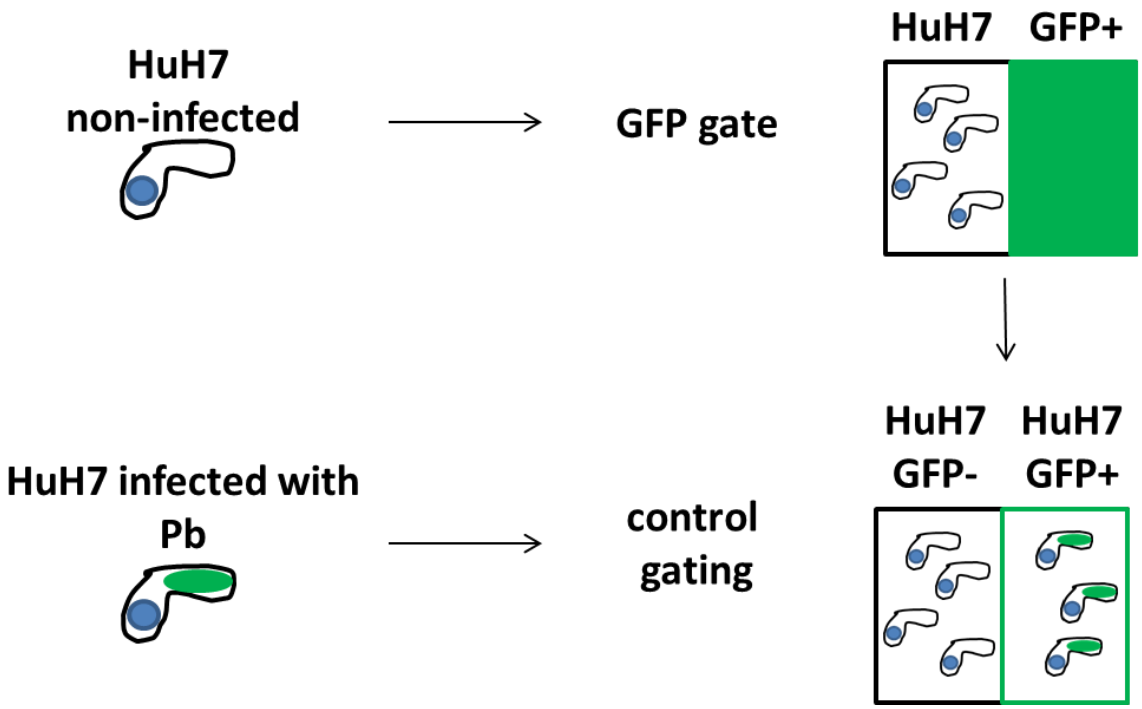

Figure 42 Gating strategy for HuH7 cells infected by *P. berghei*
Flow cytometry gating strategy of GFP positive cells detected in HuH7 cells. Non-infected HuH7 cells were used to set the gate for GFP positive cells (GFP+). The GFP gating was controlled by *P. berghei* (Pb) infected HuH7 cells.

After ensuring a proper gating, the growth of *P. berghei* liver stages in the HuH7 downregulated cells was analysed. However, no decrease in growth was displayed for a downregulation of HsHsp70 (Figure 43A). Although, the power of the performed statistical test was below the desired power and in consequence it is less likely to detect a difference when one actually exists, indicating the need for more repetitions.

A flow cytometry analysis enables not only counting of a distinct cell population, but also allows comparison of the cell's size. Therefore, the geometric mean acquired from the different cells was compared (Figure 43B). Interestingly, cells treated with the scraRNA displayed a significant increase in size.

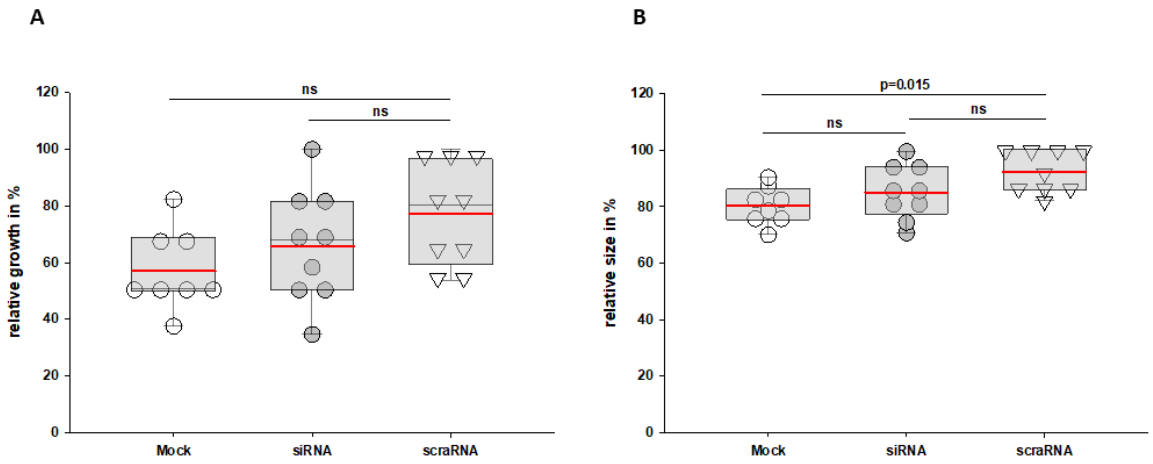

Figure 43 Growth and size of *P.berghei* in HuH7 cells with downregulated HsHsp70 amount after 48 h post-invasion

(A) Flow cytometry assay of *P. berghei* parasites in HuH7 treated with lipofectamine (mock), with 5 pmole siRNA directed against HsHsp70 (siRNA) or scraRNA (scraRNA) 48 h post-invasion. Dot blot with box marks relative growth in percent of 3 independent experiments. The highest parasitemia of each assay was set as 100%. Background of non-infected HuH7 was subtracted. The mean values are indicated by a red dash and statistical significance was determined by the One-Way ANOVA-Holm Sidak test.

(B) Analysis of geometric mean determined by flow cytometry (based on A). Dot blot with box indicates relative size in percent. The highest geometric mean of the single experiment was set as 100%. The red dash symbols statistical significance which was determined by the One-Way ANOVA-Holm Sidak test.

In summary, a specific downregulation of HsHsp70 to ~20% was achieved in HuH7 cells. Remarkably, *P. berghei* did not fail to develop in HuH7 with a decreased HsHsp70 amount. In spite of this, more experiments are needed to verify the results.

3.8 Conclusion

This study investigated the role of HsHsp70 in the asexual intra-erythrocytic life cycle of *P. falciparum*. To this end, a resealing method was successfully established, which allowed the entrapment of 30 ng pure, untagged HsHsp70^{wt} or HsHsp70^{K71M} into the rRBC. The performed growth assay with the 3D7 wildtype as well as the ΔHs70x did not demonstrate an essential function for the development of the parasite. However, it was noted that parasites displayed a significantly increased growth after 96 h in the presence of excess amounts of HsHsp70^{wt} and HsHsp70^{K71M}. Therefore, it was hypothesised that parasites used the 2 added proteins as a nutritional source, leading to a growth advantage. Nonetheless, experiments with 30 ng ovalbumin entrapped in rRBC did not support this hypothesis. Further, the comparison of the growth of RBC with rRBC

over 48 and 96 h disclosed that parasites barely propagate after 96 h in rRBC, indicating that a great deal of attention must be paid when interpreting the growth data after 96 h. Interestingly, first results demonstrated that HsHsp70 was not essential for the exo-erythrocytic development of *P.berghei*. At last, in contrast to previous translocation studies, it was not shown that HsHsp70 is involved in protein transport to the host cell cytosol.

4 Discussion

To this day, not much is known about the complex mechanisms underlying protein trafficking from the parasite to a host cell that lacks any protein transport infrastructure (Elsworth et al., 2014). However, it is well established and understood that the parasite drastically changes the appearance and the biophysical properties of the infected erythrocyte (Cowman et al., 2016; Phillips et al., 2017). These host cell modifications are closely related to the disease's pathology and are essential to the survival of the parasite (Cowman et al., 2016; Phillips et al., 2017). It was long debated how the parasite-encoded proteins are able to cross so many membranes like the PPM, PVM and can even be presented on the surface of the infected erythrocyte. In particular, the crossing of the PVM was debated intensively (Charpian and Przyborski, 2008). In the end, the discovery of the PTEX translocon located in the PVM (de Koning-Ward et al., 2009) has considerably deepened the knowledge and set the stage for new theories. As previously discussed in detail in 1.4.4 a lot of data implicated an essential role of HsHsp70 for the intra-erythrocytic development of *P. falciparum* (Alampalli et al., 2018; Ansorge et al., 1996; Banumathy et al., 2002; Charpian, 2008; Günnewig, 2016; Jha et al., 2017; Külzer et al., 2012) which was analysed in this study.

4.1 The role of HsHsp70 for intra-erythrocytic survival of the parasite

During the maturation the erythrocyte lost classical eukaryotic organelles such as the rough ER, Golgi apparatus, mitochondria and the nucleus (Gronowicz et al., 1984) making the human mature erythrocyte not an easy target for genetic manipulations. Consequently, it was not possible to generate erythrocytes that are deficient of HsHsp70. Further, the depletion of HsHsp70 e.g. by Co-IP was discharged as a possible strategy due the fact that HsHsp70 binds to hydrophobic stretches in their client proteins (Rüdiger et al., 1997). The Co-IP method might potentially not only result in the deletion of HsHsp70 from the human mature erythrocyte, but also significantly reduce the amount of client proteins and other chaperones (Berndt, 2014). It is well established that

mutations in HsHsp70 are associated with several diseases, such as multiple sclerosis, and an increased cancer risk (Boiocchi et al., 2014; Jalbout et al., 2003; Mestiri et al., 2001). Using the blood of these patients would be an alternative to study the effects of HsHsp70 for intra-erythrocytic development of *P. falciparum*. Nonetheless, it would be challenging to collect enough fresh material, since the blood cannot be older than 2 weeks as parasites cannot multiply efficiently in older cells (Kim et al., 2007). On the other hand, acquiring the official permission by the ethics committee to use the blood from patients that are already suffering from a disease might be a challenging and time consuming process.

As a result from the lack of options, a resealing or pre-loading process, which was used to introduce a dominant negative effect, was chosen to investigate the role of HsHsp70 for the intra-erythrocytic development of the parasite. The resealing method is widely used in pharmacology (Bourgeaux et al., 2016; Magnani et al., 1998, 2002; Rossi et al., 2005). Several test experiments were performed before a reproducible method with a sufficient resealing efficiency was established. Further, it was ensured that the rRBC were still infected by *P. falciparum* (Figure 13). For the dominant negative effect the HsHsp70^{K71M} mutant, which is unable to hydrolyse ATP, was chosen (O'Brien et al., 1996). First, it was tested if HsHsp70^{K71M} can be entrapped into the erythrocyte. Indeed, a 5- to 6-fold increase in HsHsp70^{K71M} compared to rRBC was accomplished (Figure 18). Then, the growth of *P. falciparum* 3D7 parasites in the presence of HsHsp70^{K71M} was analysed after 48 and 96 h. Interestingly, the growth after 48 h was not affected by the presence of HsHsp70^{K71M} (Figure 27). Also the usage of ΔHsp70x parasites did not display any difference in the growth profile for the presence of an excess amount of HsHsp70^{K71M} after 48 h (Figure 32). Notably, both parasite strains showed increased growth after 96 h upon the addition of the 2 proteins. Therefore, it was hypothesised that the improved growth was caused by increased protein amount, which might function as a nutritional source for the parasite. This theory was tested by entrapping the same amount of ovalbumin, the main protein in chicken egg white, to the erythrocyte using the same protocol as for the HsHsp70 proteins (Figure 37). Surprisingly, the addition of ovalbumin did not lead to a growth advantage for the parasite (Figure 38). In consequence,

the simple addition of more protein does not lead to a growth advantage. Yet, it might be that more repeats are needed as so many factors play role in the assay and for the growth of the parasite, which might be hiding a statistically significant effect. These ovalbumin experiments also included a control of wildtype non-resealed erythrocytes. The comparison of direct parasitemias after 48 and 96 h in erythrocytes and rRBC clearly showed that parasites cannot propagate in rRBC after 48 h (Figure 39). Consequently, considerable attention must be paid when interpreting the results after 96 h.

In addition, the different intra-erythrocytic parasite stages were analysed by a SYBR green staining. The 3D7 parasites displayed significantly less schizonts after 48 h, which would typically come along with a reduced number of ring stages after 96 h. However, this effect was not detected after 96 h (Figure 29). An explanation for this discrepancy can be found in the number of experiments. For the 3D7 strain only 2 independent experiments were performed and showed big variations in the determined numbers. Usually, SYBR green staining allows the determination of the exact number of merozoites. For this purpose, the erythrocyte membrane is permeabilised, followed by an RNase digest and subsequent staining. Unfortunately, due to the permeabilisation, the rhodamine signal marking rRBC in flow cytometry experiments was lost (data not shown). Thus, the experimental setup had to be changed and might not yet be fully adjusted to the rRBC. Another pitfall of this experiment is the missing gating control for ring/trophozoites and schizonts. Still, the strongest explanation for the discrepancy might be found in the already poor survival rate of the parasites in rRBC after 96 h. The development of the different stages for the ΔHsp70x parasites was also analysed. In general, 3 independent experiments for the ΔHsp70x parasites were conducted and also showed big variations. However, no significant differences in the number of ring/trophozoites and schizonts were spotted (Figure 33). Although, the SYBR green staining results should be interpreted with caution, however, as similar to the DAPI staining, no effect on the parasite's development in the presence of HsHsp70^{K71M} was found.

There are 2 possible explanations why the presence of HsHsp70^{K71M} did not show an effect on the intra-erythrocytic development of the parasite. Either, a technical problem with the dominant negative caused the lack of an effect, or

HsHsp70 is simply not pivotal to the survival of the parasite in the used experimental setup.

A classical dominant negative effect is achieved by overexpressing a mutated gene to such a high extent that the function of the wildtype protein is disrupted by the mutated version. This definition was established in 1987 by Herskowitz (Herskowitz, 1987). Most studies in the literature use a classical dominant negative on DNA basis and introduced a hetero- or homozygote mutation, which is overexpressed by the cell, leading to a classical dominant negative effect (Millauer et al., 1994; Zhong et al., 2003). Dominant negative mutations on Hsp70 have mostly been analysed by *in vitro* systems such as refolding and ATPase assays containing only few partners (Arakawa et al., 2011; Fontaine et al., 2015; O'Brien et al., 1996; Szabo et al., 1994). In this study, a classical dominant effect was introduced in a cell system and it is possible that the behaviour of the dominant negative might be different in this more complex system. However, some studies used HsHsc70 and HsHsp70 dominant negative mutations to assess their functions in *in vivo* systems and revealed no loss of function (Fontaine et al., 2015; Lagaudrière-Gesbert et al., 2002; Newmyer and Schmid, 2001).

Yet, sometimes these classical dominant negatives can also be without an effect as seen for a study published by Abraira and colleagues (Abraira et al., 2010). In this study, it was elucidated whether a mutated receptor tyrosine kinase ErbB is associated with the loss of Netrin-1 expression, a factor essential for the canal formation of the inner ear. A classical dominant negative was achieved by expressing a mutated ErbB from a virus that infected a chicken embryo (Abraira et al., 2010). Interestingly, in contrast to *in vitro* experiments that closely associated non-functional ErbB signalling as the cause of malformations of the inner ear canal, the *in vivo* overexpressed ErbB mutant did not alter the formation of the chicken inner ear canal (Abraira et al., 2010). Consequently, Abriaira and colleagues were not able to exclude that the low amount of remaining wildtype ErbB is enough to ensure proper signalling (Abraira et al., 2010). This would also provide a suitable explanation why HsHsp70^{K71M} did not show any effect on parasite growth.

The amount of residual endogenous HsHsp70 might be enough to provide the driving force for the translocation of essential parasite-encoded proteins. For the resealing assay a 5- to 6-fold excess amount of the mutant HsHsp70^{K71M} was introduced into the cell to disrupt or interfere with the function of the endogenous HsHsp70. A similar amount of HsHsp70^{K71M} presented a repressing effect in a previous translocation study and indicated a functional dominant negative effect (will be discussed in more detail in 4.2). In consequence, since the same amount of HsHsp70^{K71M} already blocked the function of the endogenous HsHsp70 in the translocation assay, it is tempting to speculate that a similar effect should be achieved in the rRBC.

The fact that there are lots of publications associating HsHsp70 with the transport of parasite-encoded proteins (reviewed in 1.4.4) led to the assumption that HsHsp70 might be essential to the parasite survival. Since the chaperone system is such an important system to the well-being of a cell, it cannot be ruled out that other chaperones might compensate for the dominant negative effect. Many other chaperones can be found in the erythrocyte e.g. HsHsc70, HsHsp90, HsHsp60 (TRiC) and PfHsp70x (D'Alessandro et al., 2010; Külzer et al., 2012). All those chaperones have overlapping functions and might compensate for the blocked HsHsp70 and would thereby ensure the survival of the parasite.

During the study the survival of ΔHsp70x parasites in the presence of an excess amount of HsHsp70^{K71M} was investigated, as well. Since, Hsp70x is the only parasite-encoded and exported chaperone in the host cell (Külzer et al., 2012) it would be an excellent candidate for compensation. Most strikingly, Hsp70x is only expressed in *P. falciparum* and *P. reichenowi* (infecting chimpanzee), representatives of the Laveranian species (Külzer et al., 2012). In particular, Laveranian species are known to cause more lethal malaria forms by cytoadhering to the vascular endothelium (Charnaud et al., 2017). First, it was speculated that Hsp70x might be essential for the parasite's survival due to its special link to the Laveranian species. However, Hsp70x depletion *in vitro* was not lethal to *P. falciparum* and only smaller effects on the export of EMP1, thereby reducing cytoadherence, were detected (Charnaud et al., 2017). In consequence, it might be that protein transport in ΔHsp70x parasites was assisted by HsHsp70. Nevertheless, the blockage of HsHsp70 by the dominant

negative version and usage of the ΔHsp70x parasites did not display a growth defect.

Another possible candidate is the cognate form HsHsc70. It is possible that the wrong Hsp70 was investigated in this study. In particular, the pulldown assay performed with components of the PTEX translocon point towards HsHsc70. Here, HsHsc70 was found to be 6-fold enriched at the translocon, which is highly indicative for a role in the transport of parasite-encoded proteins (de Koning-Ward et al., 2009). However, other studies e.g. Zhang and colleagues found HsHsp70 to be a member of the J-dot chaperone complex, which is closely associated with the transport of EMP1 (Külzer et al., 2012, 2010; Zhang et al., 2017). Moreover, a study using HsHsp70^{K71M} did efficiently block the transport of a parasite-encoded protein (Günnewig, 2016).

An additional interesting candidate for a role in the transport of parasite encoded proteins can be assigned to HsTRiC. Batinovic and colleagues found HsTRiC as well as HsHsp90 to be associated with EMP1. Hence, it was proposed that EMP1 trafficking and folding is performed by these human chaperones (Batinovic et al., 2017).

Apart from the experiments in *P. falciparum* also *P. berghei*, the *Plasmodium* species causing malaria in rodents, was investigated. Most strikingly, HsHsp70 was also dispensable for the development of the exo-erythrocytic liver stages (Figure 43A). However, HuH7 cells were stressed by the lipofectamine treatment indicated by lots of cell debris (see appendix Figure 49). Usually, the infection is additionally analysed and quantified by fluorescence microscopy. Here, HuH7 were infected with GFP-labelled sporozoites allowing an easy analysis. By flow cytometry a high parasitemia was detected in all samples, which was confirmed from first glances. Further, in accordance with the determined numbers by flow cytometry, HsHsp70 downregulated cells did not present fewer parasites, but due to time restrictions no quantification was performed. Notably, HsHsp70 was reduced to ~20% by siRNA addition (Figure 41B). As a result, it cannot be excluded that the residual HsHsp70 is sufficient to ensure the survival of the parasite. Furthermore, it is possible that the reduction in the HsHsp70 concentration led to an increased HsHsc70 expression. Indeed, the HsHsc70

amount was slightly elevated in the siRNA treated cells, but not significantly (Figure 41D). In general, the HuH7 experiments did not reveal an essential role in parasite survival, although a completely different stage of the parasite's life cycle and even a different parasite species were investigated. In the end, further experiments are needed to secure the phenotype.

Altogether, chaperones might be such a redundant system that it might be challenging to block protein folding and trafficking by interfering with one chaperone to provoke a fatal outcome. As seen for ΔHsp70, the parasite might sometimes survive, despite the protein transport being altered (Charnaud et al., 2017), which was also investigated in this study.

4.2 HsHsp70 and its role in protein transport across the PVM

Apart from the role of HsHsp70 for the survival of the parasite, it was also investigated whether HsHsp70 is essential to the export of parasite-encoded proteins to the host cell. A previously mentioned study conducted by J. Günnewig used a complex translocation assay to investigate the role of HsHsp70 for protein transport using a classical dominant negative assay (Günnewig, 2016). Briefly, mid-stage trophozoites were subjected to a tetanolysin permeablisation, leading to the lysis of the erythrocyte membrane, while the PVM and PPM were still intact. Afterwards, the host cell cytosol was removed by intensive washing and finally the permeabilised trophozoites were placed in a medium containing host cell cytosol of non-infected erythrocytes, which was enriched with an excess amount of the HsHsp70^{K71M}. Then, the translocation process of the marker protein GBP130 across the PVM was followed. This approach was successfully used to obtain the first experimental data that HsHsp70 is essential for the translocation of GBP130. In this study, the presence of HsHsp70^{K71M} did not affect the protein export as shown by sera experiments using neither the wildtype 3D7 parasite nor the ΔHsp70x parasites (Figure 31 and Figure 34). Further, microscopic analysis of the export of STEVOR^{GFP} and SBP^{GFP} was negative (Figure 35 and Figure 36). There are several explanations for the discrepancies between the translocation data and the findings of this study.

As previously stated and discussed in detail in 4.1, the dominant negative assay has major drawbacks concerning its efficiency. However, already for the translocation assays a similar amount of HsHsp70^{K71M} was added to host cell cytosol as for the resealing assays. In the end, both experiments used a 5- to 6-fold excess of HsHsp70 compared to the respective assay controls (Figure 18C). Thereby indicating that the used amount of HsHsp70^{K71M} entrapped in the rRBC should be enough, since the translocation assay clearly showed an effect, which is in favour of a functional dominant negative effect and weakens the hypothesis of a technical malfunction during the assay.

However, the used resealing assay is accompanied with other technical challenges. In general, if the protein transport is affected by the dominant negative, the infected erythrocyte's cytoadherence capability as well as its rigidity can be altered. Mostly, these changes are investigated by classical cytoadherence or artificial spleen assays. Due to the fragile nature of the rRBC neither of the 2 methods were available. As an alternative, infected rRBC were incubated with PHIS from the malaria-endemic area (Kelifi, Kenya) to detect differences in the surface expression. Interestingly, neither the use of wildtype parasites nor ∆Hsp70x parasites grown in the presence of HsHsp70^{K71M} blocked the surface expression of malaria antigens (Figure 31 and Figure 34). Today, it is well-established that the immune sera can already identify early exported surface proteins, including antigens like RESA (Ring-infected Erythrocyte Surface Antigen) (Coppel et al., 1984) and the major virulence factor EMP1 (Beeson et al., 2006; Chan et al., 2014). It is therefore assumed that the sera experiments performed in this study were suitable to detect a potential differential surface expression of the major virulence factor EMP1. However, the results presented here, indicate that HsHsp70 is not associated with EMP1 trafficking.

In addition to the sera experiments, a microscopic analysis using GFP-labelled SBP1 and STEVOR was conducted (Figure 35 and Figure 36). In agreement with the sera experiments, the transport of both GFP-labelled proteins was not affected by the presence of the HsHsp70^{K71M}. One explanation for the discrepancies between the translocation and resealing assays, regarding the involvement of HsHsp70, might be found in the nature of the assays. In the translocation assay the cells are treated with cycloheximide, which blocks the

parasite's protein biosynthesis, causing the parasite's death. The "dead" parasites are placed in medium containing the cell lysate of a non-infected cell. The rRBC with an excess amount of HsHsp70^{K71M} resembles the *in vivo* situation more closely and can sustain parasite propagation and survival for at least one complete cycle. In theory and in practice, the parasite is able to export proteins to the resealed host cell since the parasite relies on this protein trafficking and can survive in rRBC. In consequence, in the rRBC Hsp70x might be exported, which might compensate for the presence of the mutated HsHsp70^{K71M}. Interestingly, usage of the ∆Hsp70x parasites did not show any difference in the surface expression of the HsHsp70^{K71M}, as well. Since Hsp70x is so far the only parasite-encoded and exported chaperone to the host cell, this does not favour the strain of argumentation. However, it is still possible that thus far unidentified parasite-encoded and exported chaperones are involved in the transport. The experiments using rRBC have a higher similarity to the *in vivo* situation than the translocation assay and involve a more complex environment, which presumably caused the different outcomes in these 2 assays.

Finally, in the translocation assays a single marker protein for export was analysed. GBP130 is a non-essential exported protein and carries a PEXEL motif (Grüring et al. 2012). The protein was not included in the analysis of the sera experiments or the microscopic assay. Some proteins require the assistance of several chaperones in a random or sometimes also ordered process. One example is the von-Hippel-Lindau (vHL) protein, a well-studied tumour suppressor. For the functional vHL even a tight progression of chaperones is pivotal (Melville et al., 2003). First, this protein has to be folded by HsHsp70, before TRiC can carry out additional modifications and create the functional vHL protein (Melville et al., 2003). Thus, it is possible that GBP130 requires only HsHsp70, while the investigated EMP1, SBP1 and STEVOR need help of a whole multi-chaperone system which is redundant. Preliminary data obtained during the translocation study indicated that HsHsp70 might be only associated with the transport of GBP130, as the export of Hsp70x was analysed revealing trafficking to the host cell despite the presence of HsHsp70^{K71M} (personal communication J. Günnewig and J. Przyborski). Consequently, no effects would be detected for the investigated proteins (STEVOR, SBP and EMP1) by the

presence of HsHsp70^{K71M} and potential effects on GBP130 were missed as this protein was not analysed.

In general, it is hard to compare the results of the resealing and the translocation assays. A final conclusion regarding the involvement of HsHsp70 for the protein trafficking is impossible to draw. The HsHsp70 might be assisting in the transport to a certain extent, but at least according to the assays used in this study, is not essential for transport of parasite-encoded proteins into the host cell.

4.3 HsHsp70 localisation in the non-infected and infected erythrocyte

During the last 10 years, several efforts failed to localise HsHsp70 in the non-infected as well as infected erythrocyte using classical immunofluorescence assays (personal communication J. Przyborski). Consequently, in this study HsHsp70^{wt} was fluorescently labelled with Oregon green and subsequent pre-loading to the erythrocyte was used to visualise HsHsp70-Oregon green. In the non-infected rRBC, HsHsp70-Oregon green displayed mobile foci throughout the whole erythrocyte (Figure 20). The experimental setup included 2 controls; (i) BSA labelled with Oregon-green, and (ii) the dye itself. Both controls presented an equal fluorescence spread all over the cytosol (Figure 20). Interestingly, HsHsp70 usually shows an equal distribution in the cell cytosol of various human cell types as advertised on the webpages of several commercial antisera vendors (e.g. Abcam, Santacruz) and not as mobile foci. However, due to the controls' localisation, it is likely that HsHsp70 might indeed localise as mobile foci in the non-infected erythrocyte, even though such a localisation is rather rare. Unfortunately, the localisation studies in the infected rRBC using Cy2 labelling of the purified HsHsp70^{wt} were not satisfying. In the infected rRBC, HsHsp70^{wt}-Cy2 revealed an unexpected signal inside the parasite (Figure 21). During the course of the study it was noted that the previously cytosolic rhodamine signal presented a strong fluorescence inside the parasite particularly in the trophozoite stage. It is known that the parasite uses the host haemoglobin in the cytosol as a nutritional source (Kamchonwongpaisan et al., 1997). Therefore, the PPM creates invaginations to endocytose the host cytosol and the endosome finally fuses with the parasite's food vacuole (Aikawa et al., 1966; Slomianny, 1990). Thus, it was

hypothesised that the parasite probably internalised the rhodamine as well as the HsHsp70-Cy2, leading to the fluorescence inside the parasite, which indicates the food vacuole. The observed co-localisation for the hemozoin and rhodamine (Figure 21) strongly supports this theory. Although, another possible explanation would be that the dye was released from HsHsp70 and internalised. On the other hand, it is feasible that the dye diffused across the membranes and finally got trapped in the food vacuole.

As a dead end was reached to localise HsHsp70 in the infected erythrocyte by the fluorescently labelling and pre-loading of the erythrocytes, another approach was introduced. The parasite was genetically modified to express and export HsHsp70 to its host cell. Therefore, a fusion protein consisting of the first 80 amino acids of the STEVOR protein, which are sufficient to direct any protein to the host cell cytosol, an mCherry tag, and finally the full HsHsp70 amino acid sequence was expressed in the parasite. Most strikingly, HsHsp70^{mCherry} displayed the same dot-like mobile structures in the infected erythrocyte (Figure 23) as obtained by the Oregon-green and Cy2 labelled HsHsp70 in the non-infected erythrocyte (Figure 20 and Figure 21 respectively). Therefore, it was analysed whether HsHsp70 co-localises to known dot-like structures in the infected erythrocyte, such as the Maurer's clefts marker SBP1 and J-dot marker Hsp70x. For the Maurer's cleft marker no co-localisation with HsHsp70^{mcherry} was observed (Figure 24). In general, Maurer's clefts consist of more than one protein e.g. MAHRP (Maurer's clefts-Associated Histidine-Rich Protein) is another well-known member (Spycher et al., 2006). As a result, it cannot be ruled out that HsHsp70 is not co-localising with other Maurer's cleft components. Albeit, SBP1, due to its essential role in EMP1 trafficking (Cooke et al., 2006), would be a suitable interaction partner for a chaperone.

Further, it has to be taken into consideration that the tagging of a protein sometimes leads to a miss-localisation of the protein of interest (Hanson and Ziegler, 2004; Skube et al., 2010), which would have falsified the localisation of HsHsp70^{mCherry}. In addition, the parasite is expressing and exporting a foreign human protein. Therefore, the parasite might simply lack the requirements to ensure the proper function, thereby affecting the chaperone's activity. Yet, the most important limitation lies in the N-terminal position of the tag. HsHsp70 reacts

very sensitively to the N-terminal localisation of the tag, which affects its N-terminal SBD domain, leaving the chaperone inactive (personal communication Prof. Dr. Mayer). As a result, due to the mCherry tag, HsHsp70 is non-functional and therefore, may be miss-localised. Still, a study conducted by Zeng and colleagues used N-terminal GFP-tagged HsHsp70 to localise the protein in non- and heat-shocked HeLa cells (Henrietta-Lacks, cervix carcinoma cells) (Zeng et al., 2004). The HsHsp70^{GFP} fusion protein displayed a normal cytosolic localisation in the control cells (Zeng et al., 2004), indicating that even the inactive HsHsp70^{mCherry} protein might be properly localised. In favour are the obtained co-localisation data of HsHps70^{mcherry} with Hsp70x which revealed a partial co-localisation (Figure 24). This partial co-localisation is supported by a proteomic study conducted by Zhang and colleagues disclosing that HsHsp70 forms a complex with PFE55 (PfHsp40) and Hsp70x (Zhang et al., 2017). Further, yeast-two hybrid screens identified HsHsp70 as a promising interaction partner for J-dot proteins (Jha et al., 2017).

During the course of this study, several other approaches like immunoelectron microscopy and transiently expressing GFP-labelled HsHsp70 in HuH7 cells followed by *P. berghei* infection were tested (data not shown). Unfortunately, none were successful. In the literature several studies found HsHsp70 in various localisations, but most strikingly all those studies identified HsHsp70 by classical biochemical methods such as Co-IPs and proteomics (Banumathy et al., 2002; Jha et al., 2017; Zhang et al., 2017). The latest literature searches for a microscopy study of HsHsp70 in the infected host cell were negative, outlining the possibility that this might be a demanding task.

In the future, the deeper understanding of new stem cell technologies and usage of newly developed genetic tools can be exploited to localise HsHsp70 in the mature human infected erythrocyte. First steps towards this approach were already made towards the end of this study and collaboration with the stem cell expert Prof. Egan at the Stanford University was established. With the help of Prof. Egan, a CD34^{+} stem cell can be infected with a genetically modified lentivirus, thereby inserting a copy of HsHsp70^{GFP} to the stem cell's chromosome (Bei et al., 2010; Egan, 2018; Giarratana et al., 2005). Finally, with the help of stem cell factors like erythropoietin, these modified stem cells can be

differentiated into mature erythrocytes, a time and cost-intensive process. Subsequently, these cells can be infected with *P. falciparum*. Unfortunately, the first experiments were challenging due to a strong auto-fluorescence of the differentiated cells (personal communication J. Przyborski). In consequence, no conclusion was drawn on the localisation of HsHsp70 in the non-infected or infected erythrocyte.

In closing, more research is needed to finally resolve the localisation of HsHsp70 and to gain further information about its role in the transport of parasite-encoded proteins.

4.4 Outlook

In this study, a resealing approach was successfully established to introduce a classical dominant effect by adding an excess amount of mutated HsHsp70^{K71M} to the mature human erythrocyte. Unfortunately, under the given experimental setup, the data did not show any growth defect in the presence of the HsHsp70^{K71M}. Based on the previously mentioned drawbacks of the resealing method e.g. the chance that the dominant negative effect was not achieved or simply does not work efficiently in the used experimental setup. Clearly an approach to validate the inhibitory effect of HsHsp70^{K71M} is needed. First experiments to determine the folding capacity of haemoglobin depleted erythrocyte cytosol with luciferase refolding assays were challenging and need further development (data not shown). In general, also other mutated HsHsp70 e.g. D10A, K77Q, K77R, D199A (Arakawa et al., 2011; Seo et al., 2016) could be tested.

Nonetheless, another method is needed to validate the results. In the future, the previously explained stem cell approach can also be used to investigate the function of HsHsp70 for the intra-erythrocytic development of the parasite. By the means of a small hairpin RNA, introduced by a lentiviral transfection, the HsHsp70 can be downregulated and cells can be differentiated (Bei et al., 2010; Egan, 2018; Giarratana et al., 2005). The HsHsp70 is not identified as an essential factor for the differentiation and maturation of the cells (personal

communication E. Egan). Further, the method can be used to knock-down other known chaperones such as HsHsp90, 60 and 40. Unfortunately, HsHsc70 is essential to the differentiation and therefore, cannot be analysed by this system (personal communication E. Egan). For the investigation of HsHsc70 the resealing approach might come in handy. It is possible to purify a mutated HsHsc70^{K71M} and pre-load erythrocytes with an excessive amount. Further, the stem cell approach is rather time- as well as cost-intensive and different hairpin RNAs have to be tested for efficiency before reliable data can be collected. Therefore, the resealing approach might be a good supplement to the performed stem cell experiments. In addition, also other purified proteins can be pre-evaluated using the resealing approach and combinations of different proteins such as a dominant negative phenotype for e.g. HsHsc70 and HsHsp90 could be introduced. Moreover, the presence of HsHsp70^{K71M} can still result in abnormal knobs, an altered cytoadherence or rigidity. Regrettably, the analysis of the cytoadherence and rigidity is more than challenging with the rRBC. During the course of the study, it was noted that rRBC reacted more sensitive to fixation as classical giemsa staining failed to visualise infected erythrocytes. Cytoadherence as well as rigidity analysis often involves parasite enrichment with MACS or gelafundin, which could be due to fragile nature of rRBC more than challenging. However, irRBC could be sorted by Fluorescence Activated Cell Sorting (FACS) and afterwards fixed. With the help of Scanning Electron Microscopy (SEM) the knobs of the irRBC could be visualised and compared.

Additional studies with the translocation assays introduced by J. Günnewig should be used to analyse and narrow down the minimal host cell chaperone system involved in protein transport. Besides, other marker proteins should be used to validate that HsHsp70 is indeed not only involved in the transport of GBP130, but also targets other proteins. Furthermore, the establishment of parasites expressing GFP-labelled exported proteins e.g. the PNEP EMP1 might be used to infect the different rRBC with HsHsc70, HsHsp70, 90, 60 and 40 followed by an analysis of the effect of these chaperones on the transport of different proteins.

For the localisation of HsHsp70, the previously explained stem cell approach should be pursued. In general, further research is needed to analyse the role of HsHsp70 for the intra-erythrocytic development of the parasite.

5 References

Abraira, V. E., Satoh, T., Fekete, D. M., & Goodrich, L. V. (2010). Vertebrate Lrig3-ErbB Interactions Occur In Vitro but Are Unlikely to Play a Role in Lrig3-Dependent Inner Ear Morphogenesis. *PLoS ONE*, *5*(2), e8981.

Acharya, P., Kumar, R., & Tatu, U. (2007). Chaperoning a cellular upheaval in malaria: Heat shock proteins in Plasmodium falciparum. *Molecular and Biochemical Parasitology*, *153*(2), 85–94.

Agostini, I., Popov, S., Li, J., Dubrovsky, L., Hao, T., & Bukrinsky, M. (2000). Heat-Shock Protein 70 Can Replace Viral Protein R of HIV-1 during Nuclear Import of the Viral Preintegration Complex. *Experimental Cell Research*, *259*(2), 398–403.

Aikawa, M., Huff, C. G., & Sprinz, H. (1966). Comparative Feeding Mechanisms of Avian and Primate Malarial Parasites. *Military Medicine*, *131*(suppl_9), 969–983.

Alampalli, S. V., Grover, M., Chandran, S., Tatu, U., & Acharya, P. (2018). Proteome and Structural Organization of the Knob Complex on the Surface of the *Plasmodium* Infected Red Blood Cell. *PROTEOMICS - Clinical Applications*, *12*(4), 1600177.

Alder, N. N., Shen, Y., Brodsky, J. L., Hendershot, L. M., & Johnson, A. E. (2005). The molecular mechanisms underlying BiP-mediated gating of the Sec61 translocon of the endoplasmic reticulum. *The Journal of Cell Biology*, *168*(3), 389–399.

Amino, R., Thiberge, S., Blazquez, S., Baldacci, P., Renaud, O., Shorte, S., & Ménard, R. (2007). Imaging malaria sporozoites in the dermis of the mammalian host. *Nature Protocols*, *2*, 1705–1712.

Ansorge, I., Benting, J., Bhakdi, S., & Lingelbach, K. (1996). Protein sorting in Plasmodium falciparum-infected red blood cells permeabilized with the pore-forming protein streptolysin O. *The Biochemical Journal*, *315 (Pt 1)*(Pt 1), 307–314.

Arakawa, A., Handa, N., Shirouzu, M., & Yokoyama, S. (2011). Biochemical and structural studies on the high affinity of Hsp70 for ADP. *Protein Science*, *20*(8), 1367–1379.

Awe, K., Lambert, C., & Prange, R. (2008). Mammalian BiP controls posttranslational ER translocation of the hepatitis B virus large envelope protein. *FEBS Letters*, *582*(21–22), 3179–3184.

Bakar, N. A., Klonis, N., Hanssen, E., Chan, C., & Tilley, L. (2010). Digestive-vacuole genesis and endocytic processes in the early intraerythrocytic stages of Plasmodium falciparum. *Journal of Cell Science*, *123*(3), 441–450.

Bannister, L. H., Hopkins, J. M., Fowler, R. E., Krishna, S., & Mitchell, G. H. (2000). A brief illustrated guide to the ultrastructure of Plasmodium falciparum asexual blood stages. *Parasitology Today (Personal Ed.)*, *16*(10), 427–433.

Banumathy, G., Singh, V., & Tatu, U. (2002). Host chaperones are recruited in membrane-bound complexes by Plasmodium falciparum. *Journal of Biological Chemistry*, *277*(6), 3902–3912.

Baruch, D. I., Pasloske, B. L., Singh, H. B., Bi, X., Ma, X. C., Feldman, M., Taraschi, T. F., & Howard, R. J. (1995). Cloning the P. falciparum gene encoding PfEMP1, a malarial variant antigen and adherence receptor on the surface of parasitized human erythrocytes. *Cell*, *82*(1), 77–87.

Basco, L. K., Marquet, F., Makler, M. M., & Le Bras, J. (1995). Plasmodium falciparum and Plasmodium vivax: lactate dehydrogenase activity and its application for in vitro drug susceptibility assay. *Experimental Parasitology*, *80*(2), 260–271.

Batinovic, S., McHugh, E., Chisholm, S. A., Matthews, K., Liu, B., Dumont, L., Charnaud, S. C., Schneider, M. P., Gilson, P. R., de Koning-Ward, T. F., Dixon, M. W. A., & Tilley, L. (2017). An exported protein-interacting complex involved in the trafficking of virulence determinants in Plasmodium-infected erythrocytes. *Nature Communications*, *8*, 16044.

Baumeister, S., Endermann, T., Charpian, S., Nyalwidhe, J., Duranton, C., Huber, S., Kirk, K., Lang, F., & Lingelbach, K. (2003). A biotin derivative blocks parasite induced novel permeation pathways in Plasmodium falciparum-infected erythrocytes. *Molecular and Biochemical Parasitology*, *132*(1), 35–45.

Baumeister, S., Winterberg, M., Duranton, C., Huber, S. M., Lang, F., Kirk, K., & Lingelbach, K. (2006). Evidence for the involvement of Plasmodium falciparum proteins in the formation of new permeability pathways in the erythrocyte membrane. *Molecular Microbiology*, *60*(2), 493–504.

References

Beeson, J. G., Mann, E. J., Byrne, T. J., Caragounis, A., Elliott, S. R., Brown, G. V, & Rogerson, S. J. (2006). Antigenic differences and conservation among placental Plasmodium falciparum-infected erythrocytes and acquisition of variant-specific and cross-reactive antibodies. *The Journal of Infectious Diseases*, *193*(5), 721–730.

Bei, A. K., Brugnara, C., & Duraisingh, M. T. (2010). In vitro genetic analysis of an erythrocyte determinant of malaria infection. *The Journal of Infectious Diseases*, *202*(11), 1722–1727.

Berndt, V. (2014). *The role of HsHsp70 in host cell modification of Plasmodium falciparum*. Philipps Universität Marburg.

Billker, O., Lindo, V., Panico, M., Etienne, A. E., Paxton, T., Dell, A., Rogers, M., Sinden, R. E., & Morris, H. R. (1998). Identification of xanthurenic acid as the putative inducer of malaria development in the mosquito. *Nature*, *392*, 289–292.

Blackman, M. J., & Bannister, L. H. (2001). Apical organelles of Apicomplexa: biology and isolation by subcellular fractionation. *Molecular and Biochemical Parasitology*, *117*, 11–25.

Blatch, G. L., & Lässle, M. (1999). The tetratricopeptide repeat: a structural motif mediating protein-protein interactions. *BioEssays*, *21*(11), 932–939.

Blisnick, T., Morales Betoulle, M. E., Barale, J.-C., Uzureau, P., Berry, L., Desroses, S., Fujioka, H., Mattei, D., & Braun Breton, C. (2000). Pfsbp1, a Maurer's cleft Plasmodium falciparum protein, is associated with the erythrocyte skeleton. *Molecular and Biochemical Parasitology*, *111*(1), 107–121.

Boddey, J. A., Carvalho, T. G., Hodder, A. N., Sargeant, T. J., Sleebs, B. E., Marapana, D., Lopaticki, S., Nebl, T., & Cowman, A. F. (2013). Role of Plasmepsin V in Export of Diverse Protein Families from the *Plasmodium falciparum* Exportome. *Traffic*, *14*(5), 532–550.

Boddey, J. A., & Cowman, A. F. (2013). *Plasmodium* Nesting: Remaking the Erythrocyte from the Inside Out. *Annual Review of Microbiology*, *67*(1), 243–269.

Boddey, J. A., Hodder, A. N., Günther, S., Gilson, P. R., Patsiouras, H., Kapp, E. A., Pearce, J. A., de Koning-Ward, T. F., Simpson, R. J., Crabb, B. S., & Cowman, A. F. (2010). An aspartyl protease directs malaria effector proteins to the host cell. *Nature*, *463*(7281), 627–631.

Boiocchi, C., Osera, C., Monti, M. C., Ferraro, O. E., Govoni, S., Cuccia, M., Montomoli, C., Pascale, A., & Bergamaschi, R. (2014). Are Hsp70 protein expression and genetic polymorphism implicated in multiple sclerosis inflammation? *Journal of Neuroimmunology*, *268*(1–2), 84–88.

Botha, M., Pesce, E.-R., & Blatch, G. L. (2007). The Hsp40 proteins of Plasmodium falciparum and other apicomplexa: Regulating chaperone power in the parasite and the host. *The International Journal of Biochemistry & Cell Biology*, *39*(10), 1781–1803.

Bourgeaux, V., Lanao, J. M., Bax, B. E., & Godfrin, Y. (2016). Drug-loaded erythrocytes: on the road toward marketing approval. *Drug Design, Development and Therapy*, *10*, 665–676.

Brehme, M., & Voisine, C. (2016). Model systems of protein-misfolding diseases reveal chaperone modifiers of proteotoxicity. *Disease Models & Mechanisms*, *9*(8), 823–838.

Bullen, H. E., Charnaud, S. C., Kalanon, M., Riglar, D. T., Dekiwadia, C., Kangwanrangsan, N., Torii, M., Tsuboi, T., Baum, J., Ralph, S. A., Cowman, A. F., de Koning-Ward, T. F., Crabb, B. S., & Gilson, P. R. (2012). Biosynthesis, Localization, and Macromolecular Arrangement of the *Plasmodium falciparum* Translocon of Exported Proteins (PTEX). *Journal of Biological Chemistry*, *287*(11), 7871–7884.

Chan, J. A., Fowkes, F. J. I., & Beeson, J. G. (2014). Surface antigens of Plasmodium falciparum-infected erythrocytes as immune targets and malaria vaccine candidates. *Cellular and Molecular Life Sciences : CMLS*, *71*(19), 3633–3657.

Chang, H. H., Falick, A. M., Carlton, P. M., Sedat, J. W., DeRisi, J. L., & Marletta, M. A. (2008). N-terminal processing of proteins exported by malaria parasites. *Molecular and Biochemical Parasitology*, *160*(2), 107–115.

Charnaud, S. C., Dixon, M. W. A., Nie, C. Q., Chappell, L., Sanders, P. R., Nebl, T., … Gilson, P. R. (2017). The exported chaperone Hsp70-x supports virulence functions for Plasmodium falciparum blood stage parasites. *PloS One*, *12*(7), e0181656.

Charpian, S. (2008). *Proteintranslokation über die Membran der parasitophoren Vakuole im Plasmodium falciparum-infezierten Erythrozyten*. Philipps Universität Marburg.

Charpian, S., & Przyborski, J. M. (2008). Protein transport across the parasitophorous vacuole of Plasmodium falciparum: Into the great wide open. *Traffic*, *9*(2), 157–165.

Clausen, T. M., Christoffersen, S., Dahlbäck, M., Langkilde, A. E., Jensen, K. E., Resende, M., … Salanti, A. (2012). Structural and Functional Insight into How the *Plasmodium falciparum* VAR2CSA Protein Mediates Binding to Chondroitin Sulfate A in Placental Malaria. *Journal of Biological Chemistry*, *287*(28), 23332–23345.

Cooke, B. M., Buckingham, D. W., Glenister, F. K., Fernandez, K. M., Bannister, L. H., Marti, M., Mohandas, N., & Coppel, R. L. (2006). A Maurer's cleft-associated protein is essential for expression of the major malaria virulence antigen on the surface of infected red blood cells. *Journal of Cell Biology*, *172*(6), 899–908.

Coppel, R. L., Cowman, A. F., Anders, R. F., Bianco, A. E., Saint, R. B., Lingelbach, K. R., Kemp, D. J., & Brown, G. V. (1984). Immune sera recognize on erythrocytes a Plasmodium falciparum antigen composed of repeated amino acid sequences. *Nature*, *310*(5980), 789–792.

Cowman, A. F., Healer, J., Marapana, D., & Marsh, K. (2016). Malaria: Biology and Disease. *Cell*, *167*(3), 610–624.

Craig, E. A. (2018). Hsp70 at the membrane: driving protein translocation. *BMC Biology*, *16*(1), 11.

D'Alessandro, A., Righetti, P. G., & Zolla, L. (2010). The Red Blood Cell Proteome and Interactome: An Update. *Journal of Proteome Research*, *9*(1), 144–163.

Daniyan, M. O., Boshoff, A., Prinsloo, E., Pesce, E.-R., & Blatch, G. L. (2016). The Malarial Exported PFA0660w Is an Hsp40 Co-Chaperone of PfHsp70-x. *PLOS ONE*, *11*(2), e0148517.

Das, S., Hertrich, N., Perrin, A. J., Withers-Martinez, C., Collins, C. R., Jones, M. L., Watermeyer, J. M., Fobes, E. T., Martin, S. R., Saibil, H. R., Wright, G. J., Treeck, M., Epp, C., & Blackman, M. J. (2015). Processing of Plasmodium falciparum Merozoite Surface Protein MSP1 Activates a Spectrin-Binding Function Enabling Parasite Egress from RBCs. *Cell Host & Microbe*, *18*(4), 433–444.

de Koning-Ward, T. F., Gilson, P. R., Boddey, J. A., Rug, M., Smith, B. J., Papenfuss, A. T., Sanders, P. R., Lundie, R. J., Maier, A. G., Cowman, A. F., & Crabb, B. S. (2009). A newly discovered protein export machine in malaria parasites. *Nature*, *459*(7249), 945–949.

Dekker, S. L., Kampinga, H. H., & Bergink, S. (2015). DNAJs: more than substrate delivery to HSPA. *Frontiers in Molecular Biosciences*, *2*, 35.

Dimopoulos, G., Seeley, D., Wolf, A., & Kafatos, F. C. (1998). Malaria infection of the mosquito Anopheles gambiae activates immune-responsive genes during critical transition stages of the parasite life cycle. *EMBO Journal*, *17*, 6115–6123.

Egan, E. S. (2018). Beyond Hemoglobin: Screening for Malaria Host Factors. *Trends in Genetics*, *34*(2), 133–141.

Eilers, M., & Schatz, G. (1986). Binding of a specific ligand inhibits import of a purified precursor protein into mitochondria. *Nature*, *322*(6076), 228–232.

Elsworth, B., Crabb, B. S., & Gilson, P. R. (2014). Protein export in malaria parasites: an update. *Cellular Microbiology*, *16*(3), 355–363.

Elsworth, B., Matthews, K., Nie, C. Q., Kalanon, M., Charnaud, S. C., Sanders, P. R., … de Koning-Ward, T. F. (2014). PTEX is an essential nexus for protein export in malaria parasites. *Nature*, *511*(7511), 587–591.

Elsworth, B., Sanders, P. R., Nebl, T., Batinovic, S., Kalanon, M., Nie, C. Q., Charnaud, S. C., Bullen, H. E., de Koning Ward, T. F., Tilley, L., Crabb, B. S., & Gilson, P. R. (2016). Proteomic analysis reveals novel proteins associated with the *Plasmodium* protein exporter PTEX and a loss of complex stability upon truncation of the core PTEX component, PTEX150. *Cellular Microbiology*, *18*(11), 1551–1569.

Fontaine, S. N., Rauch, J. N., Nordhues, B. A., Assimon, V. A., Stothert, A. R., Jinwal, U. K., Sabbagh, J. J., Chang, L., Stevens, S. M., Zuiderweg, E. R. P., Gestwicki, J. E., & Dickey, C. A. (2015). Isoform-selective Genetic Inhibition of Constitutive Cytosolic Hsp70 Activity Promotes Client Tau Degradation Using an Altered Co-chaperone Complement. *Journal of Biological Chemistry*, *290*(21), 13115–13127.

Frankland, S., Adisa, A., Horrocks, P., Taraschi, T. F., Schneider, T., Elliott, S. R., Rogerson, S. J., Knuepfer, E., Cowman, A. F., Newbold, C. I., & Tilley, L. (2006). Delivery of the malaria virulence protein PfEMP1 to the erythrocyte surface requires cholesterol-rich domains. *Eukaryotic Cell*, *5*(5), 849–860.

Freeman, B. C., Myers, M. P., Schumacher, R., & Morimoto, R. I. (1995). Identification of a regulatory motif in Hsp70 that affects ATPase activity, substrate binding and interaction with HDJ-1. *The EMBO Journal*, *14*(10), 2281–2292.

Gambill, B. D., Voos, W., Kang, P. J., Miao, B., Langer, T., Craig, E. A., & Pfanner, N. (1993). A dual role for mitochondrial heat shock protein 70 in membrane translocation of preproteins. *The Journal of Cell Biology*, *123*(1), 109–117.

References

Garcia, G. E., Wirtz, R. A., Barr, J. R., Woolfitt, A., & Rosenberg, R. (1998). Xanthurenic Acid Induces Gametogenesis in Plasmodium, the Malaria Parasite. *Journal of Biological Chemistry*, *273*, 12003–12005.

Garten, M., Nasamu, A. S., Niles, J. C., Zimmerberg, J., Goldberg, D. E., & Beck, J. R. (2018). EXP2 is a nutrient-permeable channel in the vacuolar membrane of Plasmodium and is essential for protein export via PTEX. *Nature Microbiology*, *3*(10), 1090–1098.

Gehde, N., Hinrichs, C., Montilla, I., Charpian, S., Lingelbach, K., & Przyborski, J. M. (2009). Protein unfolding is an essential requirement for transport across the parasitophorous vacuolar membrane of Plasmodium falciparum. *Molecular Microbiology*, *71*(3), 613–628.

Giarratana, M.-C., Kobari, L., Lapillonne, H., Chalmers, D., Kiger, L., Cynober, T., Marden, M. C., Wajcman, H., & Douay, L. (2005). Ex vivo generation of fully mature human red blood cells from hematopoietic stem cells. *Nature Biotechnology*, *23*(1), 69–74.

Gidalevitz, T., Stevens, F., & Argon, Y. (2013). Orchestration of secretory protein folding by ER chaperones. *Biochimica et Biophysica Acta (BBA) - Molecular Cell Research*, *1833*(11), 2410–2424.

Gilson, P. R., Charnaud, S. C., & Crabb, B. S. (2014). The Role of Parasite Heat Shock Proteins in Protein Trafficking and Host Cell Remodeling. In *Heat Shock Proteins of Malaria* (pp. 99–117).

Ginsburg, H., Kutner, S., Krugliak, M., & Cabantchik, Z. I. (1985). Characterization of permeation pathways appearing in the host membrane of Plasmodium falciparum infected red blood cells. *Molecular and Biochemical Parasitology*, *14*(3), 313–322.

Goloubinoff, P. (2017). Editorial: The HSP70 Molecular Chaperone Machines. *Frontiers in Molecular Biosciences*, *4*, 1.

Greenwood, B. M., Fidock, D. A., Kyle, D. E., Kappe, S. H. I., Alonso, P. L., Collins, F. H., & Duffy, P. E. (2008). Malaria : progress, perils, and prospects for eradication. *Journal of Clinical Investigation*, *118*, 1266–1276.

Gromov, P. S., & Celis, J. E. (1991). Identification of two molecular chaperons (HSX70, HSC70) in mature human erythrocytes. *Experimental Cell Research*, *195*(2), 556–559.

Gronowicz, G., Swift, H., & Steck, T. L. (1984). Maturation of the reticulocyte in vitro. *Journal of Cell Science*, *71*, 177–197.

Gruenberg, J., Allred, D. R., & Sherman, I. W. (1983). Scanning electron microscope-analysis of the protrusions (knobs) present on the surface of Plasmodium falciparum-infected erythrocytes. *The Journal of Cell Biology*, *97*(3), 795–802.

Grüring, C., Heiber, A., Kruse, F., Flemming, S., Franci, G., Colombo, S. F., Fasana, E., Schoeler, H., Borgese, N., Stunnenberg, H. G., Przyborski, J. M., Gilberger, T.-W., & Spielmann, T. (2012). Uncovering common principles in protein export of malaria parasites. *Cell Host & Microbe*, *12*(5), 717–729.

Günnewig, J. (2016). *Die Rolle des humanen Hsp70 im Proteintransport von Plasmodium falciparum*. Philipps Universität Marburg.

Haase, S., Herrmann, S., Grüring, C., Heiber, A., Jansen, P. W., Langer, C., … Spielmann, T. (2009). Sequence requirements for the export of the *Plasmodium falciparum* Maurer's clefts protein REX2. *Molecular Microbiology*, *71*(4), 1003–1017.

Hanson, D. A., & Ziegler, S. F. (2004). Fusion of green fluorescent protein to the C-terminus of granulysin alters its intracellular localization in comparison to the native molecule. *Journal of Negative Results in Biomedicine*, *3*, 1–3.

Hatherley, R., Blatch, G. L., & Bishop, Ö. T. (2014). *Plasmodium falciparum* Hsp70-x: a heat shock protein at the host–parasite interface. *Journal of Biomolecular Structure and Dynamics*, *32*(11), 1766–1779.

Hennessy, F., Nicoll, W. S., Zimmermann, R., Cheetham, M. E., & Blatch, G. L. (2005). Not all J domains are created equal: Implications for the specificity of Hsp40-Hsp70 interactions. *Protein Science*, *14*(7), 1697–1709.

Herskowitz, I. (1987). Functional inactivation of genes by dominant negative mutations. *Nature*, *329*(6136), 219–222.

Hiller, N. L., Bhattacharjee, S., van Ooij, C., Liolios, K., Harrison, T., Lopez-Estraño, C., & Haldar, K. (2004). A Host-Targeting Signal in Virulence Proteins Reveals a Secretome in Malarial Infection. *Science*, *306*(5703), 1934–1937.

Horst, M., Oppliger, W., Rospert, S., Schönfeld, H. J., Schatz, G., & Azem, A. (1997). Sequential action of two hsp70 complexes during protein import into mitochondria. *The EMBO Journal*, *16*(8), 1842–1849.

Jalbout, M., Bouaouina, N., Gargouri, J., Corbex, M., Ben Ahmed, S., & Chouchane, L. (2003). Polymorphism of the stress protein HSP70-2 gene is associated with the susceptibility to the nasopharyngeal carcinoma. *Cancer Letters*,

193(1), 75–81.

Javid, B., MacAry, P. A., & Lehner, P. J. (2007). Structure and function: heat shock proteins and adaptive immunity. *Journal of Immunology (Baltimore, Md. : 1950)*, *179*(4), 2035–2040. Retrieved from

Jha, P., Laskar, S., Dubey, S., Bhattacharyya, M. K., & Bhattacharyya, S. (2017). Plasmodium Hsp40 and human Hsp70: A potential cochaperone-chaperone complex. *Molecular and Biochemical Parasitology*, *214*, 10–13.

Kakhniashvili, D. G., Bulla, L. A., & Goodman, S. R. (2004). The Human Erythrocyte Proteome. *Molecular & Cellular Proteomics*, *3*(5), 501–509.

Kamchonwongpaisan, S., Samoff, E., & Meshnick, S. . (1997). Identification of hemoglobin degradation products in Plasmodium falciparum. *Molecular and Biochemical Parasitology*, *86*(2), 179–186.

Kampinga, H. H., & Craig, E. A. (2010). The HSP70 chaperone machinery: J proteins as drivers of functional specificity. *Nature Reviews. Molecular Cell Biology*, *11*(8), 579–592.

Kim, C. C., Wilson, E. B., & Derisi, J. L. (2010). Improved methods for magnetic purification of malaria parasites and haemozoin. *Malaria Journal*, *9*(1).

Kim, Y. A., Cha, J. E., Ahn, S. Y., Ryu, S. H., Yeom, J. S., Lee, H. Il, Kim, C. G., Seoh, J. Y., & Park, J. W. (2007). Plasmodium falciparum cultivation using the Petri Dish: revisiting the effect of the “age” of erythrocytes and the interval of medium change. *Journal of Korean Medical Science*, *22*(6), 1022–1025.

Kirk, K., Horner, H. A., Elford, B. C., Ellory, J. C., & Newbold, C. I. (1994). Transport of diverse substrates into malaria-infected erythrocytes via a pathway showing functional characteristics of a chloride channel. *The Journal of Biological Chemistry*, *269*(5), 3339–3347.

Kirk, K., Staines, H. M., Martin, R. E., & Saliba, K. J. (1999). Transport properties of the host cell membrane. *Novartis Foundation Symposium*, *226*, 55-66; discussion 66-73.

Konieczny, I., & Zylicz, M. (1999). Role of bacterial chaperones in DNA replication. *Genetic Engineering*, *21*, 95–111.

Koning-ward, T. F. De, Gilson, P. R., Boddey, J. a, Rug, M., Smith, B. J., Papenfuss, A. T., … Crabb, B. S. (2009). A novel protein export machine in malaria parasites. *Nature*, *459*(7249), 945–949.

Kooyman, D. L., Byrne, G. W., McClellan, S., Nielsen, D., Tone, M., Waldmann, H., Coffman, T. M., McCurry, K. R., Platt, J. L., & Logan, J. S. (1995). In vivo transfer of GPI-linked complement restriction factors from erythrocytes to the endothelium. *Science (New York, N.Y.)*, *269*(5220), 89–92.

Külzer, S., Charnaud, S., Dagan, T., Riedel, J., Mandal, P., Pesce, E. R., Blatch, G. L., Crabb, B. S., Gilson, P. R., & Przyborski, J. M. (2012). Plasmodium falciparum-encoded exported hsp70/hsp40 chaperone/co-chaperone complexes within the host erythrocyte. *Cellular Microbiology*, *14*(11), 1784–1795.

Külzer, S., Rug, M., Brinkmann, K., Cannon, P., Cowman, A., Lingelbach, K., Blatch, G. L., Maier, A. G., & Przyborski, J. M. (2010). Parasite-encoded Hsp40 proteins define novel mobile structures in the cytosol of the P. falciparum-infected erythrocyte. *Cellular Microbiology*, *12*(10), 1398–1420.

Kumar, N., Koski, G., Harada, M., Aikawa, M., & Zheng, H. (1991). Induction and localization of Plasmodium falciparum stress proteins related to the heat shock protein 70 family. *Molecular and Biochemical Parasitology*, *48*(1), 47–58.

Kumar, N., Syin, C. A., Carter, R., Quakyi, I., & Miller, L. H. (1988). Plasmodium falciparum gene encoding a protein similar to the 78-kDa rat glucose-regulated stress protein. *Proceedings of the National Academy of Sciences of the United States of America*, *85*(17), 6277–6281.

Kumar, N., & Zheng, H. (1992). Nucleotide sequence of a Plasmodium falciparum stress protein with similarity to mammalian 78-kDa glucose-regulated protein. *Molecular and Biochemical Parasitology*, *56*(2), 353–356.

Lagaudrière-Gesbert, C., Newmyer, S. L., Gregers, T. F., Bakke, O., & Ploegh, H. L. (2002). Uncoating ATPase Hsc70 is recruited by invariant chain and controls the size of endocytic compartments. *Proceedings of the National Academy of Sciences of the United States of America*, *99*(3), 1515–1520.

Lambros, C., & Vanderberg, J. P. (1979). Synchronization of Plasmodium falciparum erythrocytic stages in culture. *The Journal of Parasitology*, *65*(3), 418–420.

Langreth, S. G., Reese, R. T., Motyl, M. R., & Trager, W. (1979). Plasmodium falciparum: Loss of knobs on the infected erythrocyte surface after long-term cultivation. *Experimental Parasitology*, *48*(2), 213–219.

Lanzer, M., Wickert, H., Krohne, G., Vincensini, L., & Braun Breton, C. (2006). Maurer’s clefts: A novel multi-functional

organelle in the cytoplasm of Plasmodium falciparum-infected erythrocytes. *International Journal for Parasitology*, *36*(1), 23–36.

Lindquist, S. (1986). The Heat-Shock Response. *Annual Review of Biochemistry*, *55*(1), 1151–1191.

Lingelbach, K., & Joiner, K. A. (1998). The parasitophorous vacuole membrane surrounding Plasmodium and Toxoplasma: an unusual compartment in infected cells. *Journal of Cell Science*, *111 (Pt 11)*, 1467–1475.

Longeville, S., & Stingaciu, L.-R. (2017). Hemoglobin diffusion and the dynamics of oxygen capture by red blood cells. *Scientific Reports*, *7*(1), 10448.

Magnani, M., Rossi, L., D'ascenzo, M., Panzani, I., Bigi, L., & Zanella, a. (1998). Erythrocyte engineering for drug delivery and targeting. *Biotechnology and Applied Biochemistry*, *28 (Pt 1)*, 1–6. Retrieved from

Magnani, M., Rossi, L., Fraternale, A., Bianchi, M., Antonelli, A., Crinelli, R., & Chiarantini, L. (2002). Erythrocyte-mediated delivery of drugs, peptides and modified oligonucleotides. *Gene Therapy*, *9*(11), 749–751.

Maier, A. G., Cooke, B. M., Cowman, A. F., & Tilley, L. (2009). Malaria parasite proteins that remodel the host erythrocyte. *Nature Reviews Microbiology*, *7*(5), 341–354.

Maier, A. G., Rug, M., O'Neill, M. T., Brown, M., Chakravorty, S., Szestak, T., … Cowman, A. F. (2008). Exported Proteins Required for Virulence and Rigidity of Plasmodium falciparum-Infected Human Erythrocytes. *Cell*, *134*(1), 48–61.

Markwalter, C. F., Davis, K. M., & Wright, D. W. (2016). Immunomagnetic capture and colorimetric detection of malarial biomarker Plasmodium falciparum lactate dehydrogenase. *Analytical Biochemistry*, *493*, 30–34.

Marti, M., Good, R. T., Rug, M., Knuepfer, E., & Cowman, A. F. (2004). Targeting Malaria Virulence and Remodeling Proteins to the Host Erythrocyte. *Science*, *306*(5703), 1930–1933.

Matlack, K. E., Misselwitz, B., Plath, K., & Rapoport, T. A. (1999). BiP acts as a molecular ratchet during posttranslational transport of prepro-alpha factor across the ER membrane. *Cell*, *97*(5), 553–564.

Mayer, M. P., & Bukau, B. (2005). Hsp70 chaperones: Cellular functions and molecular mechanism. *Cellular and Molecular Life Sciences*, *62*(6), 670–684.

Mayer, M. P., & Kityk, R. (2015). Insights into the molecular mechanism of allostery in Hsp70s. *Frontiers in Molecular Biosciences*, *2*, 58.

Melville, M. W., McClellan, A. J., Meyer, A. S., Darveau, A., & Frydman, J. (2003). The Hsp70 and TRiC/CCT chaperone systems cooperate in vivo to assemble the von Hippel-Lindau tumor suppressor complex. *Molecular and Cellular Biology*, *23*(9), 3141–3151.

Mestiri, S., Bouaouina, N., Ahmed, S. Ben, Khedhaier, A., Jrad, B. B., Remadi, S., & Chouchane, L. (2001). Genetic variation in the tumor necrosis factor-? promoter region and in the stress protein hsp70-2. *Cancer*, *91*(4), 672–678.

Millauer, B., Shawver, L. K., Plate, K. H., Risaui, W., & Ullrich, A. (1994). Glioblastoma growth inhibited in vivo by a dominant-negative Flk-1 mutant. *Nature*, *367*(6463), 576–579.

Miller, L. H., Baruch, D. I., Marsh, K., & Doumbo, O. K. (2002). The pathogenic basis of malaria. *Nature*, *415*(6872), 673–679.

Morán Luengo, T., Kityk, R., Mayer, M. P., Rüdiger, S. G. D., T, M. L., R, K., MP, M., & SGD., R. (2018). Hsp90 Breaks the Deadlock of the Hsp70 Chaperone System. *Molecular Cell*, *70*(3), 545–552.e9.

Mota, M. M., Pradel, G., Vanderberg, J. P., Hafalla, J. C., Frevert, U., Nussenzweig, R. S., Nussenzweig, V., & Rodríguez, A. (2001). Migration of Plasmodium Sporozoites Through Cells Before Infection. *Science*, *291*(5501), 141–144.

Nakabayashi, H., Taketa, K., Miyano, K., Yamane, T., & Sato, J. (1982). Growth of human hepatoma cells lines with differentiated functions in chemically defined medium. *Cancer Research*, *42*(9), 3858–3863. Retrieved from

Neupert, W., & Brunner, M. (2002). The protein import motor of mitochondria. *Nature Reviews Molecular Cell Biology*, *3*(8), 555–565.

Newmyer, S. L., & Schmid, S. L. (2001). Dominant-interfering Hsc70 mutants disrupt multiple stages of the clathrin-coated vesicle cycle in vivo. *The Journal of Cell Biology*, *152*(3), 607–620.

Njunge, J. M., Ludewig, M. H., Boshoff, A., Pesce, E.-R., & Blatch, G. L. (2013). Hsp70s and J proteins of Plasmodium parasites infecting rodents and primates: structure, function, clinical relevance, and drug targets. *Current Pharmaceutical Design*, *19*(3), 387–403.

Nye, E. R. (2002). Alphonse Laveran (1845–1922): Discoverer of the Malarial Parasite and Nobel Laureate, 1907. *Journal of Medical Biography*, *10*(2), 81–87.

O'Brien, M. C., Flaherty, K. M., & McKay, D. B. (1996). Lysine 71 of the chaperone protein Hsc70 Is essential for ATP hydrolysis. *The Journal of Biological Chemistry*, *271*(27), 15874–15878.

Pasini, E. M., Kirkegaard, M., Mortensen, P., Lutz, H. U., Thomas, A. W., & Mann, M. (2006). In-depth analysis of the membrane and cytosolic proteome of red blood cells. *Blood*, *108*(3), 791–801.

Pasvol, G., Wilson, R. J., Smalley, M. E., & Brown, J. (1978). Separation of viable schizont-infected red cells of Plasmodium falciparum from human blood. *Annals of Tropical Medicine and Parasitology*, *72*(1), 87–88.

Paunola, E., Suntio, T., Jämsä, E., & Makarow, M. (1998). Folding of active beta-lactamase in the yeast cytoplasm before translocation into the endoplasmic reticulum. *Molecular Biology of the Cell*, *9*(4), 817–827.

Phillips, M. A., Burrows, J. N., Manyando, C., van Huijsduijnen, R. H., Van Voorhis, W. C., & Wells, T. N. C. (2017). Malaria. *Nature Reviews Disease Primers*, *3*, 17050.

Pradel, G. (2007). Proteins of the malaria parasite sexual stages: expression, function and potential for transmission blocking strategies. *Parasitology*, *134*, 1911–1929.

Przyborski, J. M., Diehl, M., & Blatch, G. L. (2015). Plasmodial HSP70s are functionally adapted to the malaria parasite life cycle. *Frontiers in Molecular Biosciences*, *2*, 34.

Przyborski, J. M., Miller, S. K., Pfahler, J. M., Henrich, P. P., Rohrbach, P., Crabb, B. S., & Lanzer, M. (2005). Trafficking of STEVOR to the Maurer's clefts in Plasmodium falciparum-infected erythrocytes. *The EMBO Journal*, *24*(13), 2306–2317.

Przyborski, J. M., Nyboer, B., & Lanzer, M. (2016). Ticket to ride: Export of proteins to the P. falciparum-infected erythrocyte. *Molecular Microbiology*, *101*(May), 1–11.

Rhiel, M., Bittl, V., Tribensky, A., Charnaud, S. C., Strecker, M., Müller, S., Lanzer, M., Sanchez, C., Schaeffer-Reiss, C., Westermann, B., Crabb, B. S., Gilson, P. R., Külzer, S., & Przyborski, J. M. (2016). Trafficking of the exported P. falciparum chaperone PfHsp70x. *Scientific Reports*, *6*(1), 36174.

Riglar, D. T., Rogers, K. L., Hanssen, E., Turnbull, L., Bullen, H. E., Charnaud, S. C., Przyborski, J., Gilson, P. R., Whitchurch, C. B., Crabb, B. S., Baum, J., & Cowman, A. F. (2013). Spatial association with PTEX complexes defines regions for effector export into Plasmodium falciparum-infected erythrocytes. *Nature Communications*, *4*, 1415.

Rossi, L., Serafini, S., Pierigé, F., Antonelli, A., Cerasi, A., Fraternale, A., Chiarantini, L., & Magnani, M. (2005). *Erythrocyte-based drug delivery*. *5247*(August).

Rüdiger, S., Buchberger, A., & Bukau, B. (1997). Interaction of Hsp70 chaperones with substrates. *Nature Structural Biology*, *4*(5), 342–349.

Saibil, H. (2013). Chaperone machines for protein folding, unfolding and disaggregation. *Nature Reviews Molecular Cell Biology*, *14*(10), 630–642.

Salanti, A., Dahlbäck, M., Turner, L., Nielsen, M. A., Barfod, L., Magistrado, P., Jensen, A. T. R., Lavstsen, T., Ofori, M. F., Marsh, K., Hviid, L., & Theander, T. G. (2004). Evidence for the Involvement of VAR2CSA in Pregnancy-associated Malaria. *The Journal of Experimental Medicine*, *200*(9), 1197.

Salanti, A., Staalsoe, T., Lavstsen, T., Jensen, A. T. R., Sowa, M. P. K., Arnot, D. E., Hviid, L., & Theander, T. G. (2003). Selective upregulation of a single distinctly structured var gene in chondroitin sulphate A-adhering Plasmodium falciparum involved in pregnancy-associated malaria. *Molecular Microbiology*, *49*(1), 179–191.

Sargeant, T., Marti, M., Caler, E., Carlton, J., Simpson, K., Speed, T., & Cowman, A. (2006). Lineage-specific expansion of proteins exported to erythrocytes in malaria parasites. *Genome Biology*, *7*(2), R12.

Saridaki, T., Fröhlich, K. S., Braun-Breton, C., & Lanzer, M. (2009). Export of PfSBP1 to the *Plasmodium falciparum* Maurer's Clefts. *Traffic*, *10*(2), 137–152.

Schifferli, J. A., & Taylor, R. P. (1989). Physiological and pathological aspects of circulating immune complexes. *Kidney International*, *35*(4), 993–1003.

Schröder, H., Langer, T., Hartl, F. U., & Bukau, B. (1993). DnaK, DnaJ and GrpE form a cellular chaperone machinery capable of repairing heat-induced protein damage. *The EMBO Journal*, *12*(11), 4137–4144.

Seo, J. H., Park, J.-H., Lee, E. J., Vo, T. T. L., Choi, H., Kim, J. Y., … Kim, K.-W. (2016). ARD1-mediated Hsp70 acetylation balances stress-induced protein refolding and degradation. *Nature Communications*, *7*(1), 12882.

Seyffer, F., Kummer, E., Oguchi, Y., Winkler, J., Kumar, M., Zahn, R., Sourjik, V., Bukau, B., & Mogk, A. (2012). Hsp70 proteins bind Hsp100 regulatory M domains to activate AAA+ disaggregase at aggregate surfaces. *Nature Structural & Molecular Biology*, *19*(12), 1347–1355.

Shi, L.-X., & Theg, S. M. (2010). A stromal heat shock protein 70 system functions in protein import into chloroplasts in the moss Physcomitrella patens. *The Plant Cell*, *22*(1), 205–220.

Shonhai, A. (2010). Plasmodial heat shock proteins: Targets for chemotherapy. *FEMS Immunology and Medical Microbiology*, *58*(1), 61–74.

Silvestrini, F., Alano, P., & Williams, J. (2000). Commitment to the production of male and female gametocytes in the human malaria parasite Plasmodium falciparum. *Parasitology*, *121*, 465–471.

Sinden, R.E., Butcher, G.A., Billker, O., and Fleck, S. L. (1996). Regulation of infectivity of Plasmodium to the mosquito vector. *Adv Parasitol*, *38*, 53–117.

Sinden, R. E., Butcher, G. A., Billker, O., & Fleck, S. L. (1983). Sexual development of malarial parasites. *Advances in Parasitology*, *22*, 153–216.

Skube, S. B., Chaverri, J. M., & V. Goodson, H. (2010). Effect of GFP tags on the localization of EB1 and EB1 fragments in vivo. *Cytoskleton*, *67*, 1–12.

Slater, A. F. G., & Cerami, A. (1992). Inhibition by chloroquine of a novel haem polymerase enzyme activity in malaria trophozoites. *Nature*, *355*(6356), 167–169.

Slater, A. F., Swiggard, W. J., Orton, B. R., Flitter, W. D., Goldberg, D. E., Cerami, A., & Henderson, G. B. (1991). An iron-carboxylate bond links the heme units of malaria pigment. *Proceedings of the National Academy of Sciences of the United States of America*, *88*(2), 325–329.

Slomianny, C. (1990). Three-dimensional reconstruction of the feeding process of the malaria parasite. *Undefined*.

Smith, J. D., Chitnis, C. E., Craig, A. G., Roberts, D. J., Hudson-Taylor, D. E., Peterson, D. S., Pinches, R., Newbold, C. I., & Miller, L. H. (1995). Switches in expression of Plasmodium falciparum var genes correlate with changes in antigenic and cytoadherent phenotypes of infected erythrocytes. *Cell*, *82*(1), 101–110.

Spielmann, T., Gardiner, D. L., Beck, H.-P., Trenholme, K. R., & Kemp, D. J. (2006). Organization of ETRAMPs and EXP-1 at the parasite-host cell interface of malaria parasites. *Molecular Microbiology*, *59*(3), 779–794.

Spielmann, T., & Gilberger, T.-W. (2010). Protein export in malaria parasites: do multiple export motifs add up to multiple export pathways? *Trends in Parasitology*, *26*(1), 6–10.

Spycher, C., Klonis, N., Spielmann, T., Kump, E., Steiger, S., Tilley, L., & Beck, H.-P. (2003). MAHRP-1, a Novel Plasmodium falciparum Histidine-rich Protein, Binds Ferriprotoporphyrin IX and Localizes to the Maurer's Clefts. *Journal of Biological Chemistry*, *278*(37), 35373–35383.

Spycher, C., Rug, M., Klonis, N., Ferguson, D. J. P., Cowman, A. F., Beck, H.-P., & Tilley, L. (2006). Genesis of and Trafficking to the Maurer's Clefts of Plasmodium falciparum-Infected Erythrocytes. *Molecular and Cellular Biology*, *26*(11), 4074.

Staines, H. M., Rae, C., & Kirk, K. (2000). Increased permeability of the malaria-infected erythrocyte to organic cations. *Biochimica et Biophysica Acta (BBA) - Biomembranes*, *1463*(1), 88–98.

Sturm, A., Amino, R., van de Sand, C., Regen, T., Retzlaff, S., Rennenberg, A., Krueger, A., Pollok, J.-M., Menard, R., & Heussler, V. T. (2006). Manipulation of Host Hepatocytes by the Malaria Parasite for Delivery into Liver Sinusoids. *Science*, *313*(5791), 1287–1290.

Su, X., Hayton, K., & Wellems, T. E. (2007). Genetic linkage and association analyses for trait mapping in Plasmodium falciparum. *Nature Reviews. Genetics*, *8*(7), 497–506.

Su, X. Z., Heatwole, V. M., Wertheimer, S. P., Guinet, F., Herrfeldt, J. A., Peterson, D. S., Ravetch, J. A., & Wellems, T. E. (1995). The large diverse gene family var encodes proteins involved in cytoadherence and antigenic variation of Plasmodium falciparum-infected erythrocytes. *Cell*, *82*(1), 89–100.

Szabo, A., Langer, T., Schröder, H., Flanagan, J., Bukau, B., & Hartl, F. U. (1994). The ATP hydrolysis-dependent reaction cycle of the Escherichia coli Hsp70 system DnaK, DnaJ, and GrpE. *Proceedings of the National Academy of Sciences of the United States of America*, *91*(22), 10345–10349.

Tavares, J., Formaglio, P., Thiberge, S., Mordelet, E., Van Rooijen, N., Medvinsky, A., Ménard, R., & Amino, R. (2013). Role of host cell traversal by the malaria sporozoite during liver infection. *The Journal of Experimental Medicine*, *210*(5), 905–915.

Tomkiewicz, D., Nouwen, N., & Driessen, A. J. M. (2007). Pushing, pulling and trapping - Modes of motor protein supported protein translocation. *FEBS Letters*, *581*(15), 2820–2828.

Towbin, H., Staehelin, T., & Gordon, J. (1979). Electrophoretic transfer of proteins from polyacrylamide gels to nitrocellulose sheets: procedure and some applications. *Proceedings of the National Academy of Sciences of the United States of America*, *76*(9), 4350–4354.

Trager, W., & Jensen, J. B. (1976). Human malaria parasites in continuous culture. *Science (New York, N.Y.)*, *193*(4254), 673–675.

Walker, D., Chaddock, A. M., Chaddock, J. A., Roberts, L. M., Lord, J. M., & Robinson, C. (1996). Ricin A Chain Fused to a Chloroplast-targeting Signal Is Unfolded on the Chloroplast Surface Prior to Import across the Envelope Membranes. *Journal of Biological Chemistry*, *271*(8), 4082–4085.

Walliker, D., Quakyi, I. A., Wellems, T. E., McCutchan, T. F., Szarfman, A., London, W. T., Corcoran, L. M., Burkot, T. R., & Carter, R. (1987). Genetic analysis of the human malaria parasite Plasmodium falciparum. *Science (New York, N.Y.)*, *236*(4809), 1661–1666.

Waters, A. P., Thomas, A. W., van Dijk, M. R., & Janse, C. J. (1997). Transfection of Malaria Parasites. *Methods*, *13*(2), 134–147.

Wells, T. N. C., van Huijsduijnen, R. H., & Van Voorhis, W. C. (2015). Malaria medicines: a glass half full? *Nature Reviews Drug Discovery*, *14*(6), 424–442.

WHO. (2018). *WHO Malaria Report 2018*.

Wickham, M. E., Rug, M., Ralph, S. A., Klonis, N., McFadden, G. I., Tilley, L., & Cowman, A. F. (2001). Trafficking and assembly of the cytoadherence complex in Plasmodium falciparum-infected human erythrocytes. *The EMBO Journal*, *20*(20), 5636–5649.

Yam, X. Y., Niang, M., Madnani, K. G., & Preiser, P. R. (2017). Three Is a Crowd – New Insights into Rosetting in Plasmodium falciparum. *Trends in Parasitology*, *33*(4), 309–320.

Young, J. C., Hoogenraad, N. J., & Hartl, F. U. (2003). Molecular chaperones Hsp90 and Hsp70 deliver preproteins to the mitochondrial import receptor Tom70. *Cell*, *112*(1), 41–50

Zeng, X.-C., Bhasin, S., Wu, X., Lee, J.-G., Maffi, S., Nichols, C. J., Lee, K. J., Taylor, J. P., Greene, L. E., & Eisenberg, E. (2004). Hsp70 dynamics in vivo: effect of heat shock and protein aggregation. *Journal of Cell Science*, *117*(21), 4991–5000.

Zhang, Q., Ma, C., Oberli, A., Zinz, A., Engels, S., & Przyborski, J. M. (2017). Proteomic analysis of exported chaperone/co-chaperone complexes of P. falciparum reveals an array of complex protein-protein interactions. *Scientific Reports*, *7*(1), 42188.

Zhong, R., Morrison, W. H., Freshour, G. D., Hahn, M. G., & Ye, Z.-H. (2003). Expression of a Mutant Form of Cellulose Synthase AtCesA7 Causes Dominant Negative Effect on Cellulose Biosynthesis. *PLANT PHYSIOLOGY*, *132*(2), 786–795.

6 Appendix

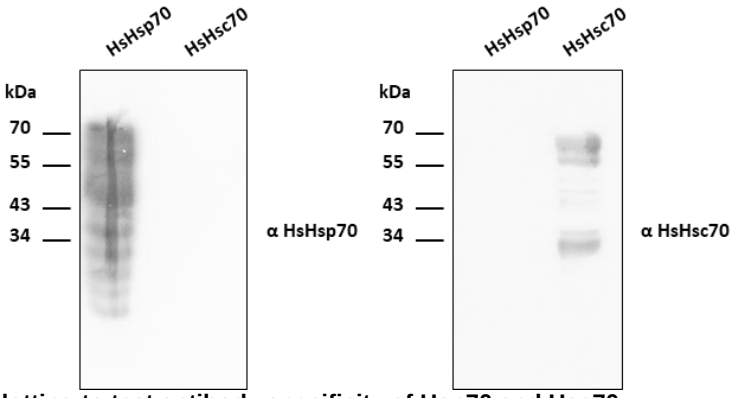

Figure 44 Immunoblotting to test antibody specificity of Hsp70 and Hsc70
Recombinant HsHsp70 and HsHsc70 were separated on a SDS gel followed by immunoblotting using sera directed HsHsp70 and HsHsc70. Size marker in kDa is indicated on left side.

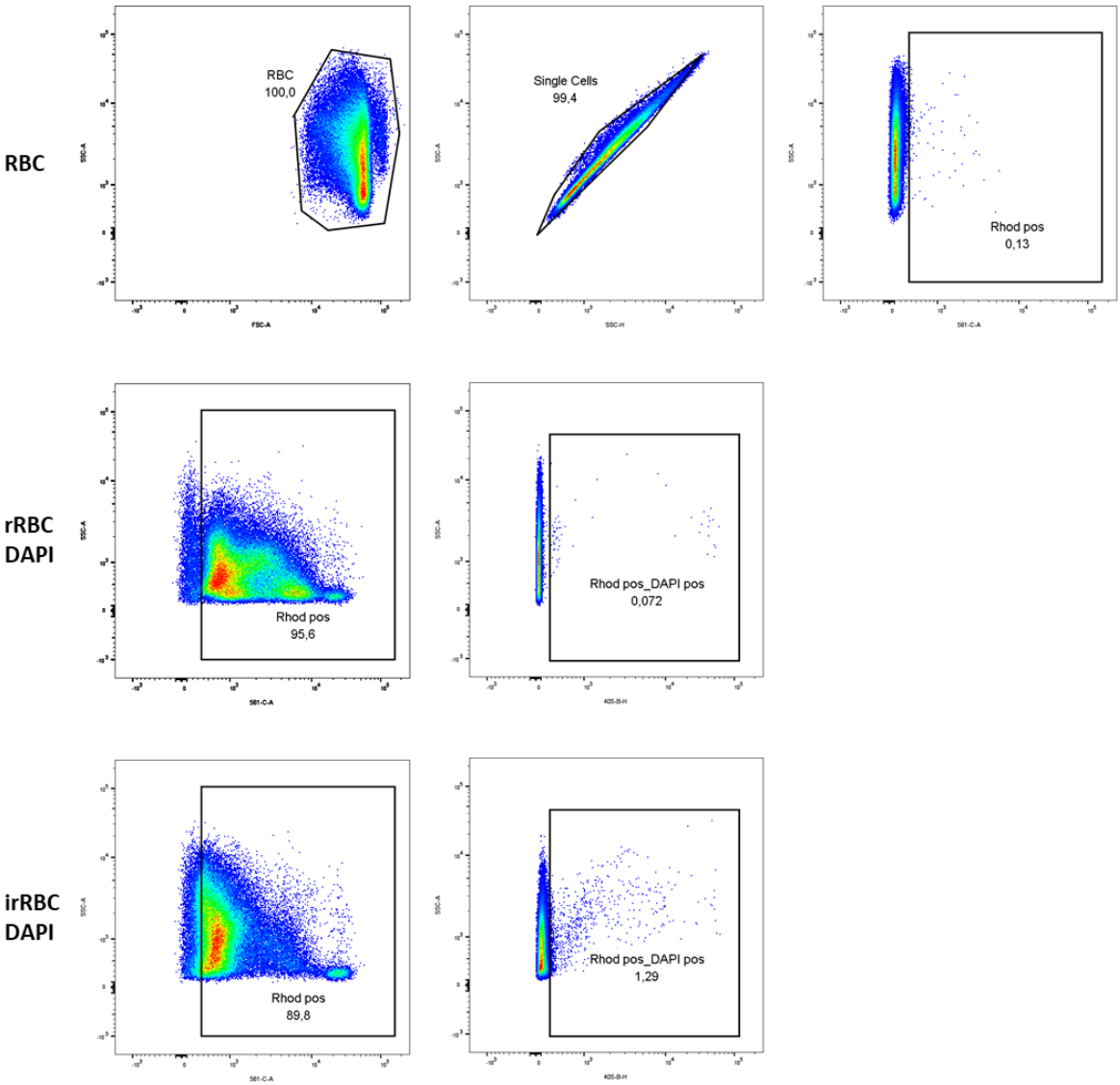

Figure 45 Gating example: DAPI positive cells in rRBC
Flow cytometry gating strategy of DAPI positive cells detected in rRBC. First, all cells were displayed in the Side SCatter (SSC), indicating the granularity of the cells, versus the Forward SCatter (FSC), measuring the size of the cells. From this population, the single cells were gated with the help of setting the SSC-Area (SSC-A) against the SSC-Height (SSC-H). Afterwards, the gate was set where rhodamine positive cells were expected by the SSC-A vs the 561-CA laser with the help of a sample of wildtype non-infected RBC (RBC). A sample with rRBC that were non-infected, but stained with DAPI was used to confirm the rhodamine gate and to set the gate for the DAPI positive cells using the SSC-A vs the 405-B-H laser (rRBC DAPI). At last, the gating process was checked by infected rRBC which were stained with DAPI (irRBC DAPI). SSC: Side SCatter, FSC: Forward SCatter, A: Area, H: Height, Rhod_pos: Rhodamine positive cells, DAPI_pos: DAPI positive cells.

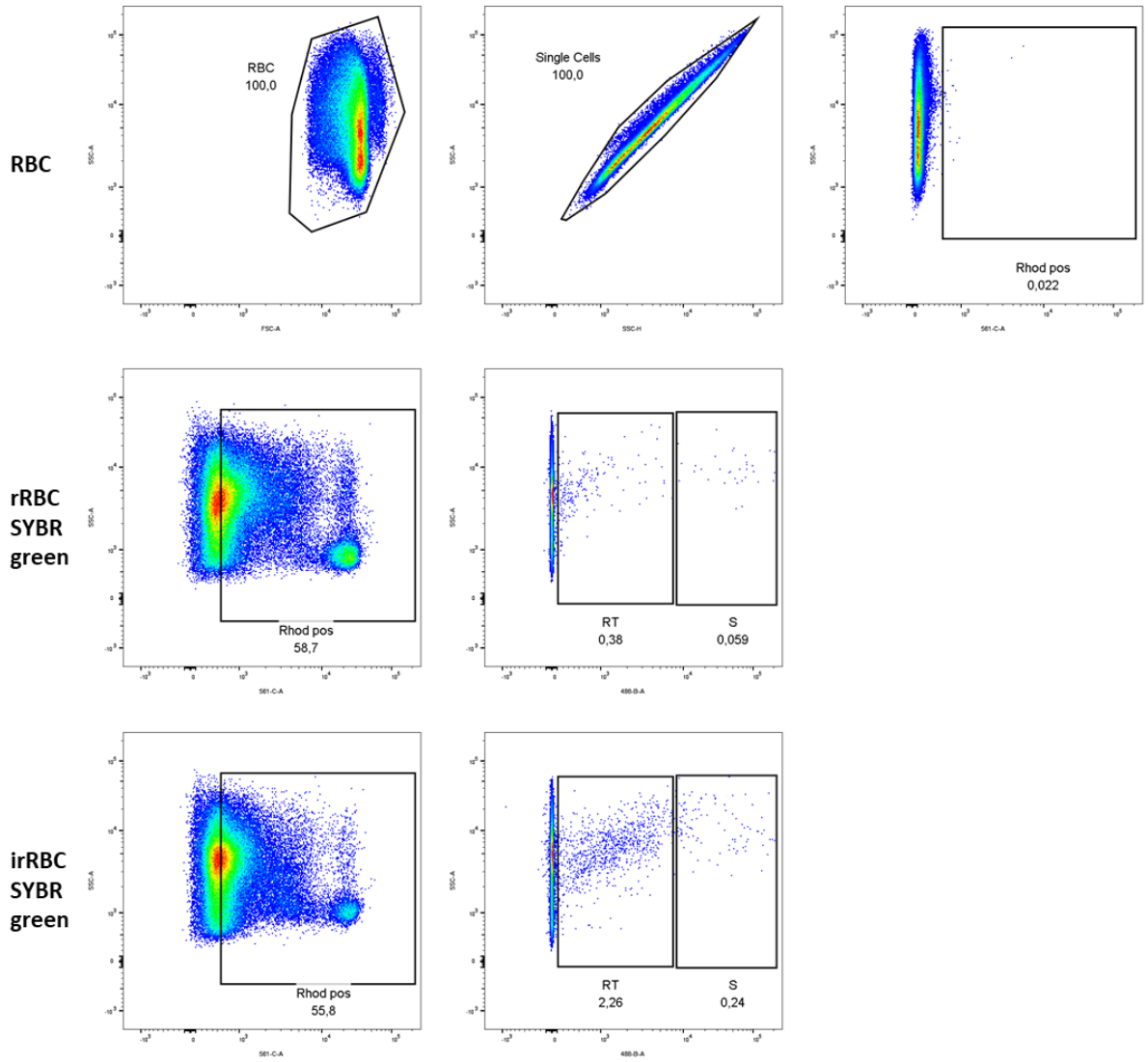

Figure 46 Gating example: SYBR green positive cells in rRBC
Flow cytometry gating strategy of SYBR green positive cells detected in rRBC to differentiate single-nucleated ring/trophozoites (RT) and multi-nucleated schizonts (S). Again, all cells, single cells and rhodamine positive cells were gated as described in Figure 45. This time, non-infected and SYBR green stained rRBC were used set the gates for the ring/trophozoite stage (RT) and the schizont stage (S) exploiting the SSC-A vs the 488-BA laser. Unfortunately, no control of a synchronised schizont and mixed ring/trophozoite culture grown in the rRBC were used in this experimental setup, therefore gates for the ring/trophozoite and schizont stage had to be assumed based on experience. Finally, a sample of infected rRBC stained with SYBR green (iRBC SYBR green) was used to control all set gates. SSC: Side SCatter, FSC: Forwards SCatter, A: Area, H: Height, Rhod_pos: Rhodamine positive cells, RT: Ring/Trophozoit, S: Schizont.

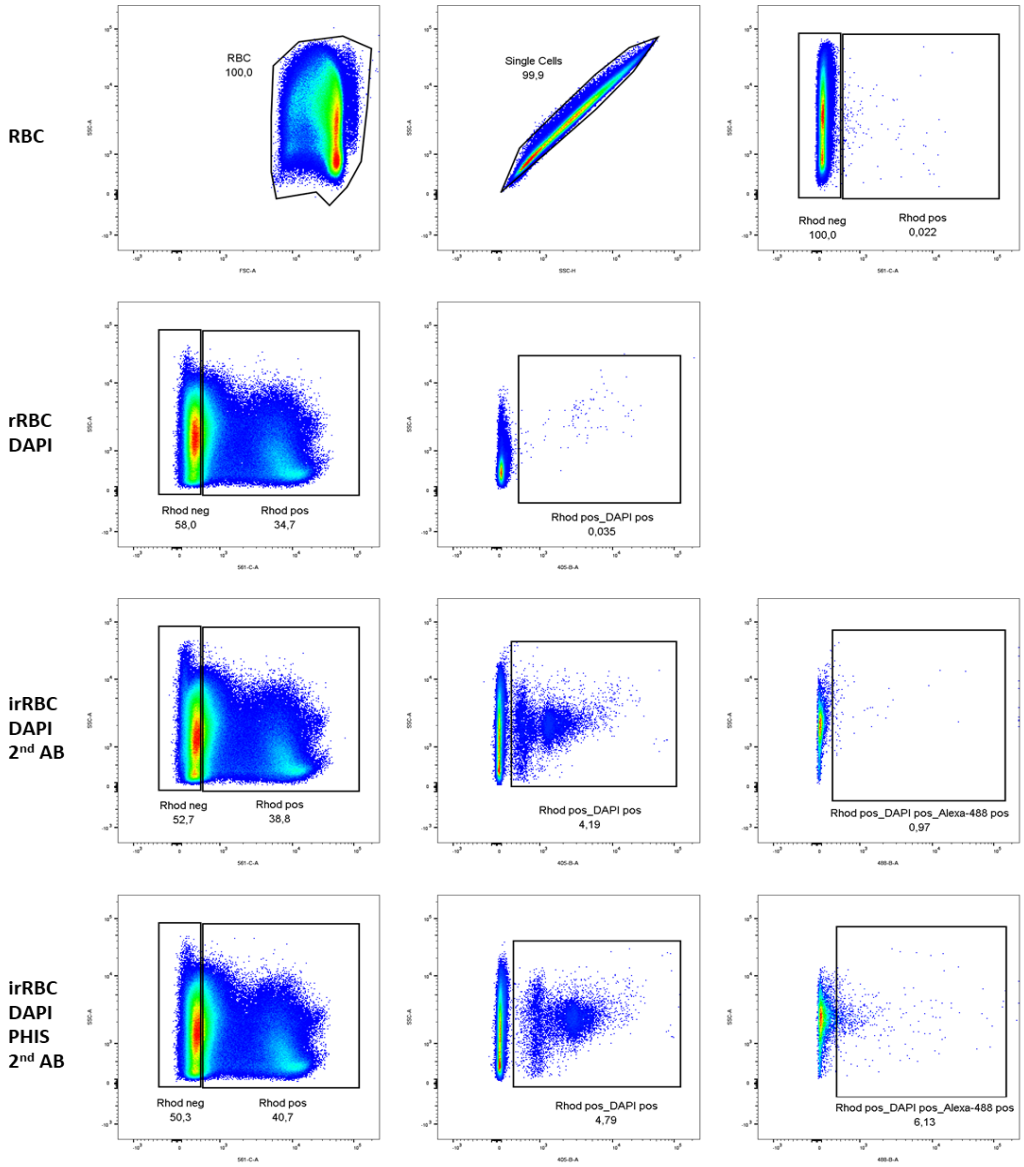

Figure 47 Gating example of irRBC stained with Alexa-488

Flow cytometry gating strategy of Alexa-488 positive cells detected in rRBC treated with PHIS from Kelifi, Kenya. First as previously explained, from all cells the single cells were gated (Figure 45). Rhodamine gate was set with the help of non-infected and non-resealed RBC (RBC). rRBC non-infected but stained with DAPI (rRBC DAPI) were used for the DAPI gating. A sample of infected rRBC stained by DAPI and incubated with the secondary antibody (irRBC DAPI 2nd AB) was used to set the gate of the Alexa-488 positive cells. Finally, infected rRBC treated with PHIS and stained with DAPI as well as the secondary antibody (irRBC DAPI PHIS 2^{nd} AB) were used to ensure a proper gating. SSC: Side SCatter, FSC: Forward SCatter, A: Area, H: Height, Rhod_pos: Rhodamine positive cells, 2^{nd} AB: secondary antibody (anti-human Alexa-488), PHIS: (Pool of HyperImmune Sera from Kelifi, Kenya).

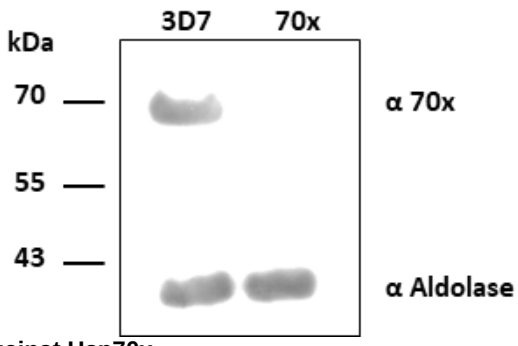

Figure 48 Immunoblotting against Hsp70x
3D7 and Hsp70x (70x) parasites (10^7 iRBC) were separated on a SDS gel followed by immunoblotting against Hsp70x, and aldolase as a loading control. Size marker in kDa is indicated on left side.

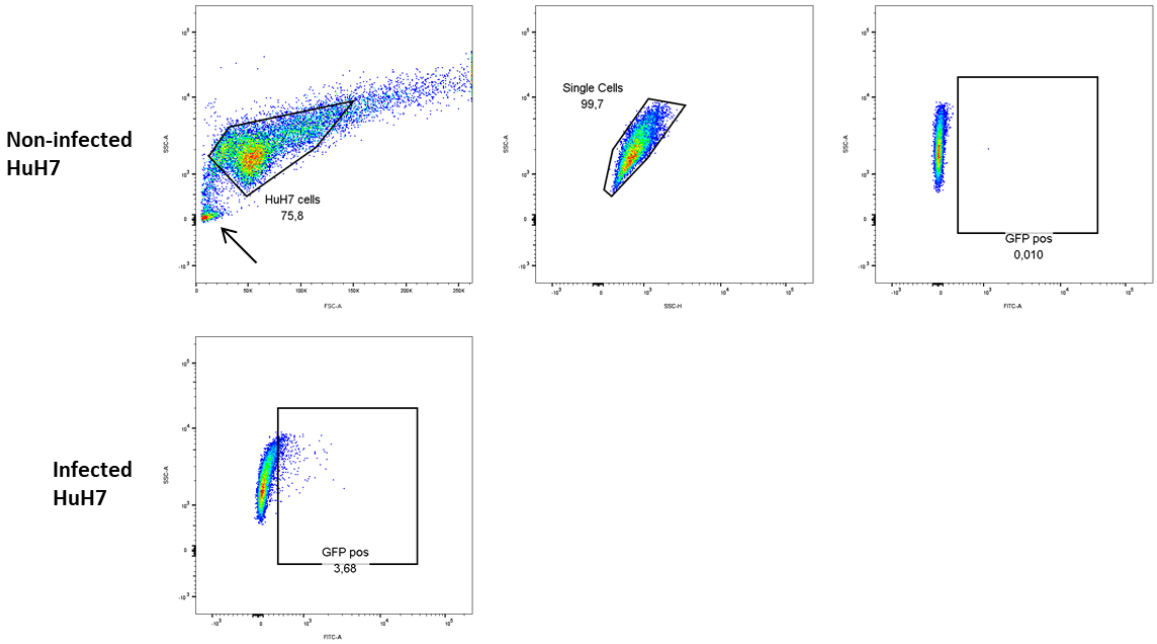

Figure 49 Gating example: HuHu7 cells infected by *P. berghei*
Flow cytometry gating strategy of GFP positive cells detected in HuH7 (liver carcinoma) cells. First, from all cells displayed in SSC-A vs FSC-A, single cells were gated using the SSC-A vs SSC-H. Non-infected HuH7 cells were used to set the gate for GFP positive cells (GFP pos). The GFP gating was controlled by infected HuH7 cells. Notably, lots of cell debris was seen (arrow), indicating that cells died during the experiment. Most likely cells died due to the lipofectamine, since irrelevant of the treatment (e.g with siRNA, scraRNA or only lipofectamine) equal amounts of cell debris can be found in all samples (data not shown) SSC: Side SCatter, FSC: Forward Scatter, GFP pos: GFP positive cells.